NASA CONTRACTOR REPORT

NASA CR-1169

ANALYTICAL INVESTIGATION OF INCOMPRESSIBLE TURBULENT SWIRLING FLOW IN PIPES

by Avelino P. Rochino and Zalman Lavan

Prepared by
ILLINOIS INSTITUTE OF TECHNOLOGY
Chicago, Ill.
for Lewis Research Center

NATIONAL AERONAUTICS AND SPACE ADMINISTRATION • WASHINGTON, D. C. • SEPTEMBER 1968

NASA CR-1169

ANALYTICAL INVESTIGATION OF INCOMPRESSIBLE TURBULENT SWIRLING FLOW IN PIPES

By Avelino P. Rochino and Zalman Lavan

Prepared under Grant No. NsG 694 by
ILLINOIS INSTITUTE OF TECHNOLOGY
Chicago, Ill.

for

Lewis Research Center

NATIONAL AERONAUTICS AND SPACE ADMINISTRATION

For sale by the Clearinghouse for Federal Scientific and Technical Information
Springfield, Virginia 22151 – CFSTI price $3.00

FOREWORD

Research related to advanced nuclear rocket propulsion is described herein. This work was performed under NASA Grant NsG-694 with Mr. Maynard F. Taylor, Nuclear Systems Division, NASA Lewis Research Center as Technical Manager.

ABSTRACT

Turbulent swirling flows in ducts were investigated analytically using mixing length theories. The governing equations for the mean flow were derived using G. I. Taylor's modified vorticity transport theory and the concept of isotropy of the transport coefficients. The similarity theory of von Karman was extended to swirling flows in a cylindrical geometry considering a three-dimensional fluctuating velocity field. The resulting similarity conditions were used to formulate the expression for eddy diffusivity in the entire flow field except a small region near the pipe wall where a mixing length expression analogous to that assumed by Prandtl for parallel flow in channels was used. The tangential equation of motion was then solved numerically to study the decay of angular momentum in a swirling flow field inside a stationary pipe. It should be pointed out that for pure rotational as well as irrotational flow, some of the similarity conditions become indeterminate suggesting that the said formulation may not be valid for these situations.

The theoretical results were compared with two sets of experimental measurements. In the first (taken at IITRI in 1967) the fluid was air and the swirl was generated by means of radial blades. Axial Reynold's Numbers ranged from 58,900 to 279,000 and the swirl ratio from 4.7 to 11.8 with data taken as far as 136 radii downstream. The second set of measurements (taken by Musolf in 1963) dealt with water where the swirl was generated by tape inserts inside the pipe. Measurements were taken as far as 100 radii

downstream at an axial Reynold's Number of 48,000 and a swirl ratio of approximately 0.50.

For both cases the agreement between experimental and predicted values was, in general, good. As might have been expected, some discrepancies occurred when the flow field was predominantly irrotational or in solid body rotation.

TABLE OF CONTENTS

Table of Contents (Cont'd)

LIST OF FIGURES

List of Figures (Cont'd)

List of Figures (Cont'd)

LIST OF SYMBOLS

Symbol	Definition
a	Initial coordinate of a fluid particle along the x-axis.
A	Velocity scale in the turbulent flow field.
b	Initial coordinate of a fluid particle along the y axis.
B	Coefficient of the partial derivative in the angular momentum equation (Eq. 95).
c	Initial coordinate of a fluid particle along the z-axis.
C	Constant in the eddy viscosity expression given in Equation 99.
$C_n (n = 1,2,3,\ldots)$	Integration constants.
D	Coefficient of the partial derivatives in the angular momentum equation (Eq. 95).
$\frac{D}{Dt}$	Substantial derivative
e_m	Kinematic eddy viscosity in the swirl equation.
$e_{m(r)}$, $e_{m(\theta)}$, $e_{m(z)}$	Kinematic eddy viscosity in the radial, tangential and axial component of the equation of motion.
$f(r)$	Initial tangential velocity profile.
$\underline{F}$	Body force vector.
$\overline{F}_r$, $\overline{F}_\theta$, $\overline{F}_z$	Average body forces in the radial, tangential and axial direction.
$\overline{H}$	Defined after Equation 5.
h_1, h_2	Roots of the characteristic equation given in Equation 71.

List of Symbols (Cont'd)

i	$\sqrt{-1}$, imaginary number.
K, $K_n (n = 1, 2, \ldots.)$	Similarity constants in the free region.
L	Length scale in the turbulent flow field.
$\underline{L}$	Mixing length vector.
L_1, L_2, L_3	Components of the mixing length vector in the x, y and z directions.
M	K_3/K_1
N	K_2/K_1
N_{Re}	Axial Reynolds' Number based on the maximum axial velocity of the fully developed profile, the radius of the pipe and the kinematic molecular viscosity at 85°F and 14.7 psia pressure.
p	Instantaneous pressure defined in Equation 1.
P, p'	Mean and fluctuating pressure.
Q	$P/\rho + \overline{\underline{v}'}^2/2$
r	Radial coordinate.
r_i	Radius of inner cylinder.
r_{max}	Radius having maximum tangential velocity.
r_w	Radius of the pipe, or of the outer cylinder.
S	K_2/K_3
t	Time
T_{ij}	Reynolds' stress acting on a plane perpendicular to the i-th axis and parallel to the j-direction.
$\underline{V}$	Instantaneous velocity vector.
$\overline{\underline{V}}$, $\underline{v}'$, v_i'	Mean and fluctuating velocity vector.
U, V, W	Components of the mean velocity vector in the radial, tangential and axial directions.

u', v', w'	Components of the fluctuating velocity vector in the radial, tangential and axial directions.
W_m	Maximum axial velocity of the fully developed profile.
z	Axial coordinate.
α, α_1	Constants from dimensional analysis.
β	Angular momentum.
β_j^n	$\beta(j\Delta r, n\Delta z)$
Δr	Grid size in the radial direction.
Δz	Grid size in the axial direction.
τ, γ, ϕ	Defined after Equation II-3.
Γ	Swirl ratio; $= 2V_{max}/W_{ave}$, where V_{max}, the maximum tangential velocity and W_{ave}, the average axial velocity are evaluated at the first downstream station ($z = 4R$).
Ψ	Amplification matrix.
∇	Del operator
∇^2	Laplace operator
∇x	Curl operator
$\underline{\Omega}$	Instantaneous vorticity vector.
$\bar{\underline{\Omega}}$; $\underline{\Omega}'$	Mean and fluctuating vorticity vector.
ω_r, ω_θ, ω_z	Component of the instantaneous vorticity vector in the radial, tangential and axial directions.
ξ, η, ζ	Component of the mean vorticity vector in the radial, tangential and axial directions, defined in Equation 20. (x,y,z directions in Appendix I and II.)

ξ', η', ζ'	Component of the fluctuating vorticity vector in the radial, tangential and axial directions. (x,y,z directions in App. I & II.)
λ	As defined after Equation 91.
μ	Molecular viscosity.
ν	Kinematic viscosity.
ρ	Density of the incompressible fluid.
ρ_t	Instantaneous density, defined in Equation 1.
$\bar{\rho}$, ρ'	Mean and fluctuating density.
θ	Coordinate in tangential direction.

Subscripts

o	Reference values.
Rot	Based on mean rotation.
Sh	Based on shear velocity.
Ang	Based on angular momentum gradient in the axial direction.
max	Based on the point with maximum tangential velocity.
m	Based on the maximum value of the fully developed profile.
j	Grid point number in the radial direction.
r, θ, z	Indicates radial, tangential and axial direction.

Superscripts

*	Similarity parameters.
'	Fluctuating flow variables.
n	Grid point number in the axial direction.
$\bar{}$	Denotes temporal average.

ANALYTICAL INVESTIGATION OF INCOMPRESSIBLE TURBULENT SWIRLING FLOW IN PIPES

I. INTRODUCTION

Turbulent flows are encountered in almost every application where fluid motion is involved. Hinze[1] defined it as "an irregular condition of flow in which various quantities related to it show a random variation with time and space coordinates so that statistically distinct average values can be discerned." According to this definition, the irregular behavior of the motion can be described by the law of probability, thus making it accessible to mathematical treatment.

While both Eulerian and Lagrangian mean values can be considered, the former is more commonly employed.[2] The Eulerian average values can be taken at a certain point over a long interval of time (temporal mean values), or over a large region at a particular instant of time (spatial mean values), or finally over a great number of realizations represented by identical fields at corresponding points and instants (statistical mean values).[2]

When we deal with the mean values of the turbulent motion, the common concept is such that a fictitious "laminar flow" is present.[1],[2],[3],[4] In analogy to the laminar case, the flow is endowed with properties called "eddy viscosity" and "eddy conductivity." These properties bear no relation to the ordinary diffusion properties of the fluid and are intimately related to the flow itself. Furthermore, their numerical values may be hundreds of times larger.[2] Several phenomenological theories substantially

contributed to the present understanding of some important aspects of turbulence.[5],[6],[7] For this reason this approach has been employed in the present investigation of turbulent swirling flow.

It was generally believed[4] that the different features of turbulent flow such as mean velocity distribution and frictional effects bear, in general, little resemblance to those found in laminar flow. This is due to the fact that the diffusion mechanism in turbulent flow is far stronger than molecular diffusion. When the effect of both turbulent and molecular diffusion is considered, it is commonly assumed that the two are additive in the field of flow.

In addition to phenomenological models, statistical approaches were also used to study turbulence. This approach is mathematically more elegant and may indeed lead to a more fundamental and detailed understanding of the nature of turbulent motion. In the present state, however, this method does not yield complete solutions to turbulent flow problems since the mathematical formulation lacks closure, i.e., higher order correlation functions are successively introduced when studying the dynamic behavior of correlations of a given order. Attempts made to express these functions in terms of a fourier series resulted either in complete divergence or at best in extremely slow convergence. While it it possible to pursue this approach by introducing rather arbitrary assumptions into the analysis, it was decided to utilize the simpler and more commonly used phenomenological approach in the present investigation.

Review of Swirling and Rotating Flow Investigations

The dye experiment of O. Reynolds[8] first noted the irregular motion of the fluid elements for the case of parallel flow through a pipe of circular cross-section. The transition from laminar to turbulent motion took place at a definite value of what is now known as the Reynolds' Number. The flow between concentric rotating cylinders was first considered experimentally by Mallock[9] who found that when the inner cylinder was fixed, the steady flow was stable so long as the angular velocity of the outer one did not exceed a certain limit. When it exceeded that limit the flow was definitely unstable. On the other hand, when the outer cylinder was fixed he found that the steady motion was unstable for all speeds of revolution of the inner cylinder that he tried.

The problem caught the attention of G. I. Taylor who studied it both mathematically and experimentally and obtained definite results. In 1922[10] his results showed that when the inner cylinder was at rest, the steady motion was stable for a wide range of rotational speeds of the outer cylinder, and when the outer cylinder was fixed the flow was stable for sufficiently low rotation of the inner cylinder. He also measured the tangential velocity distribution in the turbulent region between the cylinders and found out that the flow in a large part of the annular space was irrotational.[7] The same observation was made by Wattendorf[11] for turbulent flow in curved channels.

The fictitious "laminar flow" concept of turbulent motion was used by past investigators in the analysis of rotating and swirling turbulent flow.

Kassner and Knoernschild[12] studied friction laws and energy transfer in rotating flow in an attempt to explain the Hilsch or Ranque effect in a vortex tube. They showed that in such a flow the shearing stress is proportional to the shear velocity, the proportionality factor being the eddy viscosity which is in turn a function of the shear velocity and the mixing length. Ragsdale[13] used Kassner's formulation of the eddy viscosity to investigate the correlation of his experimental vortex data with mixing length expressions given by Prandtl[14] and von Karman's similarity hypothesis.[15] He concluded that Karman's mixing length function correlates the data better than that assumed by Prandtl.

Einstein and Li,[16] in their treatment of turbulent vortex motion of incompressible fluids showed analytically that in the tangential component of the Navier-Stokes equation, turbulent flow has an effect similar to that of laminar flow if the eddy viscosity (ρe_m) is considered a constant. Deissler and Perlmutter[17] extended this statement to compressible fluids in their study of the Ranque-Hilsch phenomenon. Their theoretical results agree reasonably well with the experimental data of Hartnett and Eckert.[18] Reynolds[19] and Sibulkin[20] have studied a number of problems on vortical flows to explain and analyze the same effect.

Kreith and Sonju[21] made a semi-theoretical analysis of the decay of a turbulent swirl of an incompressible fluid in pipes. They used an empirical expression of the kinematic eddy viscosity (e_m) in the linearized swirl equation and obtained good agreement with experimental data as far as the turbulent swirl decay is concerned. The predicted mean tangential velocity distribution, however, deviated from experimental values far downstream.

Studies of the effect of turbulent swirling flow in heat transfer in tubes were carried out by Kreith and Margolis,[22] Smithbern and Landis,[23] Gambil, Bundy and Wansbrough[24] and others. Ragsdale,[25] Keyes[26] and Karrebrock and Meghreblian[27] have analyzed other types of vortex flows in an effort to develop a method suitable for the containment of gases in a nuclear rocket.

For the laminar case, Lavan and Fejer[28] obtained a numerical solution for swirling flow in the entrance region of pipes using the complete Navier-Stokes equation. Collatz and Goertler[29] and Talbot[30] considered small swirl components superimposed on a fully developed parallel pipe flow. They thus linearized the equations of motion thereby reducing them to an eigenvalue problem.

Recently, R. B. Kinney[31] extended von Karman's similarity theory to a cylindrical geometry and established the similarity conditions for plane turbulent rotating flow. He derived a universal velocity profile and an eddy viscosity expression from these similarity conditions and evaluated a universal constant in the eddy viscosity equation from Taylor's velocity and wall stress measurements.[32]

While these investigations, as well as others not mentioned here, contributed to the understanding of turbulent swirling and rotating flow, considerably more research is required in order to understand these problems more completely. The present investigation will attempt to study the problem of turbulent swirling flow in a cylindrical pipe using the phenomenological models of the turbulent flow mechanism. The decay of angular

momentum will be studied over a relatively large axial distance from the point of swirl generation. The swirl equation will be deduced from Taylor's modified vorticity transport theory using an eddy viscosity expression derived by extending von Karman's similarity hypothesis to a cylindrical geometry with a fully turbulent swirling flow. In order to include the region near the wall in the analysis, pertinent modification in the swirl and eddy viscosity expressions will be made. The theoretical results will be compared with experimental data obtained by other investigators.[33],[34]

II. CONTINUITY AND NAVIER-STOKES EQUATION FOR TURBULENT FLOW

To study the time-dependent properties of turbulent flow it is usually assumed that the motion can be separated into a mean flow with a fluctuating flow superimposed on it. The instantaneous value of any dependent variable is then the sum of the mean and fluctuating values of this variable.

Due to the complexity of the instantaneous turbulent motion an averaging technique is employed and the investigation concerns itself with the average motion that includes mean values as well as products of fluctuating components. Of the Eulerian mean values mentioned previously, the temporal type is commonly used in methods of measurement and observation (Reference 2, p. 81). The average of any quantity, say F, is

$$\bar{F} = \frac{1}{T} \int_0^T F \, dt$$

where T is large compared to the time scale of the fluctuations. This renders the mean value of the fluctuating components as zero. The mean value of the product of two quantities that can be expressed as

$$\bar{A} + A' \qquad \text{and} \qquad \bar{B} + B'$$

is therefore

$$\bar{A}\,\bar{B} + \overline{A'\,B'}$$

Hinze[1] and Schlichting[4] give a detailed account of the averaging procedure.

Figure 1 depicts the cylindrical polar coordinate system that will be used where u, v, w, p and ρ_t are the instantaneous velocities, pressure and density. These variables are in turn given by

$$
\begin{aligned}
u &= \bar{U} + u' \\
v &= \bar{V} + v' \\
w &= \bar{W} + w' \\
p &= \bar{P} + p' \\
\rho_t &= \bar{\rho} + \rho'
\end{aligned}
\tag{1}
$$

where the bar denotes mean values and the primes the fluctuating components.

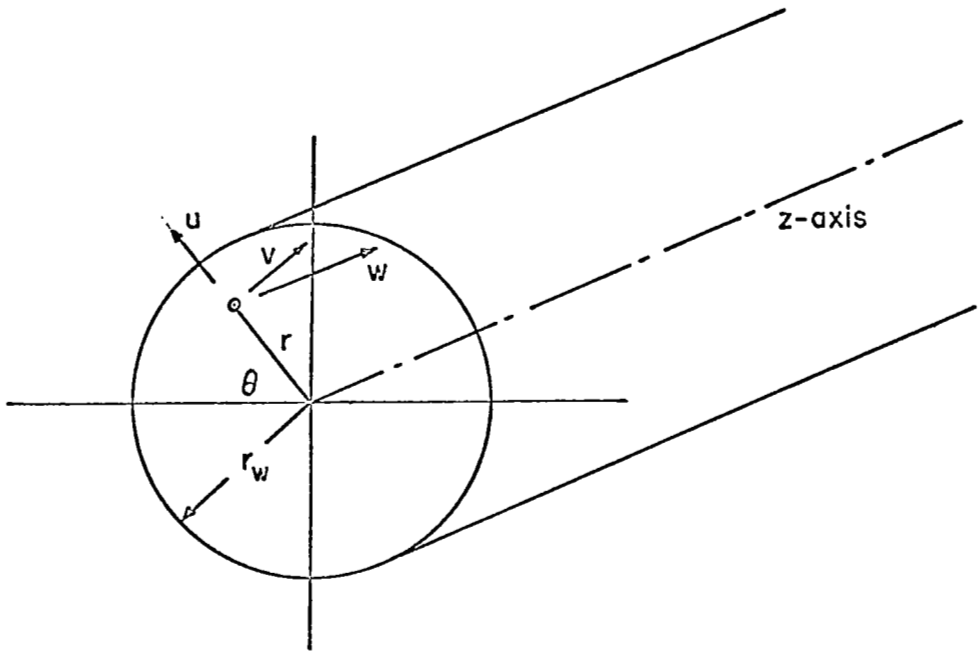

Figure 1: Coordinate System and Velocity Notation

The fluctuating component of physical quantities like viscosity, specific heat and coefficient of heat conductivity can be neglected (Reference 2, p. 82).

Inserting the instantaneous values (Equation 1) into the continuity and Navier-Stokes equations, taking time averages and considering constant molecular viscosity, we obtain the following equations for compressible flow.

A. COMPRESSIBLE FLOW

1. Continuity Equation

$$\frac{\partial \bar{\rho}}{\partial t} + \frac{\partial(\bar{\rho}\,\bar{U})}{\partial r} + \frac{\bar{\rho}\,\bar{U}}{r} + \frac{1}{r}\frac{\partial(\bar{\rho}\,\bar{V})}{\partial \theta} + \frac{\partial(\bar{\rho}\,\bar{W})}{\partial z} + \frac{1}{r}\overline{\rho' u'}$$

$$+ \frac{\partial(\overline{\rho' u'})}{\partial r} + \frac{1}{r}\frac{\partial(\overline{\rho' v'})}{\partial \theta} + \frac{\partial(\overline{\rho' w'})}{\partial z} = 0 \qquad (2)$$

2. Equations of Motion

(a) Radial Component

$$\bar{\rho}\left[\frac{\partial \bar{U}}{\partial t} + \bar{U}\frac{\partial \bar{U}}{\partial r} + \frac{\bar{V}}{r}\frac{\partial \bar{U}}{\partial \theta} + \bar{W}\frac{\partial \bar{U}}{\partial z} - \frac{\bar{V}^2}{r}\right] = -\frac{\partial \bar{P}}{\partial r} + \frac{1}{3}\mu\frac{\partial \bar{H}}{\partial r}$$

$$+ \mu\left[\nabla^2 \bar{U} - \frac{\bar{U}}{r^2} - \frac{2}{r^2}\frac{\partial \bar{V}}{\partial \theta}\right] - \bar{\rho}\left[\overline{u'\frac{\partial u'}{\partial r}} + \overline{\frac{v'}{r}\frac{\partial u'}{\partial \theta}} + \overline{w'\frac{\partial u'}{\partial r}}\right.$$

$$- \frac{1}{r}\overline{v'^2}\Bigg] - \overline{\rho'\frac{\partial u'}{\partial t}} - \overline{\rho' u'}\frac{\partial \bar{U}}{\partial r} - \overline{\rho' v'}\left(\frac{1}{r}\frac{\partial \bar{U}}{\partial \theta} - \frac{2\bar{V}}{r}\right)$$

$$- \overline{\rho' w'\frac{\partial u'}{\partial r}} - \overline{\rho'\frac{\partial u'}{\partial r}}\cdot\bar{U} - \overline{\rho'\frac{\partial u'}{r\partial\theta}}\cdot\bar{V} - \overline{\rho' w'}\frac{\partial \bar{U}}{\partial r}$$

$$- \overline{\rho'\frac{\partial u'}{\partial r}}\cdot\bar{W} + \frac{1}{r}\overline{\rho' v'^2} - \overline{\frac{\rho' v'}{r}\frac{\partial u'}{\partial \theta}} - \overline{\rho' u'\frac{\partial u'}{\partial r}} + \bar{F}_r \qquad (3)$$

(b) Tangential Component

$$\bar{\rho}\left[\frac{\partial \bar{V}}{\partial t} + \bar{U}\frac{\partial \bar{V}}{\partial r} + \frac{\bar{V}}{r}\frac{\partial \bar{V}}{\partial \theta} + \bar{W}\frac{\partial \bar{V}}{\partial z} + \frac{\bar{U}\bar{V}}{r}\right] = -\frac{1}{r}\frac{\partial \bar{P}}{\partial \theta}$$

$$+ \frac{1}{3}\frac{\mu}{r}\frac{\partial \bar{H}}{\partial \theta} + \mu\left(\nabla^2\bar{V} - \frac{\bar{V}}{r^2} + \frac{2}{r}\frac{\partial \bar{U}}{\partial \theta}\right) - \bar{\rho}\left(\overline{u'\frac{\partial v'}{\partial r}}\right.$$

$$\left. + \overline{\frac{v'}{r}\frac{\partial v'}{\partial \theta}} + \overline{w'\frac{\partial v'}{\partial z}} + \overline{\frac{u'v'}{r}}\right) - \overline{\rho'\frac{\partial v'}{\partial t}} - \overline{\rho' u'}\left(\frac{\partial \bar{V}}{\partial r} + \frac{\bar{V}}{r}\right)$$

$$- \overline{\rho' v'}\left(\frac{\partial \bar{V}}{r\partial\theta} + \frac{\bar{U}}{r}\right) - \overline{\rho' w'}\frac{\partial \bar{V}}{\partial z} - \overline{\rho'\frac{\partial v'}{\partial r}}\cdot\bar{U} - \overline{\rho'\frac{\partial v'}{r\partial\theta}}\cdot\bar{V}$$

$$- \overline{\rho'\frac{\partial v'}{\partial z}}\cdot\bar{W} - \overline{\frac{\rho' u' v'}{r}} - \overline{\rho' u'\frac{\partial v'}{\partial r}} - \overline{\frac{\rho' v'}{r}\frac{\partial v'}{\partial \theta}} - \overline{\rho' w'\frac{\partial v'}{\partial z}} + \bar{F}_\theta$$

(4)

(c) Axial Component

$$\bar{\rho}\left[\frac{\partial \bar{W}}{\partial t} + \bar{U}\frac{\partial \bar{W}}{\partial r} + \frac{\bar{V}}{r}\frac{\partial \bar{W}}{\partial \theta} + \bar{W}\frac{\partial \bar{W}}{\partial z}\right] = -\frac{\partial \bar{P}}{\partial z} + \frac{1}{3}\mu\frac{\partial \bar{H}}{\partial z}$$

$$+ \mu\left[\nabla^2 \bar{W}\right] - \bar{\rho}\left[\overline{u'\frac{\partial w'}{\partial r}} + \overline{\frac{v'}{r}\frac{\partial w'}{\partial \theta}} + \overline{w'\frac{\partial w'}{\partial z}}\right]$$

$$- \overline{\rho' u'}\frac{\partial \bar{W}}{\partial r} - \overline{\frac{\rho' v'}{r}}\frac{\partial \bar{W}}{\partial \theta} - \overline{\rho' w'}\frac{\partial \bar{W}}{\partial z} - \overline{\rho'\frac{\partial w'}{\partial r}} \cdot \bar{U}$$

$$- \overline{\rho'\frac{\partial w'}{r\partial \theta}} \cdot \bar{V} - \overline{\rho'\frac{\partial w'}{\partial z}} \cdot \bar{W} - \overline{\rho' u'\frac{\partial w'}{\partial r}} - \overline{\frac{\rho' v'}{r}\frac{\partial w'}{\partial \theta}}$$

$$- \overline{\rho' w'\frac{\partial w'}{\partial z}} + \bar{F}_z. \qquad (5)$$

Where:

$$\bar{H} = \frac{\partial \bar{U}}{\partial r} + \frac{\bar{U}}{r} + \frac{\partial \bar{V}}{r\partial \theta} + \frac{\partial \bar{W}}{\partial z}$$

$$\nabla^2 = \frac{\partial^2}{\partial r^2} + \frac{\partial}{r\partial r} + \frac{\partial^2}{r^2\partial^2\theta} + \frac{\partial^2}{\partial z^2}$$

μ = Molecular viscosity

$$\left.\begin{matrix}\bar{F}_r \\ \bar{F}_\theta \\ \bar{F}_z\end{matrix}\right\} = \text{Average external forces in the radial, tangential and axial direction.}$$

The coupled non-linear system of Equations 2 - 5 is very complex and requires the addition of the energy equation if compressible flows are to be considered.

To simplify the problem we consider incompressible flow, thus decoupling the energy equation and eliminating the triple correlation functions. Also, $\bar{H}$ is now zero. In addition, we assume that the mean flow is steady, axi-symmetric and no body forces are present.

With the above simplifications and considering that the fluctuating flow satisfies the continuity equation (Reference 22, p. 19), Equations 2 - 5 reduce to:

B. INCOMPRESSIBLE FLOW

1. Continuity Equation

$$\frac{\partial \bar{W}}{\partial z} + \frac{1}{r}\frac{\partial (r\bar{U})}{\partial r} = 0 \qquad (6)$$

2. Equations of Motion

(a) Radial Component

$$\bar{U}\frac{\partial \bar{U}}{\partial r} + \bar{W}\frac{\partial \bar{U}}{\partial z} - \frac{\bar{V}^2}{r} = -\frac{1}{\rho}\frac{\partial \bar{P}}{\partial r} + \nu\left[\frac{\partial^2 \bar{U}}{\partial r^2} + \frac{1}{r}\frac{\partial \bar{U}}{\partial r}\right.$$

$$\left. + \frac{\partial^2 \bar{U}}{\partial z^2} - \frac{\bar{U}}{r^2}\right] - \left[\frac{\partial(\overline{u'w'})}{\partial z} + \frac{1}{r}\frac{\partial(\overline{ru'^2})}{\partial r} - \frac{\overline{v'^2}}{2}\right] \qquad (7)$$

(b) Tangential Component

$$\bar{W}\frac{\partial \bar{V}}{\partial z} + \bar{U}\frac{\partial \bar{V}}{\partial r} + \frac{\bar{U}\bar{V}}{r} = \nu\left[\frac{\partial^2 \bar{V}}{\partial z^2} + \frac{\partial^2 \bar{V}}{\partial r^2} + \frac{1}{r}\frac{\partial \bar{V}}{\partial r} - \frac{\bar{V}}{r^2}\right]$$

$$- \left[\frac{\partial(\overline{w'v'})}{\partial z} + \frac{\partial(\overline{u'v'})}{\partial r} + \frac{2\overline{u'v'}}{r}\right] \qquad (8)$$

(c) Axial Component

$$\bar{W}\frac{\partial \bar{W}}{\partial z} + \bar{U}\frac{\partial \bar{W}}{\partial r} = -\frac{1}{\rho}\frac{\partial \bar{P}}{\partial z} + \nu\left[\frac{\partial^2 \bar{W}}{\partial z^2} + \frac{\partial^2 \bar{W}}{\partial r^2} + \frac{1}{r}\frac{\partial \bar{W}}{\partial r}\right]$$

$$- \left[\frac{\partial}{\partial z}(\overline{w'^2}) + \frac{1}{r}\frac{\partial}{\partial r}(r\overline{w'u'})\right] \qquad (9)$$

Where ν = kinematic viscosity = $\frac{\mu}{\rho}$.

Apparently, the hydrodynamical equations for a turbulent incompressible fluid have a form similar to the original Navier-Stokes equation with constant viscosity except that additional dependent variables called Reynolds' stresses are present. These fictitious stresses characterize the turbulent friction in the field and when multiplied by the mean velocity gradients give the rate of production of turbulent energy. Hinze[1] explains the physical interpretation of these fictitious forces and discussed the energy relations in the turbulent field.

The system of Equations 6 - 9 has more dependent variables than available equations, hence additional relationships are required. Boussinesq[35] realized this problem and introduced the concept that the turbulent stresses behave like viscous stresses, i.e., they are proportional to the mean velocity gradients. He termed the proportionality factor as "eddy viscosity."

Although the existence of this idea is due largely to the analogy with laminar flow, this property of the turbulent fluid is not like molecular viscosity nor are they related as discussed earlier. One may therefore raise a serious objection to the whole scheme. In support, Hinze (1,p.22) commented: "There is nothing against the formal introduction of the term 'eddy viscosity' if we are fully aware of its specific office, namely to express the behavior of the turbulent stresses in terms of the mean velocity gradients in a flowing fluid."

The mathematical nature of the eddy viscosity is not yet generally ascertained. Stanisic and Groves[36] argued that although it transforms

properly when assumed to be a second order tensor, it is not sufficiently general to assure the existence of six linearly independent Reynolds' stresses. They hinted the possibility that it is a fourth order tensor.

To account for the different values in different directions, there were suggestions that the eddy viscosity be treated as a vector.[37] This is permissible provided the assumption that the Reynolds' stresses are proportional to the mean deformation tensor is not used in the analysis. The expression of the turbulence stresses in terms of the velocity gradients has to be ascertained by some other means (for example, with the aid of phenomenological theories).

If the eddy viscosity is to be treated as a scalar, the average turbulence pressure from the turbulent stresses must be taken as a separate term in the formulation expressing the turbulence stress tensor in terms of the mean deformation tensor. In this way, the two sides of the equation become identically zero for an incompressible fluid (Reference 1, p.21).

In this investigation, the eddy viscosity function was derived with the use of Karman's similarity hypothesis. It was found that for swirling flow, eddy viscosity exists at two perpendicular planes of a fluid element (see Figure 12), due to the presence of mean velocity gradients perpendicular to such planes. Assuming that the similarity conditions are simultaneously satisfied at every point in the field and treating the eddy viscosity as a vector, a resultant expression was obtained. The evaluation of the similarity constant was based on Kinney's[31] investigation. (A detailed discussion is given in Chapter VII.)

III. PHENOMENOLOGICAL THEORIES

Three elementary theories are commonly used to describe the turbulent flow mechanism, namely:

1) Prandtl's Momentum Transport Theory

2) Taylor's Vorticity Transport Theory

3) von Karman's Similarity Theory

Each of these theories are based on assumptions that are not general in application so that it is possible that one may apply in one case or in a part of the flow field while the others do not. Schlichting[4] gives a good introductory account of these theories.

The above-mentioned theories use the concept of a "mixing length" which is that characteristic distance over which an agglomeration of fluid particles is considered to preserve a transferable property. After traversing this distance the fluid particles mix with the new surrounding fluid. The fluctuation of the transferable property is related to the difference between the value of this property at the two different lamina separated by this length. In a manner, this concept of the mixing length is somewhat analogous with the mean free path in the kinetic theory of gases. The difference is that the latter concerns itself with the microscopic motion of individual molecules strictly obeying the conditions assumed, while the former deals with the macroscopic motion of a lump of fluid particles that may undergo continuous changes due to external and viscous effects. The assumptions made are, therefore, only approximately fulfilled.

Von Karman's Similarity Theory considers the mixing length to be a length scale of the turbulence mechanism. It advocates that the turbulent flow patterns at different points in the immediate neighborhood of the reference point are similar and differ only in the scales of length and velocity. With this concept, the mixing length is considered to be independent of the magnitude of velocity and is only a function of the velocity gradients as well as of the higher order derivatives.

For parallel flows in pipes and channels, Prandtl assumed the mixing length to be proportional to the distance from the wall.[14] In this case the length is related to the path of the fluid element and is therefore a "Lagrangian length." Karman's length is an "Eulerian length" since it is considered to be a length scale in the flow field.

Prandtl's and Karman's formulation of the mixing length can be used in conjunction with either momentum or vorticity transport theory. Goldstein[5] investigated the validity of Karman's mixing length function to parallel flow in pipes and channels using both momentum and vorticity transport theories in each case. He found that for turbulent parallel pipe flows the predicted velocity distribution using the vorticity transport theory's formulation for the shearing stress agreed well with the experimental results of Stanton and Nikuradse as shown in Figure 2, where W_m = maximum velocity, W_* = friction velocity (wall shear stress/ρ)$^{1/2}$, and W = local velocity. The figure shows a comparison of theoretically predicted and experimentally measured velocity profile for turbulent parallel flow in pipes after S. Goldstein.[5] The velocity distribution was

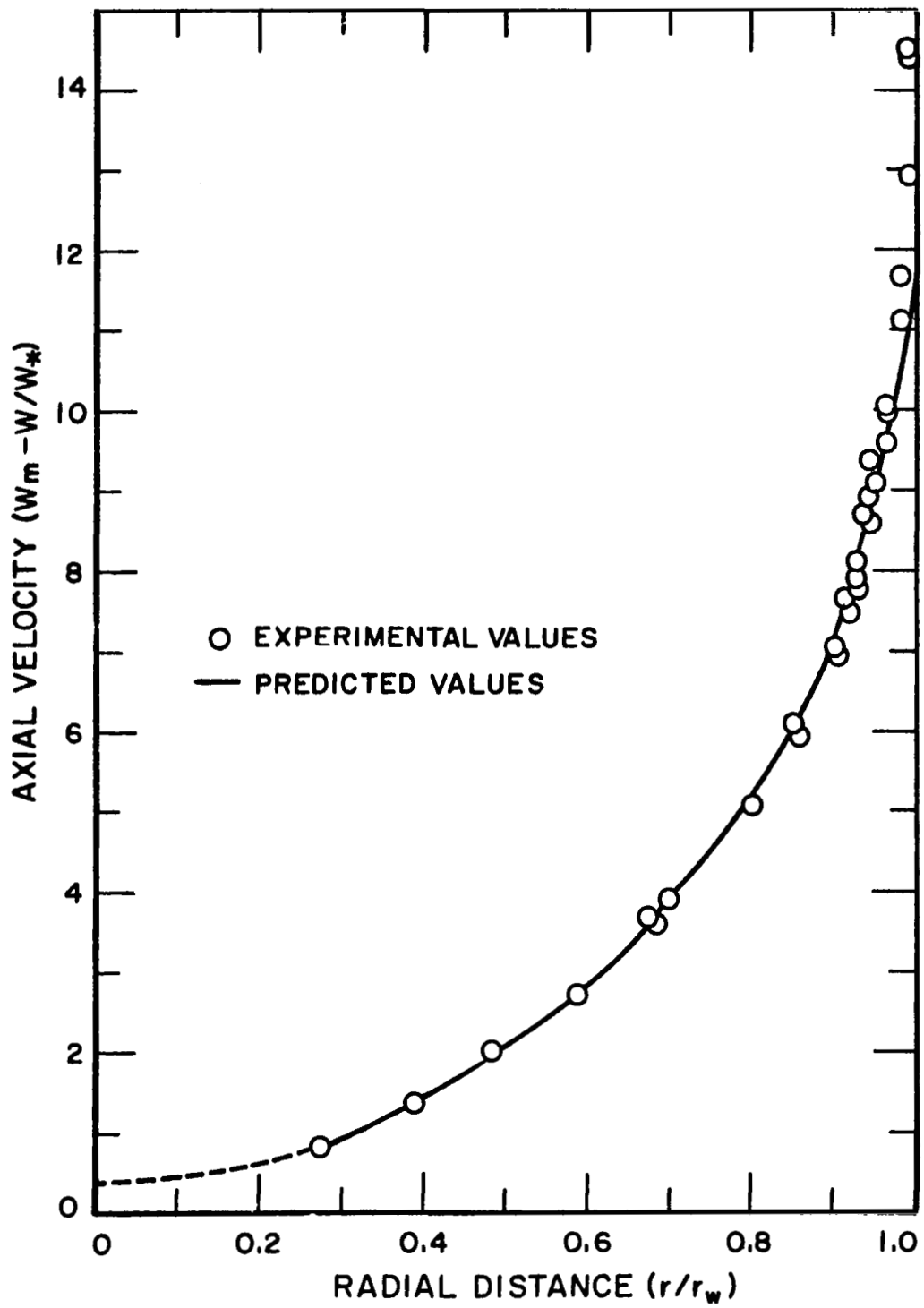

FIGURE 2. PREDICTED AXIAL VELOCITY PROFILE IN PIPES AFTER GOLDSTEIN [5] USING VORTICITY TRANSPORT AS WELL AS SIMILARITY THEORY.

obtained using Taylor's vorticity transport theory as well as the mixing length expression derived from Karman's similarity theory.

For turbulent channel flow, the velocity distribution predicted by the momentum transport theory agrees with experiment better than that using the vorticity transport theory.

G. I. Taylor[6] made a similar investigation for turbulent parallel pipe and channel flows using his theory as well as Prandtl's momentum transport theory. He took Prandtl's expression of the mixing length and his results show that for turbulent parallel pipe flow, the velocity distribution predicted by his theory agrees with experimental data better than that predicted by the other theory. The agreement is shown in Figure 3 where the notations are the same as those in Figure 2. For turbulent channel flow, there is nothing to choose between the results of the two theories since the disagreement with experimental data are the same for both.

Based on the above results it appears that Taylor's vorticity transport theory gives good results for pipe flows. This is due to the fact that for a two-dimensional flow the transport of vorticity in unimpeded in the flow field. This can be seen from the vorticity equation which for conservative forces takes the form:

$$\frac{\partial \underline{\Omega}}{\partial t} + (\underline{V} \cdot \nabla)\underline{\Omega} - (\underline{\Omega} \cdot \nabla)\underline{V} - \nu \nabla^2 \underline{\Omega} = 0 \qquad (10)$$

where: $\underline{V}$ = the instantaneous velocity vector

$\underline{\Omega}$ = the instantaneous vorticity vector

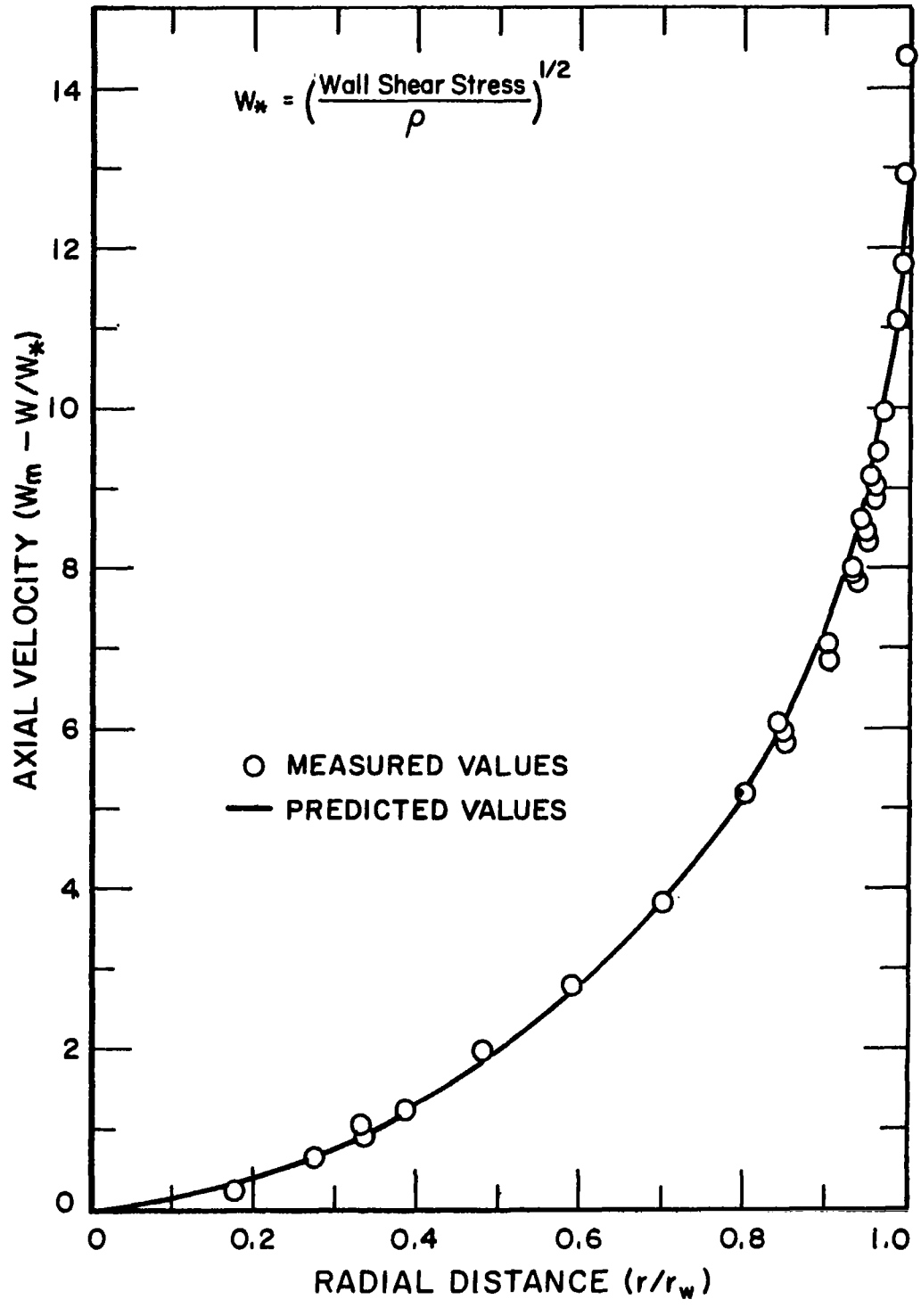

FIGURE 3. PREDICTED AXIAL VELOCITY PROFILE IN PIPES AFTER TAYLOR [6] USING VORTICITY TRANSPORT AND PRANDTL'S MIXING LENGTH ASSUMPTION.

In a cylindrical geometry with axisymmetric flow, the term $(\underline{\Omega} \cdot \nabla)\ \underline{V}$, which represents the "rate of change of vorticity when the vortex line moves with the fluid and the strength of the vortices remain constant",[3] vanishes and the remaining terms result in a diffusion-like equation. In pipe flow unlike channel flow, the secondary flows present are not large enough to destroy the two-dimensionality concept. Hence the fundamental assumption of the vorticity transport theory is essentially fulfilled in pipe flows.

In 1935, Taylor[7] applied his theory in a modified form to turbulent flow between concentric rotating cylinders (see Chapter V). When the inner cylinder is rotating while the outer one is fixed he experimentally verified that in over 83% of the annular space between the cylinders the flow is definitely of the type predicted by his modified vorticity transport theory. The remaining space near the inner and outer cylinders has a flow of the type predicted by the momentum transport theory. This result is shown in Figure 4 where the constancy of the angular momentum (as predicted by the vorticity transport theory) prevails in a large region of the flow. Wattendorf,[11] in his experiments on turbulent flows in curved channels and rotating cylinders, also made similar observations.

The above mentioned results suggest that Taylor's vorticity transport theory should be applicable for investigating turbulent swirling flow in pipes. However, in order to surmount the mathematical difficulties involved, additional assumptions will be made. Furthermore, as the theory does not yield a mathematical formulation of the mixing length parameter, von Karman's similarity theory for turbulent motion will be used to achieve this end.

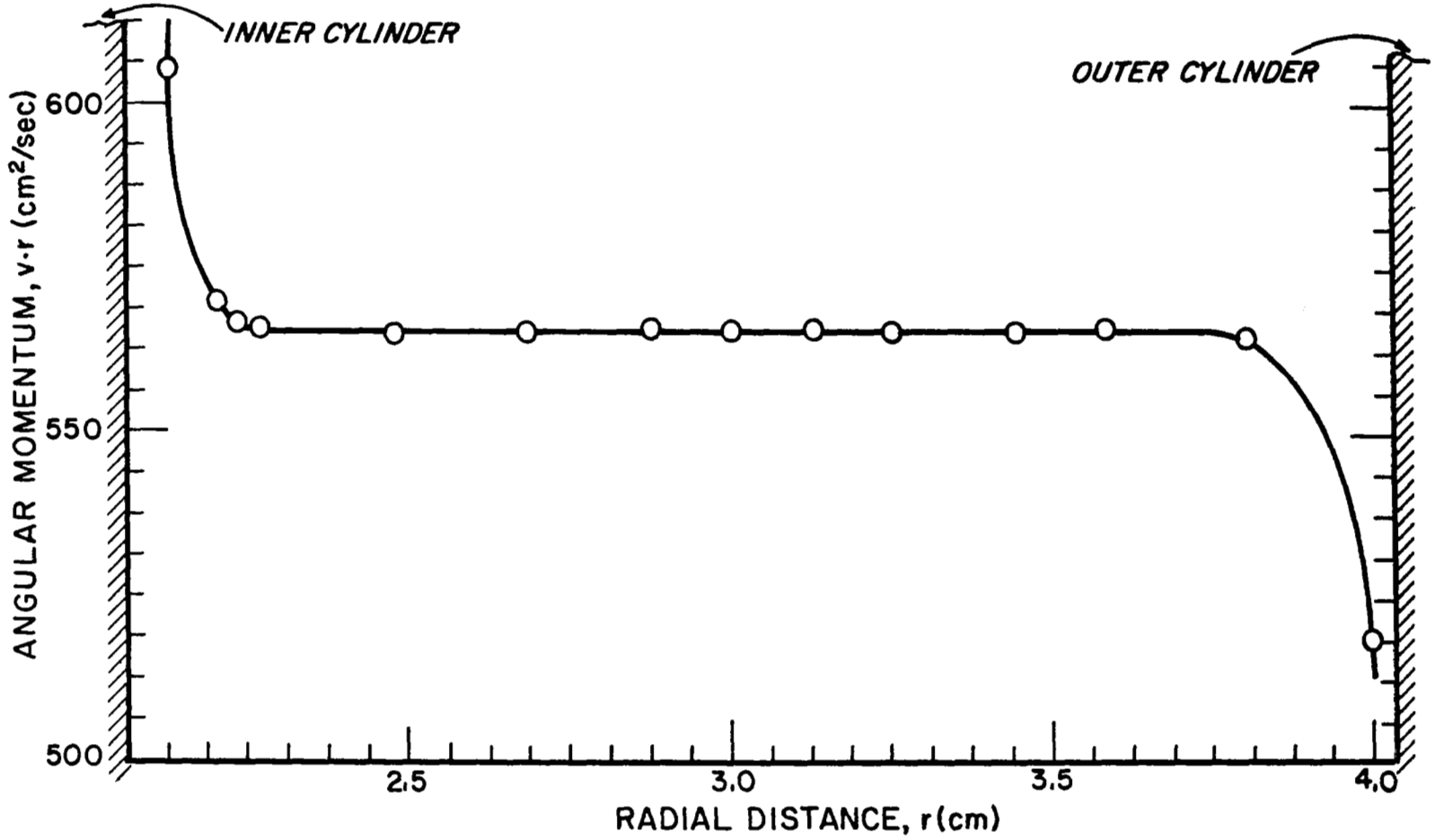

FIGURE 4. DISTRIBUTION OF ANGULAR MOMENTUM IN THE ANNULAR SPACE BETWEEN TWO CONCENTRIC CYLINDERS (INNER CYLINDER ROTATING) AFTER G. I. TAYLOR[7].

IV. FORMULATION OF THE INCOMPRESSIBLE TURBULENT FLOW EQUATIONS OF MOTION USING THE VORTICITY TRANSPORT THEORY

The equations of motion for an incompressible fluid with constant viscosity are:

$$\frac{\partial \underline{V}}{\partial t} + (\underline{V} \cdot \nabla)\underline{V} = \frac{1}{\rho}\left[-\nabla P + \underline{F} + \mu\nabla^2\underline{V}\right] \tag{11}$$

where $\underline{V}$ = velocity vector

P = pressure

$\underline{F}$ = body force vector

ρ = density

t = time

μ = molecular viscosity

Since

$$(\underline{V} \cdot \nabla)\underline{V} = \nabla\left(\frac{\underline{V}^2}{2}\right) - \underline{V} \times (\nabla \times \underline{V})$$

and defining

$$\nabla \times \underline{V} = \underline{\Omega} \text{ which is the vorticity vector,} \tag{11-a}$$

Equation 11 can be written as:

$$\frac{\partial \underline{V}}{\partial t} + \nabla\left(\frac{\underline{V}^2}{2}\right) - \underline{V} \times \underline{\Omega} = \frac{1}{\rho}\left[-\nabla P + \underline{F} + \mu\nabla^2\underline{V}\right] \tag{12}$$

The vorticity transport theory assumes that: 1) the molecular viscosity is negligible compared to the eddy viscosity of the turbulent fluid; 2) the mean flow is steady and axisymmetric, and 3) body forces are negligible. The instantaneous quantities are replaced by

$$\begin{aligned} \underline{V} &= \overline{\underline{V}} + \underline{v}' \\ \underline{\Omega} &= \overline{\underline{\Omega}} + \underline{\Omega}' \\ P &= \overline{P} + p' \end{aligned} \tag{13}$$

where bars denote mean values and primes denote fluctuating components.

With the above assumptions and substituting the turbulent instantaneous quantities (Equation 13) in Equation 12, and taking averages, one obtains:

$$\nabla\left(\frac{\underline{V}^2}{2}\right) - \overline{\underline{V}} \times \overline{\underline{\Omega}} = -\nabla\left(\frac{\overline{P}}{\rho} + \frac{\overline{v}'^2}{2}\right) + \overline{\underline{v}' \times \underline{\Omega}'} \tag{14}$$

In this equation the Reynolds stresses are represented in terms of the average vector product of the fluctuating velocity and vorticity vectors.

At this point we introduce the concept of the vorticity transport theory which considers that a fluid element moves a distance $\underline{L}$ (the mixing length) conserving its vorticity and after traversing this distance, the lump of fluid mixes with the new environment. Assuming $\underline{L}$ as well as its space derivative to be very small so that we can neglect its squares as well as terms quadratic in the L's and their space derivatives, an

expression for the fluctuating vorticity vector, $\underline{\Omega}'$, can be derived in terms of the mixing length and the mean vorticity vector. If we employ the lagrangian continuity expression and Cauchy's equation for expressing the vorticity at any point in terms of its vorticity at some previous position, it can be shown that (see Appendix I)

$$\underline{\Omega}' = \nabla \times (\underline{L} \times \overline{\underline{\Omega}}) \tag{15}$$

where $\underline{L}$ = mixing length vector with components (L_r, L_θ, L_z). Substituting Equation 15 into 14, we have:

$$\nabla\left(\frac{\overline{V}^2}{2}\right) - \overline{\underline{V}} \times \overline{\underline{\Omega}} = -\nabla\left(\frac{\overline{P}}{\rho} + \frac{\overline{v}'^2}{2}\right) + \overline{\underline{v}' \times \nabla \times (\underline{L} \times \overline{\underline{\Omega}})} \tag{16}$$

Equation 16 will next be expressed in cylindrical polar coordinates where the bar sign is dropped from the mean flow variables for convenience. The resulting scalar equations are:

Radial Component:

$$U\frac{\partial U}{\partial r} + W\frac{\partial U}{\partial r} - \frac{V^2}{r} = -\frac{\partial Q}{\partial r} + \xi\cdot\frac{\overline{v'\partial L_z}}{\partial r} + \eta\cdot\frac{\overline{v'\partial L_z}}{r\partial\theta}$$

$$+ \zeta\frac{\overline{v'\partial L_z}}{\partial z} - \overline{v'L_r}\cdot\frac{\partial\zeta}{\partial r} - \overline{v'L_\theta}\frac{\partial\zeta}{r\partial\theta} - \overline{v'L_z}\frac{\partial\zeta}{\partial z} - \xi\cdot\frac{\overline{w'\partial L_\theta}}{\partial r}$$

$$- \eta\left[\frac{\overline{w'\partial L_\theta}}{r\partial\theta} + \frac{\overline{w'L_r}}{r}\right] - \zeta\cdot\frac{\overline{w'\partial L_\theta}}{\partial z} + \overline{w'L_r}\frac{\partial\eta}{\partial r} + \overline{w'L_\theta}\left[\frac{\partial\eta}{r\partial\theta}\right.$$

$$\left. + \frac{\xi}{r}\right] + \overline{w'L_z}\frac{\partial\eta}{\partial z} . \qquad (17)$$

Tangential Component:

$$U\frac{\partial V}{\partial r} + W\frac{\partial V}{\partial z} + \frac{UV}{r} = \frac{\overline{w'\partial L_r}}{\partial r}\cdot\xi + \frac{\overline{w'\partial L_r}}{r\partial\theta}\cdot\eta + \frac{\overline{w'\partial L_r}}{\partial z}\cdot\zeta$$

$$- \overline{w'L_r}\frac{\partial\xi}{\partial r} - \overline{w'L_\theta}\frac{\partial\xi}{r\partial\theta} - \overline{w'L_z}\frac{\partial\xi}{\partial z} - \frac{\overline{u'\partial L_z}}{\partial r}\cdot\xi - \frac{\overline{u'\partial L_z}}{r\partial\theta}\cdot\eta$$

$$- \frac{\overline{u'\partial L_z}}{\partial z}\cdot\zeta + \overline{u'L_r}\frac{\partial\zeta}{\partial r} + \overline{u'L_\theta}\frac{\partial\zeta}{r\partial\theta} + \overline{u'L_z}\frac{\partial\zeta}{\partial z} \qquad (18)$$

Axial Component:

$$U\frac{\partial W}{\partial r} + W\frac{\partial W}{\partial z} = -\frac{\partial Q}{\partial z} + \frac{\overline{u'\partial L_\theta}}{\partial r}\cdot\xi + \eta\left[\frac{\overline{u'\partial L_\theta}}{r\partial\theta} + \frac{\overline{u'L_r}}{r}\right]$$

$$+ \frac{\overline{u'\partial L_\theta}}{\partial z}\cdot\zeta - \overline{u'L_r}\frac{\partial\eta}{\partial r} - \overline{u'L_\theta}\left[\frac{\partial\eta}{r\partial\theta} + \frac{\xi}{r}\right] - \overline{u'L_z}\frac{\partial\eta}{\partial z}$$

$$- \frac{\overline{v'\partial L_r}}{\partial r}\cdot\xi - \frac{\overline{v'\partial L_r}}{r\partial\theta}\cdot\eta - \frac{\overline{v'\partial L_r}}{\partial z}\cdot\zeta + \overline{v'L_r}\frac{\partial\xi}{\partial r}$$

$$+ \overline{v'L_\theta}\frac{\partial\xi}{r\partial\theta} + \overline{v'L_z}\frac{\partial\xi}{\partial z} \qquad (19)$$

where $Q = \frac{P}{\rho} + \frac{\overline{v'}^2}{2}$ and the vorticity components (Equation 11-a) in cylindrical coordinates are:

$$\xi = \frac{1}{r}\frac{\partial W}{\partial\theta} - \frac{\partial V}{\partial z}$$

$$\eta = \frac{\partial U}{\partial z} - \frac{\partial W}{\partial r} \qquad (20)$$

$$\zeta = \frac{1}{r}\left[\frac{\partial}{\partial r}(rV) - \frac{\partial U}{\partial\theta}\right]$$

Equations 17, 18 and 19, that are extremely complicated, can be simplified by applying Taylor's modified concept of his theory.[6],[7] A lump of fluid is conceived to leave a certain position with the local components of vorticity of the mean flow, and to retain these components till it mixes with its surroundings after traversing the mixing length. If this condition is substituted into the mathematical formulation of the process (see Appendix II) it follows that

$$\underline{L} = \text{constant} \tag{21}$$

If we further assume that the axisymmetric condition also holds for the fluctuating flow, the equations of motion reduce to:

Radial Component:

$$U\frac{\partial U}{\partial r} + W\frac{\partial U}{\partial z} - \frac{V^2}{r} = -\frac{\partial Q}{\partial r} - \overline{v'L_r}\frac{\partial \zeta}{\partial r} - \overline{v'L_z}\frac{\partial \zeta}{\partial z}$$

$$- \eta\frac{\overline{w'L_r}}{r} + \overline{w'L_r}\frac{\partial \eta}{\partial r} + \frac{\overline{w'L_\theta}}{r}\cdot\zeta + \overline{w'L_z}\frac{\partial \eta}{\partial z} \tag{22}$$

Tangential Component:

$$U\frac{\partial V}{\partial r} + W\frac{\partial V}{\partial z} + \frac{UV}{r} = -\overline{w'L_r}\frac{\partial \zeta}{\partial r} - \overline{w'L_z}\frac{\partial \zeta}{\partial z} + \overline{u'L_r}\frac{\partial \zeta}{\partial r}$$

$$+ \overline{u'L_z}\frac{\partial \zeta}{\partial z} \tag{23}$$

Axial Component:

$$U\frac{\partial W}{\partial r} + W\frac{\partial W}{\partial z} = -\frac{\partial Q}{\partial z} + \eta\cdot\frac{\overline{u'L_r}}{r} - \overline{u'L_r}\frac{\partial \eta}{\partial r} - \overline{u'L_\theta}\cdot\frac{\xi}{r}$$

$$- \overline{u'L_z}\frac{\partial \eta}{\partial z} + \overline{v'L_r}\frac{\partial \xi}{\partial r} + \overline{v'L_z}\frac{\partial \xi}{\partial z} \qquad (24)$$

The terms $\overline{u_i'L_j}$, i.e., the turbulent transport coefficients that appear in the system of Equations 22 to 24 will now be considered. Taylor, in his application of the theory to parallel pipe flow assumed the turbulent transport coefficients to be isotropic, and we will make the same assumption here. Expressed mathematically,

$$\overline{u_i'L_j} = 0 \quad \text{if} \quad i \neq j$$

$$= e_{m(i)} \quad \text{if} \quad i = j. \qquad (25)$$

where e_m is the kinematic eddy viscosity and i, j = r, θ, z.

In the following chapter, Equations 22 to 25 will be applied to different turbulent flow problems in order to check their validity. It will be seen that the resulting equations are the same governing equations that past investigators considered in the particular cases.

V. APPLICATIONS OF THE DERIVED TURBULENT FLOW EQUATIONS

CASE A: PARALLEL FLOW IN PIPES (FULLY DEVELOPED)

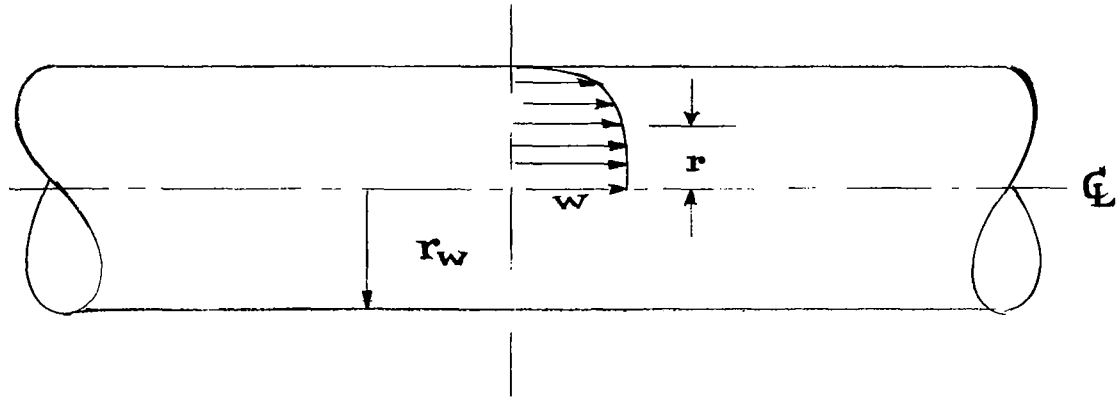

Figure 5: Flow Geometry for Case A

In this case the only mean velocity present is in the axial direction. From the continuity equation, 6, it follows that:

$$W = W(r) \quad \text{only}$$

so that by Equation 20 the mean vorticity components are:

$$\xi = 0 \qquad \eta = -\frac{dW}{dr} \qquad \zeta = 0$$

Due to the assumption that the transport coefficients are isotropic:

$$\overline{u'L_\theta} = \overline{u'L_z} = \overline{v'L_r} = \overline{v'L_z} = 0$$

and the axial component of the equation of motion (Equation 24) reduces to:

$$\frac{d}{dz}\left(\frac{P}{\rho} + \frac{\overline{v'}^2}{2}\right) = \overline{u'L_r}\left(\frac{d^2W}{dr^2} - \frac{dW}{rdr}\right) \qquad (26)$$

The term $\overline{u'L_r}$ is the kinematic eddy viscosity, e_m, which can be written as:

$$e_m = \overline{u'L_r} = -\frac{L^2 dW}{dr} \quad \text{(see Reference 5)}$$

and since the flow is fully developed, $\frac{d}{dz}\left(\frac{\overline{v'}^2}{2}\right) = 0.$

Equation 26 becomes:

$$-\frac{1}{\rho}\frac{dP}{dz} = L^2 \frac{dW}{dr}\left(\frac{d^2W}{dr^2} - \frac{dW}{rdr}\right) \qquad (27)$$

S. Goldstein[5] solved the above equation using Karman's similarity theory's formulation of the mixing length, L, (taken equal to the length scale in the turbulent field) which for parallel pipe flow is:

$$L = \text{Const} \frac{\frac{dW}{dr}}{\frac{d^2W}{dr^2} - \frac{dW}{rdr}}$$

He solved Equation 27 using the boundary condition $\frac{dW}{dr} = \infty$ at $r = r_w$ to evaluate one of the two constants of integration. The remaining constant was evaluated by the use of the experimental data of Stanton and Nikuradse.

Figure 2 shows Goldstein's results compared with experimental data. The agreement is very good indeed.

Taylor[6] solved the above problem but his mathematical formulation does not assume axisymmetry to hold for the fluctuating flow. He obtained a positive sign in the right hand term of Equation 27. Using Prandtl's assumption for the mixing length, he integrated the equation and his results are shown in Figure 3. It can be observed that the agreement between theory and experiment is also good here.

CASE B: FLOW BETWEEN ROTATING CONCENTRIC CYLINDERS

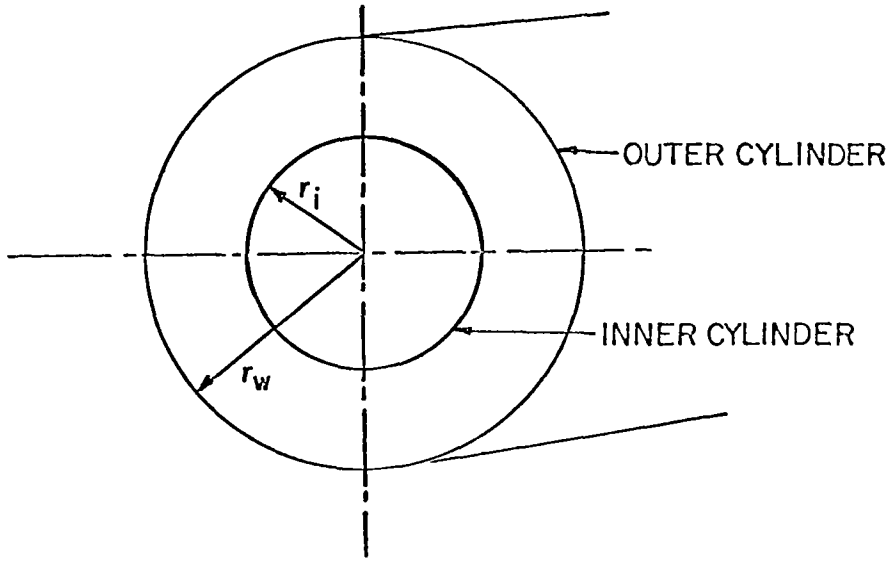

Figure 6: Flow Geometry for Case B

This problem had been considered theoretically and experimentally by G. I. Taylor[7] using the same theory for his theoretical predictions.

If the cylinders are sufficiently long and their ends are closed there is no net axial flow and end effects may be neglected. Hence

$$W = 0.$$

From the continuity equation:

$$\frac{d}{dr}(rU) = 0$$

and upon integration

$$U = \text{Constant}/r \tag{28}$$

With the inner cylinder rotating while the outer one is at rest, the following boundary condition applies:

$$U = 0 \quad \text{at} \quad r = r_w$$

Upon substitution in Equation 28, it follows that

$$\text{Constant} = 0.$$

It can be seen that only the tangential component of the mean flow is present. With $V = V(r)$, the mean vorticity components are:

$$\xi = 0, \qquad \eta = 0, \qquad \zeta = \frac{dV}{dr} + \frac{V}{r} \tag{29}$$

Substituting Equation 29 into 22, 23 and 24 with the assumption of isotropic transport coefficients, the equations of motion are:

1. Tangential Component

$$0 = \overline{u'L_r} \frac{d(\zeta)}{dr} \tag{30}$$

2. Radial Component

$$\frac{d\left(\frac{P}{\rho} + \frac{\overline{v'}^2}{2}\right)}{dr} = \frac{V^2}{r} \tag{31}$$

In Equation (30), $\overline{u'L_r}$ cannot be zero. Therefore,

$$\frac{d(\zeta)}{dr} = 0.$$

Upon integration

$$\zeta = C_1 \qquad \text{or}$$

$$\frac{d(rV)}{rdr} = C_1 \tag{32}$$

Further integration of Equation 32 gives:

$$V = C_1 r + \frac{C_2}{r} \tag{33}$$

Taylor performed an experiment to check the above theoretical predictions. He found that for the case where the inner cylinder is rotating and the outer cylinder is at rest, the angular momentum (rV) is practically constant in the central portion (83% of the annular space between the cylinders) of the flow field. In this region, he concluded that the flow is definitely of the type predicted by his theory because of the fact that it obeys Equation 32, provided C_1 must be equal to zero. The experiment further showed that the theory is not valid near the walls so that the usual no-slip condition will not apply in the mathematics of the theory.

CASE C: FLOW ANALYSIS OF THE TURBULENT VORTEX TUBE

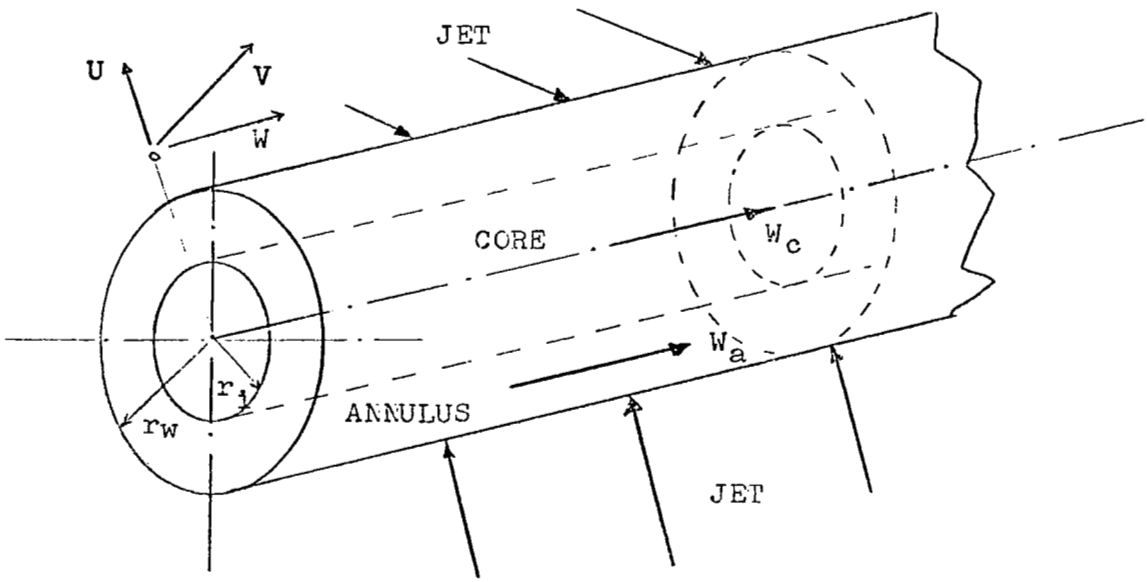

Figure 7: Flow Configuration of the Problem

This problem had been studied intensively by Deissler and Perlmutter[17] where they divided the vortex configuration into two parts, namely the core and the annulus. In a vortex tube the vortex is usually generated by jets injected at the periphery of the outer cylinder. Following their assumption that $V = V(r)$ and that the mean flow is axisymmetric, the mean vorticity components in the radial and axial directions are:

$$\xi = 0$$

$$\zeta = \frac{d(rV)}{rdr} = \frac{dV}{dr} + \frac{V}{r} .$$

When the mean vorticity values are substituted into Equation 23, we obtain the tangential component of the equation of motion for this particular case which is:

$$\frac{UdV}{dr} + \frac{UV}{r} = \overline{u'L_r}\left(\frac{d^2V}{dr^2} + \frac{dV}{rdr} - \frac{V}{r^2} \right) \tag{34}$$

Multiplying both sides of the equation by the density and recalling that $\overline{u'L_r} = e_m$, the kinematic eddy viscosity, we obtain

$$\rho\left(\frac{UdV}{dr} + \frac{UV}{r} \right) = \rho e_m \left(\frac{d^2V}{dr^2} + \frac{dV}{rdr} - \frac{V}{r^2} \right) \tag{35}$$

Equation 35 is the governing equation considered by Deissler and Perlmutter in their investigation. Furthermore, they considered ρe_m a constant. Their

theoretical results agree reasonably well with the experimental data obtained by Hartnett and Eckert.[7]

It appears that the equations of motion for turbulent flow derived by the vorticity transport theory are sufficiently general. An attempt will now be made to apply these equations to the study of turbulent swirling flow.

VI. GOVERNING EQUATIONS FOR AN INCOMPRESSIBLE SWIRLING FLOW

In axisymmetric swirling flows, all the three mean velocity components are present and they are functions of r and z. The mean vorticity components are:

$$\xi = -\frac{\partial V}{\partial z}$$

$$\eta = \frac{\partial U}{\partial z} - \frac{\partial W}{\partial r} \tag{36}$$

$$\zeta = \frac{1}{r}\frac{\partial}{\partial r}(rV)$$

Making the usual assumption of isotropic transport coefficients, and substituting Equation 36 into Equations 22, 23 and 24, the equations of motion for turbulent swirling flow are obtained.

1. Radial Component

$$U\frac{\partial U}{\partial r} + W\frac{\partial U}{\partial z} - \frac{V^2}{r} = -\frac{\partial Q}{\partial r} + e_{m(r)}\left(\frac{\partial^2 U}{\partial z^2} - \frac{\partial^2 W}{\partial r \partial z}\right) \tag{37}$$

2. Tangential Component

$$U\frac{\partial V}{\partial r} + W\frac{\partial V}{\partial z} + \frac{UV}{r} = e_{m(\theta)}\left(\frac{\partial^2 V}{\partial r^2} + \frac{1}{r}\frac{\partial V}{\partial r} - \frac{V}{r^2} + \frac{\partial^2 V}{\partial z^2}\right) \tag{38}$$

3. Axial Component

$$U\frac{\partial W}{\partial r} + W\frac{\partial W}{\partial z} = -\frac{\partial Q}{\partial z} + e_{m(z)}\left(\frac{\partial^2 W}{\partial r^2} - \frac{1}{r}\frac{\partial W}{\partial r} - \frac{\partial^2 U}{\partial r \partial z} + \frac{1}{r}\frac{\partial U}{\partial z} \right) \tag{39}$$

Where:

$$Q = \frac{P}{\rho} + \frac{\overline{V'}^2}{2}$$

$$\underline{v}' = (u', v', w')$$

$e_{m(r)}, e_{m(\theta)}, e_{m(z)}$ = the kinematic eddy viscosity in the radial, tangential and axial directions.

In the above equations (as in previous derivations) the molecular viscosity was neglected according to the first assumption of the vorticity transport theory. This assumption is, however, not valid in regions where molecular viscosity is an important feature of the flow, i.e., regions near a solid boundary. Since it is desired to include such regions in the present investigation, the equation of motion will be modified.

If we compare the tangential component of the mean turbulent Navier-Stokes equation (Equation 8) with Equation 38, we note that the turbulent

stresses behave in a manner similar to the laminar stresses where the eddy viscosity replaces the molecular viscosity. This shows that for the tangential component of the motion equation, the fictitious "laminar flow" concept of turbulent motion gives a one to one correspondence with an incompressible laminar flow. This fact has been pointed out first by Einstein and Li.[16]

Since the tangential component of the above turbulent flow equations has been derived independent of the assumption that the shearing stress is proportional to the deformation tensor, there is no restriction as to the nature of the eddy viscosity. Comparison with the same component of the laminar Navier-Stokes equation suggests that a turbulent flow with constant eddy viscosity behaves like a laminar flow. However, in turbulent swirling flow, the eddy viscosity may be a strong function of the flow field, and in this investigation the function form will be evaluated using von Karman's similarity theory.

The above arguments serve to justify the common concept that if it is desired to include the molecular diffusion in the turbulent equations, the eddy and molecular viscosities are additive.

The tangential component of the equation of motion considering molecular diffusion can therefore be written as:

$$U\frac{\partial V}{\partial r} + W\frac{\partial V}{\partial z} + \frac{UV}{r} = (\nu + e_{m(\theta)})\left(\frac{\partial^2 V}{\partial r^2} + \frac{1}{r}\frac{\partial V}{\partial r} - \frac{V}{r^2} + \frac{\partial^2 V}{\partial z^2}\right) \tag{40}$$

Turbulence near a solid boundary is suppressed and the flow tends to become laminar. Ths usual no-slip condition at the wall can now be applied in the integration of the above equation. However we will first non-dimensionalize the equations and perform an order of magnitude analysis.

Let

$$U = U^{*}U_{o}$$

$$W = W^{*}W_{o}$$

$$V = V^{*}V_{o}$$

$$r = r^{*}r_{o}$$

$$z = z^{*}z_{o}$$

where all values with asterisks are dimensionless and of order unity and those with subscript o are reference quantities. In swirling flow, the axial and tangential velocities are in general prevalent so that:

$$W_{o} = O(1)$$

$$V_{o} = O(1)$$

In considering the axial change of W, we note that the axial velocity profile changes only slightly over axial distances since the average value of the axial velocity is a constant. Therefore, with

$$r_{o} = O(1)$$

$$z_{o} = O\left(\frac{1}{\epsilon}\right)$$

where

$$\epsilon << 1,$$

$$\frac{\partial W}{\partial z} = \left(\frac{W_o}{z_o} \right) \left(\frac{\partial W^*}{\partial z^*} \right)$$

$$0(\epsilon) \qquad 0(1)$$

$$= 0(\epsilon) \tag{41}$$

Equation 41 shows that W is a weak function of z so that:

$$\frac{\partial W}{\partial r} >> \frac{\partial W}{\partial z} \tag{42}$$

To determine the order of magnitude of U, we consider the continuity equation:

$$\frac{\partial W}{\partial z} + \frac{1}{r} \frac{\partial}{\partial r} (rU) = 0$$

Integrating this equation and using the boundary condition,

$U = 0$ at $r = 0$, we have:

$$U = - \frac{W_o r_o}{z_o} \frac{1}{r^*} \int_0^{r^*} \frac{\partial W^*}{\partial z^*} \, r^* \, dr^*$$

$$0(\epsilon) \qquad 0(1)$$

Hence,

$$U_o = O(\epsilon) \quad \text{so that:}$$

$$U << W$$

$$U << V \tag{44}$$

Next we compare the change of V with respect to z to that of W with respect to z. In swirling flow, the tangential velocity decreases uniformly to zero whereas the axial velocity is unchanged on the average. It is therefore believed that the term $\frac{\partial V}{\partial z}$ is more important than $\frac{\partial W}{\partial z}$ in the tangential component of the equation of motion. This opinion is also shared by Kreith and Sonju[21] who have neglected $\frac{\partial W}{\partial z}$ in their swirling flow analysis.

Applying the same order of magnitude analysis to all the equations of motion and neglecting terms of order ϵ we have:

1. Radial Component

$$\frac{\partial}{\partial r}\left(\frac{P}{\rho} + \frac{\overline{v'}^2}{2}\right) = \frac{V^2}{r} \tag{45}$$

2. Tangential Component

$$W\frac{\partial V}{\partial z} = (\nu + e_{m(\theta)})\left(\frac{\partial^2 V}{\partial z^2} + \frac{\partial^2 V}{\partial r^2} + \frac{1}{r}\frac{\partial V}{\partial r} - \frac{V}{r^2}\right) \tag{46}$$

3. Axial Component

$$\frac{\partial}{\partial z}\left(\frac{P}{\rho} + \frac{\overline{v'}^2}{2}\right) = (e_{m(z)} + \nu)\left(\frac{\partial^2 W}{\partial r^2} - \frac{1}{r}\frac{\partial W}{\partial r}\right) \qquad (47)$$

Equation (46), also known as the "swirl equation," will be used to predict the decay of angular momentum in the axial direction. The axial velocity W will be considered as a function of r only and its average profile will be evaluated from experimental measurements at different downstream positions.

The swirl equation is non-dimensionalized as follows:

$$W = W_m W^* \qquad V = W_m V^*$$

$$r = r_w r^* \qquad z = r_w z^*$$

$$e_{m(\theta)} = \nu e_m^{*}(\theta)$$

where:

W_m = Maximum axial velocity of the fully developed profile

r_w = pipe radius

ν = Kinematic molecular viscosity

Effecting the transformation, the dimensionless swirl equation is:

$$W^* \frac{\partial V^*}{\partial z^*} = \frac{(1 + e_{m(\theta)})}{N_{Re}} \left(\frac{\partial^2 V^*}{\partial r^{*2}} + \frac{\partial V^*}{r^* \partial r^*} - \frac{V^*}{r^{*2}} + \frac{\partial^2 V^*}{\partial z^{*2}} \right) \tag{48}$$

with $N_{Re} = \frac{W_m r_w}{\nu}$, the axial Reynold's Number. The asterisks can be omitted in the above equation with a convention that all variables are dimensionless.

In the present investigation, it is necessary to go as far as 100 radii downstream. Taking this as a reference value for z, we note that $\frac{\partial V}{\partial z}$ is of order 1/100 and $\frac{\partial^2 V}{\partial z^2}$ of the order 1/10000. The latter is small enough that it can be neglected in the present investigation. Furthermore, Kreith and Sonju[10] pointed out that in turbulent flow, one can safely assume the term $e_{m(\theta)} \frac{\partial^2 V}{\partial z^2}$ to be negligible compared with $W \frac{\partial V}{\partial z}$. Thus, the swirl equation finally becomes

$$W \frac{\partial V}{\partial z} = \frac{(1 + e_{m(\theta)})}{N_{Re}} \left(\frac{\partial^2 V}{\partial r^2} + \frac{1}{r} \frac{\partial V}{\partial r} - \frac{V}{r^2} \right) \tag{49}$$

Equation 49 has been solved by Kreith and Sonju[10] with the assumption that the eddy viscosity is independent of the radial and axial distance, being a function only of the axial Reynold's number. In the following chapter, the eddy viscosity function will be derived using von Karman's similarity theory for turbulent flow extended to a cylindrical geometry. The subscript θ of the eddy viscosity rotation in the swirl equation will be dropped with a convention that henceforth, e_m applies to the swirl equation.

VII. SIMILARITY CONDITIONS FOR TURBULENT ROTATING AND SWIRLING FLOWS

A. THE INSTANTANEOUS VORTICITY EQUATION

If we neglect molecular viscosity, the equation of motion is:

$$\frac{\partial \underline{V}}{\partial t} + \nabla\left(\frac{1}{2}\underline{V}^2\right) - (\underline{V} \times \underline{\Omega}) = \frac{1}{\rho}\underline{F} - \frac{1}{\rho}\nabla P \tag{50}$$

To derive the vorticity equation we take the curl of both sides of Equation 50 and obtain:

$$\frac{\partial \underline{\Omega}}{\partial t} + (\underline{V}\cdot\nabla)\underline{\Omega} - (\underline{\Omega}\cdot\nabla)\underline{V} + \underline{\Omega}(\nabla\cdot\underline{V}) + \underline{V}(\nabla\cdot\underline{\Omega}) = 0 \tag{51}$$

Since for an incompressible fluid $\nabla\cdot\underline{V} = 0$, and $\nabla\cdot\underline{\Omega} = \nabla\cdot(\nabla\times\underline{V}) \equiv 0$ Equation 51 further becomes

$$\frac{\partial \underline{\Omega}}{\partial t} + (\underline{V}\cdot\nabla)\underline{\Omega} - (\underline{\Omega}\cdot\nabla)\underline{V} = 0 \tag{52}$$

Equation 52 in polar cylindrical coordinates is:

1. Radial Component

$$\frac{\partial \omega_r}{\partial t} + u\frac{\partial \omega_r}{\partial r} + \frac{v}{r}\frac{\partial \omega_r}{\partial \theta} + w\frac{\partial \omega_r}{\partial z} - \omega_r\frac{\partial u}{\partial r} - \frac{\omega_\theta}{r}\frac{\partial u}{\partial \theta}$$

$$- \omega_z\frac{\partial u}{\partial z} = 0 \tag{53}$$

2. Tangential Component

$$\frac{\partial \omega_\theta}{\partial t} + u\frac{\partial \omega_\theta}{\partial r} + \frac{v}{r}\frac{\partial \omega_\theta}{\partial \theta} + w\frac{\partial \omega_\theta}{\partial z} + \frac{v}{r}\omega_r - \omega_r\frac{\partial v}{\partial r} - \frac{\omega_\theta}{r}\frac{\partial v}{\partial \theta}$$

$$- \omega_z\frac{\partial v}{\partial z} - \frac{\omega_\theta u}{r} = 0 \qquad (54)$$

3. Axial Component

$$\frac{\partial \omega_z}{\partial t} + u\frac{\partial \omega_2}{\partial r} + \frac{v}{r}\frac{\partial \omega_z}{\partial \theta} + w\frac{\partial \omega_z}{\partial z} - \omega_r\frac{\partial w}{\partial r} - \frac{\omega_\theta}{r}\frac{\partial w}{\partial \theta} - \omega_z\frac{\partial w}{\partial z}$$

$$= 0 \qquad (55)$$

Where the instantaneous quantities

$$\underline{V} = (u, v, w)$$

$$\underline{\Omega} = (\omega_r, \omega_\theta, \omega_z)$$

B. SIMILARITY CONDITIONS FOR FULLY TURBULENT ROTATING FLOWS

1. Mathematical Analysis

For a fully turbulent rotating flow the mean velocities in the radial and axial directions are not present while all the fluctuating flow components are present. The instantaneous velocity vector has, therefore, the following components:

$$\underline{V} = (u', V + v', w') \tag{56}$$

With V = V(r) and assuming the mean flow as axially symmetric one obtains:

$$\xi = 0$$
$$\eta = 0$$
$$\zeta = \frac{1}{r}\frac{d(rV)}{dr}$$

for the mean vorticity components, and the instantaneous vorticity vector is

$$\underline{\Omega} = \left(\xi' : \eta' : \zeta' + \frac{dV}{dr} + \frac{V}{r} \right) \tag{57}$$

Substituting Equations 56 and 57 into Equations 53, 54 and 55 we obtain the following equations:

(a) Radial Component

$$\frac{V}{r}\frac{\partial \xi'}{\partial \theta} - \frac{1}{r}\frac{d(rV)}{dr} \cdot \frac{\partial u'}{\partial z} + \frac{\partial \xi'}{\partial t} + u'\frac{\partial \xi'}{\partial r} + \frac{v'}{r}\frac{\partial \xi'}{\partial \theta} + w'\frac{\partial \xi'}{\partial z}$$

$$- \xi'\frac{\partial u'}{\partial r} - \frac{\eta'}{r}\frac{\partial u'}{\partial \theta} - \zeta'\frac{\partial u'}{\partial z} = 0 \tag{58}$$

(b) Tangential Component

$$\frac{V}{r}\frac{\partial \eta'}{\partial \theta} - r\frac{d}{dr}\left(\frac{V}{r}\right) \cdot \xi' - \frac{1}{r}\frac{d}{dr}(rV) \cdot \frac{\partial v'}{\partial z} + \frac{\partial \eta'}{\partial t} + u'\frac{\partial \eta'}{\partial r}$$

$$+ \frac{v'}{r}\frac{\partial \eta'}{\partial \theta} + w'\frac{\partial \eta'}{\partial z} + \frac{v'\xi'}{r} - \xi'\frac{\partial v'}{\partial r} - \frac{\eta'}{r}\frac{\partial v'}{\partial \theta} - \zeta'\frac{\partial v'}{\partial z} - \frac{\eta' u'}{r}$$

$$= 0 \tag{59}$$

(c) Axial Component

$$\frac{V}{r}\frac{\partial \zeta'}{\partial \theta} - \frac{1}{r}\frac{d}{dr}(rV)\frac{\partial w'}{\partial z} + \left[\frac{d}{dr}\left(\frac{dV}{dr} + \frac{V}{r}\right)\right] u' + \frac{\partial \zeta'}{\partial t} + u'\frac{\partial \zeta'}{\partial r}$$

$$+ \frac{v'}{r}\frac{\partial \zeta'}{\partial \theta} + w'\frac{\partial \zeta'}{\partial z} - \xi'\frac{\partial w'}{\partial r} - \frac{\eta'}{r}\frac{\partial w'}{\partial \theta} - \zeta'\frac{\partial w'}{\partial z} = 0 \qquad (60)$$

Consider a turbulent rotating field as shown in Figure 8 and choose any point $P(r_o, \theta_o, z_o)$ as a point of reference. Following von Karman's concept of the similarity theory it is assumed that: 1) In order for the turbulent disturbances to correlate at two different points, the field of flow that must be considered is restricted to the immediate neighborhood of the reference point P. 2) In the neighborhood of the reference point, the flow patterns are similar, i.e., they differ only from point to point in the scale of length and velocity. 3) The frame of reference is moving with the mean velocity at point P and that the turbulent disturbances in the immediate neighboring points around it are transported by the mean flow. Also, since we are considering only the immediate neighborhood of point P, for $\frac{d(rV)}{dr}$, $\frac{d(dV/dr + V/r)}{dr}$ and $\frac{d(V/r)}{dr}$, we take their values at point P while for V/r, we take the first term of the Taylor expansion about point P, namely

$$\frac{V}{r} \approx (r - r_o)\left[\frac{d\left(\frac{V}{r}\right)}{dr}\right]_o$$

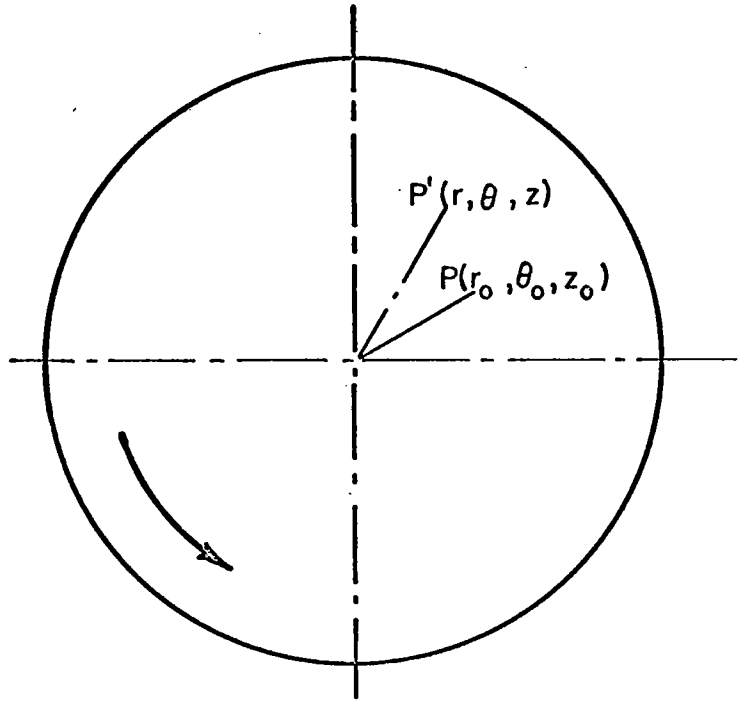

Figure 8: Turbulent Rotating Field in a Cylindrical Geometry

Also the radial coordinate can be represented by

$$\frac{1}{r} = \frac{1}{r_o}\left[1 - \frac{(r - r_o)}{r_o} + \ldots\ldots\ldots\ldots\ldots\right], \text{ and}$$

following assumption 2,

L = length scale

A = velocity scale.

Also let the variables with asterisk, that are of order unity, represent the similarity parameters in the turbulent flow field. The similarity assumption implies the following relations:

$$\left.\begin{aligned} &r - r_o = Lr^*;\ r_o(\theta - \theta_o) = L\theta^*;\ z - z_o = Lz^*;\ t = Lt^*/A; \\ &u' = Au'^*;\ v' = Av'^*;\ w' = Aw'^*;\ \xi' = A\xi'^*/L;\ \eta' = A\eta'^*/L;\ \zeta' = A\zeta'^*/L. \end{aligned}\right\} \quad (61)$$

Hence,

$$\frac{\partial r^*}{\partial r} = \frac{1}{L} \qquad \frac{\partial \theta^*}{\partial \theta} = \frac{r_o}{L}$$

$$\frac{\partial z^*}{\partial z} = \frac{1}{L} \qquad \frac{\partial t^*}{\partial t} = \frac{A}{L}$$

Substituting the above relations into Equations 58, 59 and 60, we obtain:

(a) Radial Component

$$\frac{L}{A}\left(\frac{dV}{dr} - \frac{V}{r}\right)_o - \frac{L}{A}\left(\frac{dV}{dr} + \frac{V}{r}\right)_o \frac{\partial u'^*}{\partial z^*} - \frac{L}{r_o}\left(r^* v'^* \frac{\partial \xi'^*}{\partial \theta^*}\right.$$

$$\left. - r^* \eta'^* \frac{\partial u'^*}{\partial \theta^*}\right) + \frac{\partial \xi'^*}{\partial t^*} + u'^* \frac{\partial \xi'^*}{\partial r^*} + v'^* \frac{\partial \xi'^*}{\partial \theta^*} + w'^* \frac{\partial \xi'^*}{\partial z^*}$$

$$- \xi'^* \frac{\partial u'^*}{\partial r^*} - \eta'^* \frac{\partial u'^*}{\partial \theta^*} - \zeta'^* \frac{\partial u'^*}{\partial z^*} = 0 \qquad (62)$$

(b) Tangential Component

$$\frac{L}{A}\left(\frac{dV}{dr} - \frac{V}{r}\right)_o \left(r^* \frac{\partial \eta'^*}{\partial \theta^*} - \xi'^*\right) - \frac{L}{A}\left(\frac{dV}{dr} + \frac{V}{r}\right)_o \frac{\partial v'^*}{\partial z^*}$$

$$+ \frac{\partial \eta'^*}{\partial t^*} + u'^* \frac{\partial \eta'^*}{\partial r^*} + v'^* \frac{\partial \eta'^*}{\partial \theta^*} + w'^* \frac{\partial \eta'^*}{\partial z^*} - \xi'^* \frac{\partial v'^*}{\partial r^*}$$

$$- \eta'^* \frac{\partial v'^*}{\partial \theta^*} - \zeta'^* \frac{\partial v'^*}{\partial z^*} + \frac{L}{r_o} \left(r^* \eta'^* \frac{\partial v'^*}{\partial \theta^*} - r^* v'^* \frac{\partial \eta'^*}{\partial \theta^*} \right.$$

$$\left. + v'^* \xi'^* - \eta'^* u'^* \right) = 0 \qquad (63)$$

(c) Axial Component

$$\frac{L}{A} \left(\frac{dV}{dr} - \frac{V}{r} \right)_o \left(r^* \frac{\partial \zeta'^*}{\partial \theta^*} \right) - \frac{L}{A} \left(\frac{dV}{dr} + \frac{V}{r} \right)_o \frac{\partial w'^*}{\partial z^*} + \frac{L}{A}^2 \left[\frac{d}{dr} \left(\frac{dV}{dr} \right. \right.$$

$$\left. \left. + \frac{V}{r} \right) \right]_o u'^* + \frac{\partial \zeta'^*}{\partial t^*} + u'^* \frac{\partial \zeta'^*}{\partial r^*} + v'^* \frac{\partial \zeta'^*}{\partial \theta^*} + w'^* \frac{\partial \zeta'^*}{\partial z^*}$$

$$- \xi'^* \frac{\partial w'^*}{\partial r^*} - \eta'^* \frac{\partial w'^*}{\partial \theta^*} - \zeta'^* \frac{\partial w'^*}{\partial z^*} - \frac{L}{r_o} \left(r^* v'^* \frac{\partial \zeta'^*}{\partial \theta^*} \right.$$

$$\left. + r^* \eta'^* \frac{\partial w'^*}{\partial \theta^*} \right) = 0 \qquad (64)$$

Equations 62, 63 and 64 are independent of the position of the reference point P. This implies that the following coefficients in the above equations must be constants:

$$(a') \qquad \frac{L}{r_o} = \text{Constant}$$

$$(b') \qquad \frac{L}{A} \left(\frac{dV}{dr} - \frac{V}{r} \right)_o = \text{Constant} \qquad (65)$$

$$(c') \qquad \frac{L}{A}\left(\frac{dV}{dr} + \frac{V}{r_o}\right)_o = \text{Constant}$$

$$(d') \qquad \frac{L^2}{A}\left[\frac{d\left(\frac{dV}{dr} + \frac{V}{r}\right)}{dr}\right]_o = \text{Constant} \qquad (65)$$

The reference point P can be anywhere in the field so that the subscript o can be omitted in Equation 65. The above relations yield the following similarity conditions:

$$(1) \qquad L = K_1 r \qquad \text{(using a')}$$

$$(2) \qquad L = K_2 \frac{\frac{dV}{dr} - \frac{V}{r}}{\frac{d}{dr}\left(\frac{dV}{dr} + \frac{V}{r}\right)} \qquad \text{(from b' and d')}$$

$$(3) \qquad L = K_3 \frac{\frac{dV}{dr} + \frac{V}{r}}{\frac{d}{dr}\left(\frac{dV}{dr} + \frac{V}{r}\right)} \qquad \text{(from c' and d')} \qquad (66)$$

$$(4) \qquad A = K_4 L\left(\frac{dV}{dr} - \frac{V}{r}\right) \qquad \text{(using b')}$$

$$(5) \qquad A = K_5 L\left(\frac{dV}{dr} + \frac{V}{r}\right) \qquad \text{(using c')}$$

2. Discussions

It should be noted that different expressions define the length and velocity scales in the flow field. These conditions must be simultaneously satisfied in every point of the field giving rise to a family of universal velocity profiles. It is also evident from the above conditions that more than one velocity profile that satisfies the similarity conditions can exist in different rotating flow problems. This fact is supported by actual experimentation particularly that of G. I. Taylor,[7], [32] who reported two very different velocity profiles in the field depending on which of the concentric cylinders was rotated. This particular aspect will be discussed further in a latter part of this report.

The similarity conditions can enable us to get an understanding of the turbulent mechamism in rotating fields. From Equation 61, the tangential component of the fluctuating velocity field is

$$\left|v'\right| = \left|A\, v'^{*}\right| \qquad (v'^{*} \text{ is of order unity})$$

Taking the 4th similarity condition and substitute it into the above equation we have

$$\left|v'\right| = K_4 L \left|\left(\frac{dV}{dr} - \frac{V}{r}\right)\right| \left|v'^{*}\right|$$

or

$$\left|\frac{v'}{r}\right| = L_m \left|\frac{d\left(\frac{V}{r}\right)}{dr}\right| \tag{67}$$

where the mixing length L_m is taken as $LK_4 \left|v'^{*}\right|$.

If we substitute the 5th similarity condition and following the same arguement, we have

$$\left| rv' \right| = L_m \left| \frac{d(rV)}{dr} \right| \tag{68}$$

With the usual concept of the mixing length, it appears that both angular momentum and angular velocity are transportable quantities within the field. The establishment of the fluctuating velocity field can therefore be due to the transport of either or both of these quantities.

Past experimental studies of rotating and swirling flows in pipes reveal a region of predominantly solid body rotation near the center of the pipe. The rate of increase of the tangential velocity with radius decreases continuously until a maximum velocity is reached. Thereafter the tangential velocity decreases with radius as r^{-m} where $.5 < m \leq 1$ ($m = 1$ corresponds to irrotational flow).

It is therefore obvious that a transition from rotational to irrotational flow is taking place in the flow field. Figure 9 shows a tangential velocity profile in a vortex tube at a point just a few diameters downstream from the point of swirl generation as reported by Hartnett and Eckert.[18] G. I. Taylor[7] as well as Wattendorf[11] also give evidence of this transition in turbulent rotating and curved flow fields.

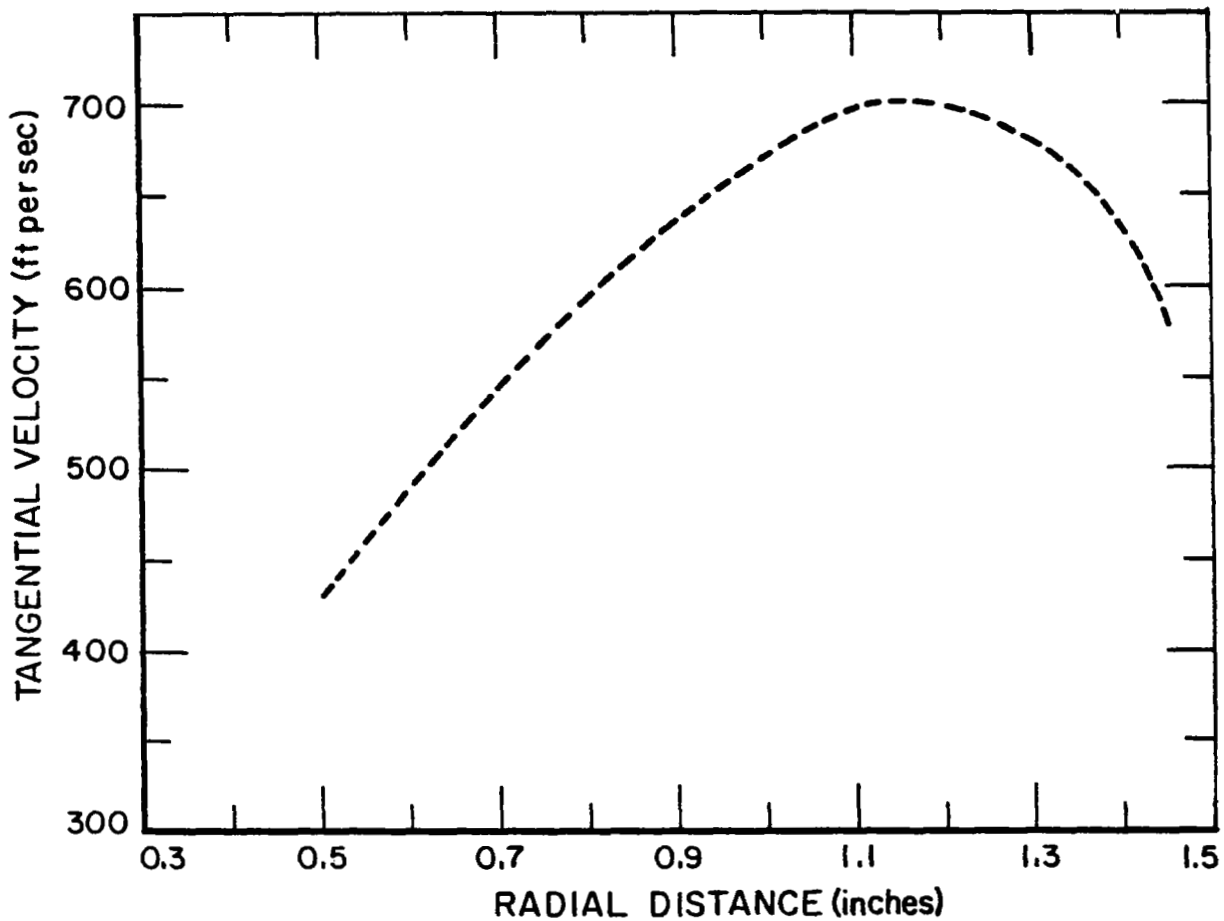

FIGURE 9. RADIAL DISTRIBUTION OF TANGENTIAL VELOCITY IN A VORTEX TUBE. AFTER HARTNETT AND ECKERT [18].

A similar transition takes place in swirling flow. E. R. Hoffman and P. N. Joubert[38] reported a comparison of laminar and turbulent velocity profiles for such flows. It appears that the turbulent profile deviated more from the laminar one in the outer region. This is probably due to the fact that in this region the ratio of turbulent to laminar transport coefficient is higher than near the central region.

The presence of a predominantly irrotational flow in the turbulent rotating field can provide an explanation as to why Taylor's vorticity transport theory yields consistent results. In a region which has a predominantly irrotational behavior the mean vorticity is very small. With this condition, Taylor's assumption in his modified theory is more nearly satisfied, namely "a lump of fluid is conceived to leave a certain position with the components of vorticity of the mean flow and to retain these components till it mixes with its surroundings after traversing the mixing length."

3. Family of Similar Velocity Profiles for Turbulent Rotating Flow

Since the conditions given in Equation 66 must be satisfied simultaneously in order for similarity to hold, a family of similar velocity profiles can be generated. The form depends upon the presence or absence of the radial gradient of the axial component of the mean vorticity, $\frac{d\zeta}{dr}$.

If we equate conditions (1) and (2) in Equation 66 we obtain:

$$\frac{d^2V}{dr^2} + \frac{1}{r}\frac{dV}{dr} - \frac{V}{r^2} = \frac{K_2}{K_1}\left(\frac{1}{r}\frac{dV}{dr} - \frac{V}{r^2}\right)$$

Letting $N = \frac{K_2}{K_1}$ yields:

$$\frac{d^2V}{dr^2} + \frac{1}{r}(1 - N)\frac{dV}{dr} - (1 - N)\frac{V}{r^2} = 0 \qquad (69)$$

Equation 69 is Euler's equation, the solution of which is

$$V = C_1 r^{h_1} + C_2 r^{h_2} \qquad \text{for } h_1 \neq h_2$$

or (70)

$$V = (C_3 + C_4 \ln r) r^{h_1} \qquad \text{for } h_1 = h_2$$

Where C_1 to C_4 are constants of integration and h_1, h_2 are the roots of the characteristic equation

$$h^2 - Nh + (N - 1) = 0 \qquad (71)$$

The roots of Equation 71 are:

$$h_1 = 1 \qquad \text{and} \qquad h_2 = N - 1.$$

Thus, if we substitute the values of h_1 and h_2 in Equation 70, the family of similar velocity profiles resulting from conditions (1) and (2) is

$$V = C_1 r + C_2 r^{N-1} \qquad \text{for } 0 \leqq N \neq 2$$

or (72)

$$V = C_3 r + C_4 r(\ln r) \qquad \text{for } N = 2$$

Equating conditions (1) and (3) in Equation 66, the resulting differential equation is:

$$\frac{d}{dr}\left(\frac{dV}{dr} + \frac{V}{r}\right) = \frac{K_3}{K_1}\left(\frac{dV}{dr} + \frac{V}{r}\right)\frac{1}{r} \quad . \tag{73-a}$$

Letting $M = \frac{K_3}{K_1}$ and integrating the above equation we obtain another form of the family of similar velocity profiles.

$$V = \frac{C_5}{r} + C_6 r^{M+1} \tag{73-b}$$

where C_5 and C_6 are constants of integration.

Similarly, taking conditions (2) and (3) we obtain:

$$K_2\left(\frac{dV}{dr} - \frac{V}{r}\right) = K_3\left(\frac{dV}{dr} + \frac{V}{r}\right) . \tag{74-a}$$

Here unlike the previous two cases, the radial gradient of the axial vorticity component $d\zeta/dr$ does not appear. Putting $S = \frac{K_2}{K_3}$ and integrating the above differential equation, we obtain the following family of similar velocity profiles:

$$V = C_7 r^{(S+1)/(S-1)} \tag{74-b}$$

where C_7 is a constant of integration.

All the three forms of similar velocity profiles derived above include the irrotational profile (V = Constant/r) that was observed experimentally by G. I. Taylor. To this end, the value of one constant of integration in

Equations 72 and 73 must be assumed arbitrarily to be zero as was also done by Taylor himself. Equations 72 and 73 include also the velocity profile that was predicted by Taylor's vorticity transport theory ($V = K_1'r + \frac{K_2'}{r}$).

For an irrotational mean flow, $\frac{d\zeta}{dr}$ is absent so that this type of flow should fall into the family of similar velocity profiles given by Equation 74 with the similarity constant S equal to zero. Furthermore, no arbitrary assumption as to the value of the constant of integration is made here. In the case of a pure rotational mean flow where $\frac{d\zeta}{dr}$ is also absent, the value of the similarity constant S in Equation 74 is plus or minus infinity. It is interesting to note that for both types of mean flow (pure rotational and irrotational), some of the similarity conditions in Equation 66 are indeterminate due to the vanishing of $\frac{d\zeta}{dr}$. For example:

For irrotational mean flow, V = Constant/r.

$$\frac{dV}{dr} + \frac{V}{r} = -\frac{\text{Constant}}{r^2} + \frac{\text{Constant}}{r^2} = 0$$

Therefore,

$$\frac{d}{dr}\left(\frac{dV}{dr} + \frac{V}{r}\right) = 0$$

Hence the third similarity condition becomes

$$L = \frac{0}{0}$$

which is indeterminate. For pure rotational flow, the second similarity condition becomes indeterminate. Due to this indeterminacy of one of the similarity conditions the assumption that all similarity conditions are simultaneously satisfied in the flow field no longer holds. From Equation 65 it follows that if $\frac{d\zeta}{dr} = 0$, the coefficient listed in (d') is non-existent. It is believed that the similarity concept is still valid for pure rotational and irrotational cases for which a new set of similarity constant results.

As was pointed out earlier, there is a gradual transition from rotational to irrotational behavior in a confined rotating flow field. Due to this phenomenon it is believed that at different regions of the flow, different forms of similar velocity profiles can exist. The form of similar velocity profiles near the axis is given by Equation 74. In the intermediate region where $\frac{d\zeta}{dr}$ is present the velocity profile may be given by Equation 72 or 73, and also 74 if the transition to irrotational flow is complete.

The region near the pipe wall requires special consideration. Here, the similarity hypothesis is not valid, and the mixing length will be taken as proportional to the distance from the wall , namely

$$L = k_1(1 - r) \tag{75}$$

This assumption is analogous to Prandtl's treatment of parallel flows in channels.

The extent of this region where the above argument applies will be discussed in Section C, Part 2 of this chapter.

While this investigation was still in progress, R. B. Kinney[20] published the results of his investigation concerning similarity in a fully turbulent rotating plane flow. He extended von Karman's similarity theory to a cylindrical geometry for the said type of flow using the same concepts as considered here. However, the similarity conditions, number (3) and (5) in Equation 66, were not revealed because of his consideration of a two-dimensional fluctuating flow field only. He evaluated a universal constant for the flow based on the experimental data of G. I. Taylor.

4. Shearing Stress and Eddy Diffusivity Expressions

The turbulent shearing stress can be written in terms of the correlation between the fluctuating velocity components. Thus,

$$T_{ij} = - \rho \overline{v_i' v_j'} \tag{76}$$

In terms of the similarity variables defined in Equation 61 the above equation can also be written as

$$T_{ij} = - \rho A^2 \overline{v_i'^* v_j'^*}$$

Since $v_i'^*$ are of order unity it can be inferred that

$$T_{ij} \sim - \rho A^2 \qquad \text{or}$$

$$= \left(\text{Constant}\right) \rho A^2 \tag{77}$$

From dimensional analysis, the kinematic eddy viscosity, e_m, can be expressed as

$$e_m = \alpha_1 \left(\frac{T_{ij}}{\rho} \right)^{1/2} L \tag{78}$$

where α_1 is a constant.

Upon substitution of Equation 77 into Equation 78 and simplifying, we have

$$e_m = \pm \alpha \, L \cdot A \qquad \text{(the + or - sign assures } e_m \text{ to be always positive.)} \tag{79}$$

If the fourth similarity condition is substituted into Equation 77 and 79, the shearing stress and the eddy viscosity can be expressed in terms of the shear velocity. We obtain

$$(T_{r\theta})_{Sh} = (\text{Constant})_1 \cdot \rho \cdot L^2 \left(\frac{dV}{dr} - \frac{V}{r} \right)^2 \tag{80-a}$$

and

$$e_m = (\text{Constant})_1 \cdot L^2 \left(\frac{dV}{dr} - \frac{V}{r} \right) \tag{80-b}$$

Combining these two expressions we get:

$$(T_{r\theta})_{Sh} = \rho e_m \left(\frac{dV}{dr} - \frac{V}{r} \right) = \rho e_m r \frac{d}{dr} \left(\frac{V}{r} \right) \tag{80-c}$$

Similarly, substituting the fifth similarity condition from Equation 66 into Equations 77 and 79 we obtain the shearing stress in terms of the mean rotation of the flow.

Hence,

$$(T_{r\theta})_{rot} = (\text{Constant})_2 \cdot \rho \cdot L^2 \left(\frac{dV}{dr} + \frac{V}{r}\right) \tag{81}$$

$$e_m = (\text{Constant})_2 \, L^2 \left(\frac{dV}{dr} + \frac{V}{r}\right)$$

and

$$(T_{r\theta})_{rot} = \rho e_m \left(\frac{dV}{dr} + \frac{V}{r}\right) = \rho e_m \left[\frac{1}{r} \frac{d}{dr} (rV)\right]$$

The above mathematical results suggest that the shearing stress in turbulent rotating flow arises due to transport of angular velocity as well as angular momentum. It should be pointed out here that the widely used hypothesis that the turbulent shear can be written as a product of a transport coefficient and the shear velocity (as is the case in laminar flow) is not sufficiently general.

Prandtl's momentum transport theory on the other hand, suggests that in rotating flows the turbulent shear should be considered as a product of a transport coefficient and the mean rotation. The present analysis serves to unify the above conflicting concepts by reducing them to special cases of a more general result.

If we assume that the stress generated by the transport of each property is additive, the total shearing stress for rotating flow becomes:

$$T_{r\theta} = (T_{r\theta})_{sh} + (T_{r\theta})_{rot}$$

or

$$T_{r\theta} = \rho \left[(\text{Constant})\ L^2 \left(\frac{dV}{dr} - \frac{V}{r} \right)^2 + (\text{Constant})\ L^2 \left(\frac{dV}{dr} + \frac{V}{r} \right)^2 \right]$$

And using Equation 74 we get:

$$T_{r\theta} = \rho\ L^2 \left[(\text{Constant}) + (\text{Constant}) \right] \frac{K_2}{K_3} \left(\frac{dV}{dr} - \frac{V}{r} \right)^2$$

$$T_{r\theta} = \rho\ L^2\ (\text{Constant}) \left(\frac{dV}{dr} - \frac{V}{r} \right)^2 \qquad (82)$$

or using Equation 80-b

$$T_{r\theta} = \rho\ e_{m(sh)} \left(\frac{dV}{dr} - \frac{V}{r} \right) \qquad (83)$$

where

$$e_{m(sh)} = (\text{Constant})\ L^2 \left(\frac{dV}{dr} - \frac{V}{r} \right)$$

With the use of the same arguments as above, the total shearing stress can also be expressed in terms of the mean rotation. We obtain:

$$T_{r\theta} = \rho\ e_{m(rot)} \left(\frac{dV}{dr} + \frac{V}{r} \right) \qquad (84)$$

where

$$e_{m(rot)} = (\text{Constant})\ L^2 \left(\frac{dV}{dr} + \frac{V}{r} \right)$$

And using Equation 74-a we can also write:

$$e_{m(rot)} = (\text{Constant})\ L^2 \left(\frac{dV}{dr} - \frac{V}{r} \right)$$

These formulations of the shearing stress have been used by previous investigators as mentioned earlier. Hoffman and Joubert,[39] for example, used Equation 84. Kassner[12] derived Equation 83 by considering a plane rotating system of coordinates with the assumption that the fluid particles are under the influence of d'Alembert forces. Ragsdale[13] used the same equation for his vortical flow investigations and Deissler and Perlmutter[17] also used the same formulation (Equation 83) for their analysis of the vortex tube. Investigators who used either expression for the shearing stress have reported agreement of theoretical and experimental results in their problems.

This is consistent with our previous finding that the turbulent shear is proportional to the mean rotation as well as to the mean shear velocity, thus explaining the apparent contradiction between the two hypotheses.

C. SIMILARITY CONDITIONS AND EDDY DIFFUSIVITY EXPRESSION FOR FULLY TURBULENT SWIRLING FLOWS

1. Similarity Conditions

In turbulent swirling flows, the mean tangential velocity is a function of the radius and the axial distance. In applying the similarity concepts for this type of flow, the axial mean velocity will be considered constant and the mean radial velocity will be meglected. These assumptions are made to simplify the mathematical analysis as well as the physical interpretation of the results.

If we use the mathematical procedure described in Section B, and include the changes described above, we obtain the same set of similarity

conditions listed in Equation 66 and also two additional conditions.

The similarity conditions for swirling flow are:

$$
\left.
\begin{aligned}
&1.\quad L = K_1 r \\
&2.\quad L = \frac{K_2 \frac{\partial V}{\partial r} - \frac{V}{r}}{\frac{\partial}{\partial r}\left(\frac{\partial V}{\partial r} + \frac{V}{r}\right)} \\
&3.\quad L = \frac{K_3 \frac{\partial V}{\partial r} + \frac{V}{r}}{\frac{\partial}{\partial r}\left(\frac{\partial V}{\partial r} + \frac{V}{r}\right)} \\
&4.\quad L = \frac{K_4 \frac{\partial V}{\partial z}}{\frac{\partial}{\partial r}\left(\frac{\partial V}{\partial r} + \frac{V}{r}\right)} \\
&5.\quad A = K_5 L\left(\frac{\partial V}{\partial r} - \frac{V}{r}\right) \\
&6.\quad A = K_6 L\left(\frac{\partial V}{\partial r} + \frac{V}{r}\right) \\
&7.\quad A = K_7 L \frac{\partial V}{\partial z}
\end{aligned}
\right\} \qquad (85)
$$

In establishing the above conditions, the radial and axial change of $\frac{\partial V}{\partial z}$ were neglected.

The seventh similarity condition shows that the axial gradient of angular momentum generates a fluctuating velocity field as well as Reynold's stresses. This can be seen by substituting condition (7) into $v' = Av'^{*}$

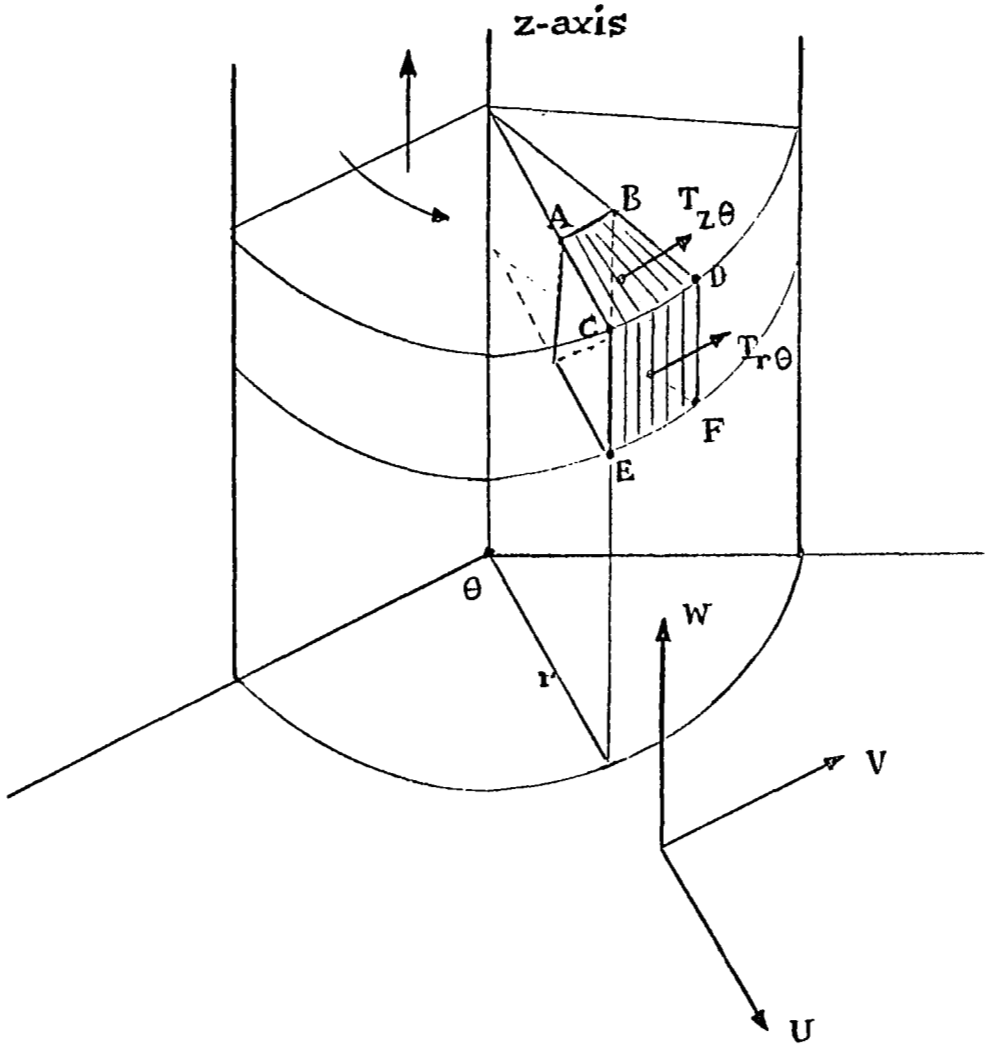

Figure 10: A Fluid Element in a Pipe with Swirling Flow

(in Equation 61) and in Equation 77. If we consider an element of fluid shown in Figure 10, it is obvious that this phenomenon is responsible for the production of a shearing stress on a plane perpendicular to the z-axis and in the θ direction (plane ABCD). The radial gradients of angular momentum, i.e. rotation, and angular velocity that is proportional to the shear velocity generate shearing stresses in the plane perpendicular to the r-axis and in the θ direction (plane CDEF). The latter was discussed in the last section.

2. Eddy Diffusivity Expression

Referring again to Figure 10, the plane CDEF, it was shown that the shearing stress is

$$T_{r\theta} = \rho e_{m(sh)} \left(\frac{\partial V}{\partial r} - \frac{V}{r} \right) \tag{83}$$

where

$$e_{m(sh)} = (\text{Constant})\ L^2 \left(\frac{\partial V}{\partial r} - \frac{V}{r} \right)$$

(partial notation is used here due to the dependence of the tangential velocity on r and z.)

In the plane ABCD, the shearing stress is

$$T_{z\theta} = \rho e_{m(ang)} \left(\frac{\partial V}{\partial z} \right) \tag{86}$$

where

$$e_{m(ang)} = (\text{Constant})\ L^2 \left(\frac{\partial V}{\partial z} \right) .$$

A resultant eddy viscosity expression for the present case, will be obtained by simultaneously satisfying the similarity conditions 2 and 4 in Equation 85.

Equating conditions 2 and 4, we have

$$\frac{\partial V}{\partial z} = \frac{K_2}{K_4} \left(\frac{\partial V}{\partial r} - \frac{V}{r} \right)$$

The eddy viscosity expression in Equation 86 now becomes

$$e_{m(ang)} = (\text{Constant})\ L^2 \left| \frac{\partial V}{\partial r} - \frac{V}{r} \right| \tag{87}$$

If we take the resultant eddy viscosity to be the vector sum of the two components, we obtain:

$$e_m = \sqrt{(e_{m(sh)})^2 + (e_{m(ang)})^2}$$

$$= L^2 \left| \left(\frac{\partial V}{\partial r} - \frac{V}{r} \right) \right| \sqrt{(\text{Constant})^2 + (\text{Constant})^2} \tag{87-a}$$

$$= (\text{Constant})\ L^2 \left| \frac{\partial V}{\partial r} - \frac{V}{r} \right|$$

Substituting the first similarity condition into Equation 85, the above equation becomes

$$e_m = K^2 r^2 \left(\frac{\partial V}{\partial r} - \frac{V}{r} \right) \tag{88}$$

where

K = Constant.

Obviously, we can also express the resultant eddy viscosity in terms of the mean rotation or the axial gradient of the mean tangential velocity. However, the above form has been used by past investigators and they have evaluated the constant K based on experimental data for rotating or vortex

flow. Kinney[31] for example, found it to be approximately equal to 0.028 using G. I. Taylor's experiment of rotating flow between concentric cylinders. Ragsdale[3] also evaluated K from his vortex flow experiments.

In the present investigation, the K^2 in Equation 88 was taken as (Kinney's Constant)^2 times $\sqrt{2}$ (according to Equation 87-a), yielding K = 0.0333. The predicted values for mean tangential velocity at different downstream positions were in good agreement with experimental data as will be shown in Chapter IX.

The length scale near the wall is assumed to be proportional to the distance from it in analogy with the first similarity condition in Equation 85. This assumption has been experimentally verified to be correct for turbulent parallel pipe flow up to a wall distance of approximately 0.10 radius (see Schlichting, "Boundary Layer Theory", p. 510). Hence, with this assumption, the eddy viscosity expression in the neighborhood of the wall was taken as:

$$e_m = K^2(1 - r)^2 \left|\frac{\partial V}{\partial r} - \frac{V}{r}\right| \qquad 0.9 < r \leq 1.0 \qquad (89)$$

In summary, the eddy viscosity expressions for the swirling flow field in dimensionless form are as follows:

$$\begin{aligned} e_m &= N_{Re} \cdot K^2 \cdot r^2 \left|\frac{\partial V}{\partial r} - \frac{V}{r}\right| && 0 \leq r \leq 0.90 \\ e_m &= N_{Re} \cdot K^2 \cdot (1 - r)^2 \left|\frac{\partial V}{\partial r} - \frac{V}{r}\right| && 0.9 < r \leq 1.0 \end{aligned} \qquad (90)$$

Equation 90 was obtained using the same reference quantities as well as the same procedure in effecting the transformation of the swirl equation into dimensionless form. (See Chapter VI). The Reynolds Number is defined as:

$$N_{Re} = \frac{W_m \cdot r_w}{\nu}$$

with ν evaluated at (85°F, 14.7 psia).

VIII. SOLUTION OF THE SWIRL EQUATION

A. THE DIFFERENTIAL EQUATION

When the eddy viscosity expressions in Equation 90 are substituted into the swirl equation (Equation 49) we obtain:

$$W(r)\frac{\partial V}{\partial z} = \left[\frac{1}{N_{Re}} + \left|K^2\lambda\left(\frac{\partial V}{\partial r} - \frac{V}{r}\right)\right|\right]\left(\frac{\partial^2 V}{\partial r^2} + \frac{1}{r}\frac{\partial V}{\partial r} - \frac{V}{r^2}\right) \tag{91}$$

where $\lambda = r^2$ for $0 \leq r \leqq 0.9$

$= (1 - r)^2$ for $0.9 < r \leqq 1.0$

and the kinematic eddy viscosity is assumed to be always positive.

The boundary conditions are:

$$\text{(a)} \quad V(1,z) = 0$$

$$\text{(b)} \quad V(r,0) = f(r) \tag{92}$$

$$\text{(c)} \quad V(0,z) = 0$$

The swirl equation (Equation 91) will be expressed in terms of the angular momentum of the fluid for convenience.

Letting

$$\beta = rV, \qquad \text{where } \beta = \beta(r,z)$$

and substituting into Equation 91 and simplifying, we obtain

$$\frac{\partial \beta}{\partial z} = \frac{1}{W}\left[\frac{1}{N_{Re}} + \left|K^2\lambda\left(\frac{\partial \beta}{\partial r} - \frac{2\beta}{r}\right)\right|\right]\left(\frac{\partial^2 \beta}{\partial r} - \frac{1}{r}\frac{\partial \beta}{\partial r}\right) \tag{93}$$

The corresponding boundary conditions are:

$$\begin{aligned} &(a)\quad \beta(r,0) = rf(r) \\ &(b)\quad \beta(0,z) = 0 \\ &(c)\quad \beta(1,z) = 0 \end{aligned} \tag{94}$$

Equation 93 is a highly non-linear partial differential equation of the parabolic type, for which a closed form solution will not be attempted here. Instead, this equation will be solved numerically on a high speed digital computer. The required boundary conditions (Equation 94) specify that the angular momentum is zero on the axis and on the stationary pipe, and that the radial distribution of tangential velocity be prescribed at some upstream axial location. In addition, the axial velocity that appears as a parameter in Equation 93 must be specified, and this is taken to be a function of radius only.

B. NUMERICAL SOLUTION OF THE ANGULAR MOMENTUM EQUATION

The angular momentum equation can be written as:

$$\frac{\partial \beta}{\partial z} = D\frac{\partial^2 \beta}{\partial r^2} + \frac{B}{r}\frac{\partial \beta}{\partial r} \tag{95}$$

where

$$D = \frac{1}{W}\left[\frac{1}{N_{Re}} + \left|K^2\lambda\left(\frac{\partial\beta}{\partial r} - \frac{2\beta}{r}\right)\right|\right]$$

$$B = -D$$

Equation 95 will now be replaced by a system of finite difference equations. The second order derivative will be replaced by three point central differences and for the first order derivatives, forward differences will be used. Figure 11 shows the grid notation for the numerical scheme.

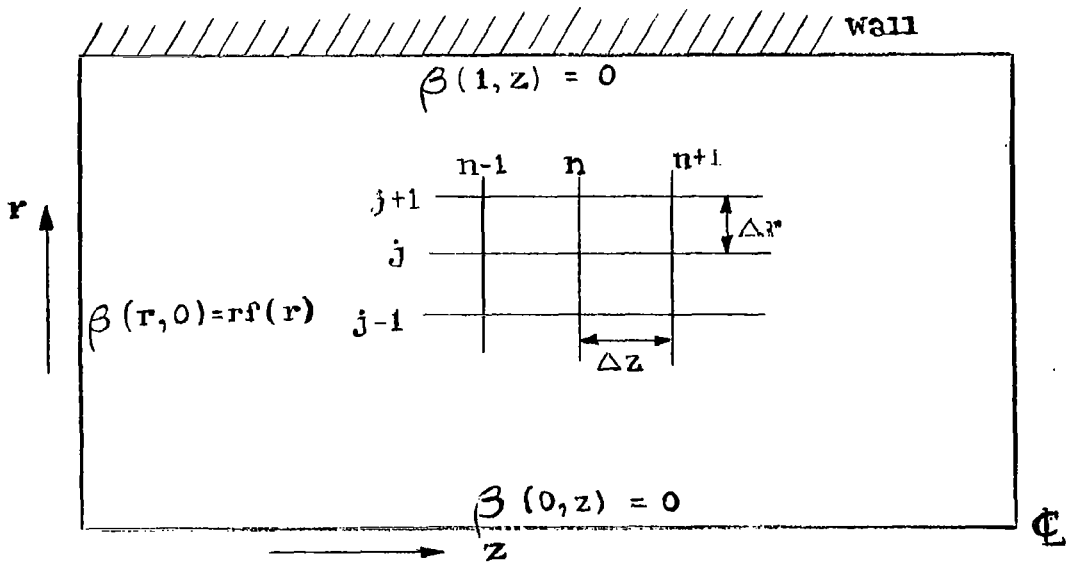

Figure 11: Grid Notation and Boundary Conditions

Let $\beta_j^n = \beta(j\Delta r, n\Delta z)$

and replacing the derivative by their finite difference approximations:

$$\frac{\partial \beta}{\partial z} = \frac{\beta_j^{n+1} - \beta_j^n}{\Delta z}$$

$$\frac{\partial \beta}{\partial r} = \frac{\beta_{j+1}^n - \beta_j^n}{\Delta r}$$

$$\frac{\partial^2 \beta}{\partial r^2} = \frac{\beta_{j+1}^n - 2\beta_j^n + \beta_{j-1}^n}{(\Delta r)^2}$$

We obtain:

$$\beta_j^{n+1} = \left[1 - \left(\frac{2D}{(\Delta r)^2} + \frac{B}{r\Delta r}\right)\Delta z\right]\beta_j^n + \left[\frac{D}{(\Delta r)^2} + \frac{B}{r\Delta r}\right]\beta_{j+1}^n \cdot \Delta z + \frac{D\cdot\Delta z}{(\Delta r)^2}\,\beta_{j-1}^n \tag{96}$$

Equation 96 is an explicit positive type-difference equation if the following inequalities are satisfied:

$$\left[\frac{2D}{(\Delta r)^2} + \frac{B}{r\Delta r}\right]\Delta z \leq 1$$

and

$$\left[\frac{D}{(\Delta r)^2} + \frac{B}{r\Delta r}\right]\Delta z \geq 0 \tag{97}$$

It can be shown that the above inequalities are always satisfied in the present problem due to the assumption that the kinematic eddy viscosity is always positive (see Equation 91).

Barakat[39] shows that for stability of the difference equation it is sufficient that the first inequality be satisfied.

The stability criterion evaluated by the use of the Fourier series method and von Neumann's condition of stability is discussed in Appendix III. It will be noted that the criterion is identical to the first condition in Equation 97, i.e.,

$$\left[\frac{2D}{(\Delta r)^2} + \frac{B}{r\Delta r}\right] \Delta z \leqq 1$$

A marching type iteration of the explicit difference equation was carried out with the use of an IBM 360 digital computer. It was assumed that the angular momentum equation is quasi-linear and the coefficients of the partial derivatives in the equation were evaluated from the known mean flow conditions at the previous z-step. Twenty subdivisions were employed in the radial direction, and as many as 500 steps were calculated in the z-direction. A typical run took approximately 15 minutes (on a 360-40).

In order to verify the theoretical analysis, the predicted decay of turbulent swirling flow in pipes was compared with experimental results obtained at IITRI and with those obtained by Musolf.

IX. RESULTS AND DISCUSSIONS

A. COMPARISON WITH IITRI'S EXPERIMENT

The experimental set-up that produced swirling flow is shown in Figure 12. It makes use of a sphere which is connected to a vacuum pump. The pressure in the sphere was initially reduced to 1.5 psia. Ambient air entered through a radial inlet section 30" in diameter that houses a cascade of adjustable blades. The swirling air enters a 3" diameter Lucite tube that is 70 diameters long. The radial distribution of both axial and tangential velocities were measured at 4 stations downstream located at 4, 36, 72 and 136 radii from the point of swirl generation.

Since air was used as the experimental fluid, one may question the validity of the previous theoretical analysis that is based on the assumption of an incompressible fluid. Lavan and Fejer[28] pointed out that for the laminar case a meaningful comparison between the incompressible solution and the experimental results for compressible swirling flows having high swirl ratios is possible. Their arguments can be extended to turbulent flow.

It is usually assumed that for a turbulent flow, the mean flow as well as the fluctuating flow fields satisfy the continuity equation. The continuity relation for the mean flow neglecting density and velocity correlation is:

$$\nabla \cdot (\rho \underline{\bar{V}}) = 0$$

or

$$\rho \nabla \cdot \underline{\bar{V}} + \rho \nabla \cdot \underline{\bar{V}} = 0$$

For flow with large swirl the density gradient is almost in the radial direction and the radial velocity component can be neglected in comparison with the tangential and axial velocity. Therefore,

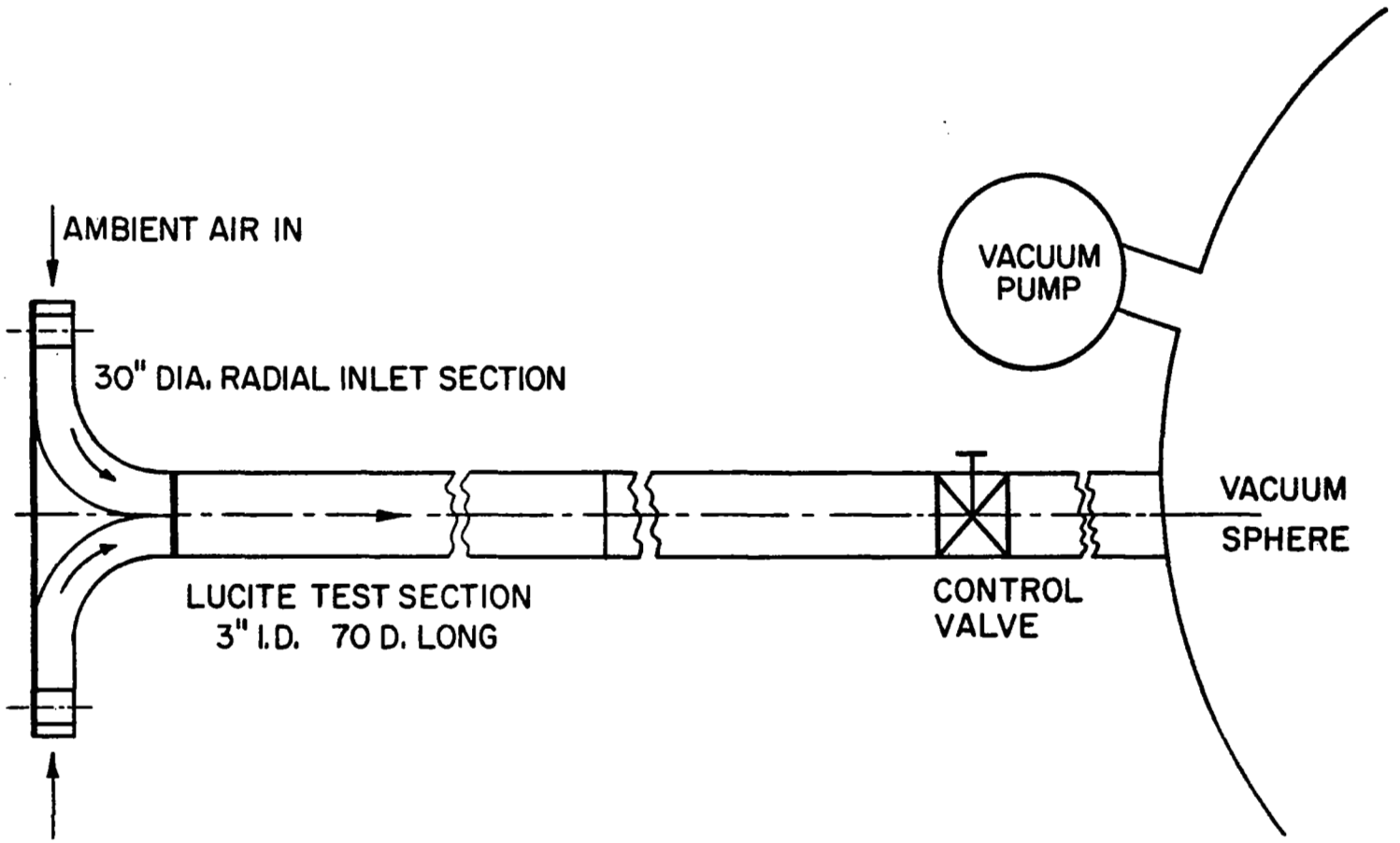

FIGURE 12. SCHEMATIC DIAGRAM OF IITRI's SWIRLING FLOW EXPERIMENTAL SET-UP.

$$\nabla\rho \approx \left(\frac{\partial\rho}{\partial r}, 0, 0 \right)$$

$$\bar{\underline{V}} \approx (0, V, W)$$

Hence,

$$\nabla\rho \cdot \bar{\underline{V}} \approx 0$$

and the continuity equation for the mean flow reduces to:

$$\nabla \cdot \bar{\underline{V}} \approx 0 \tag{98}$$

Furthermore, assuming that the density fluctuations are negligible compared to the mean flow density, then the tangential component of the equation of motion for compressible fluid is identical to Equation 8.

1. The Initial Tangential Velocity Profile

The first upstream station at which measurement of distributions of the tangential velocity were taken was situated at an axial distance of 4 radii downstream from the point of swirl generation. This data was smoothed out and used as input to the program.

Figures 13, 14, 23 and 24 show the initial conditions at Reynold's Numbers of 220,000, 58,900, 147,000 and 279,000 respectively.

2. The Average Axial Velocity Profile

The axial velocity measurements at different radial and downstream positions are shown in Figures 15, 16, 17 and 18 for the same four flow conditions. The average profile W(r) was evaluated by averaging the measured values at each radial station. The resulting average radial distribution

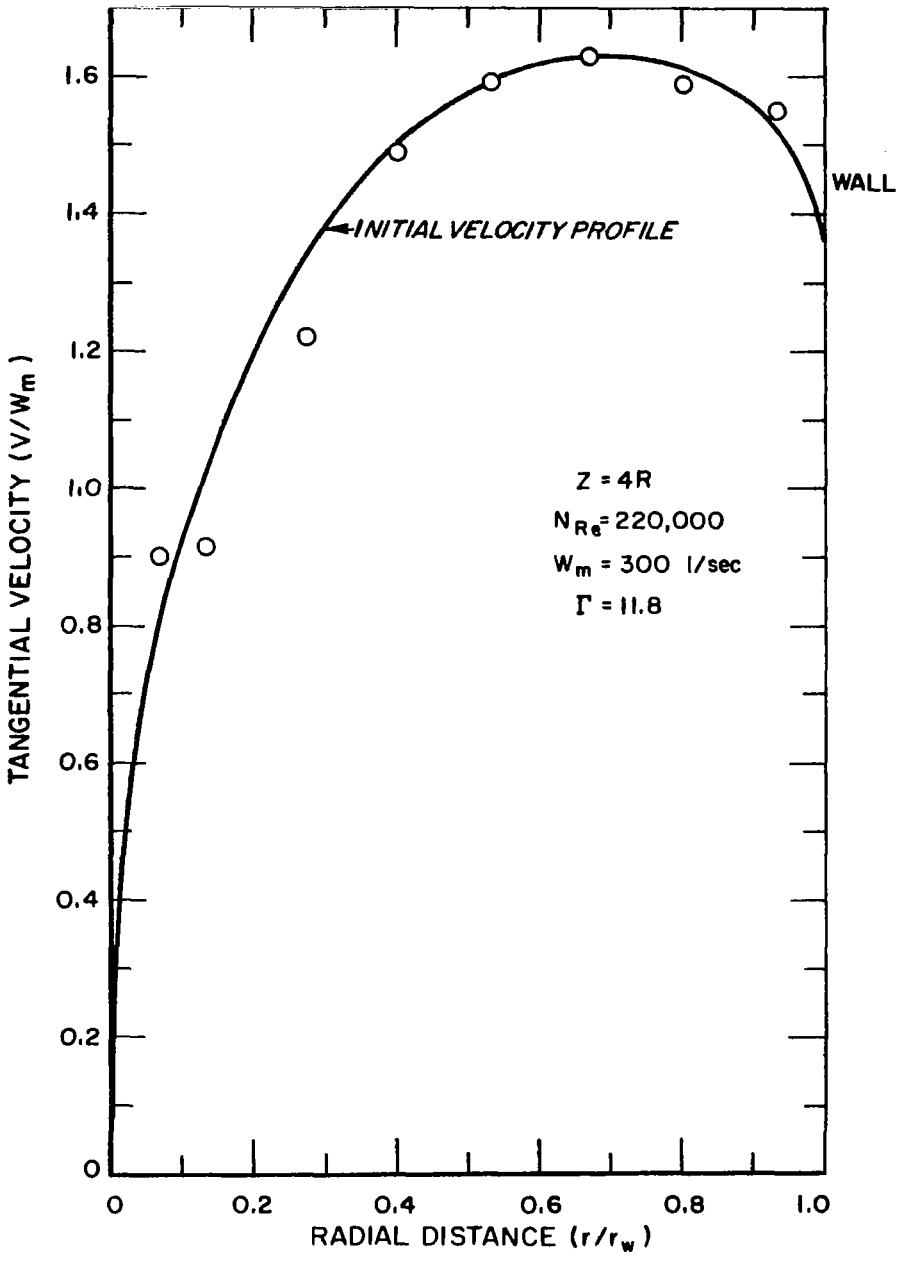

FIGURE 13. MEASURED TANGENTIAL VELOCITY PROFILE.

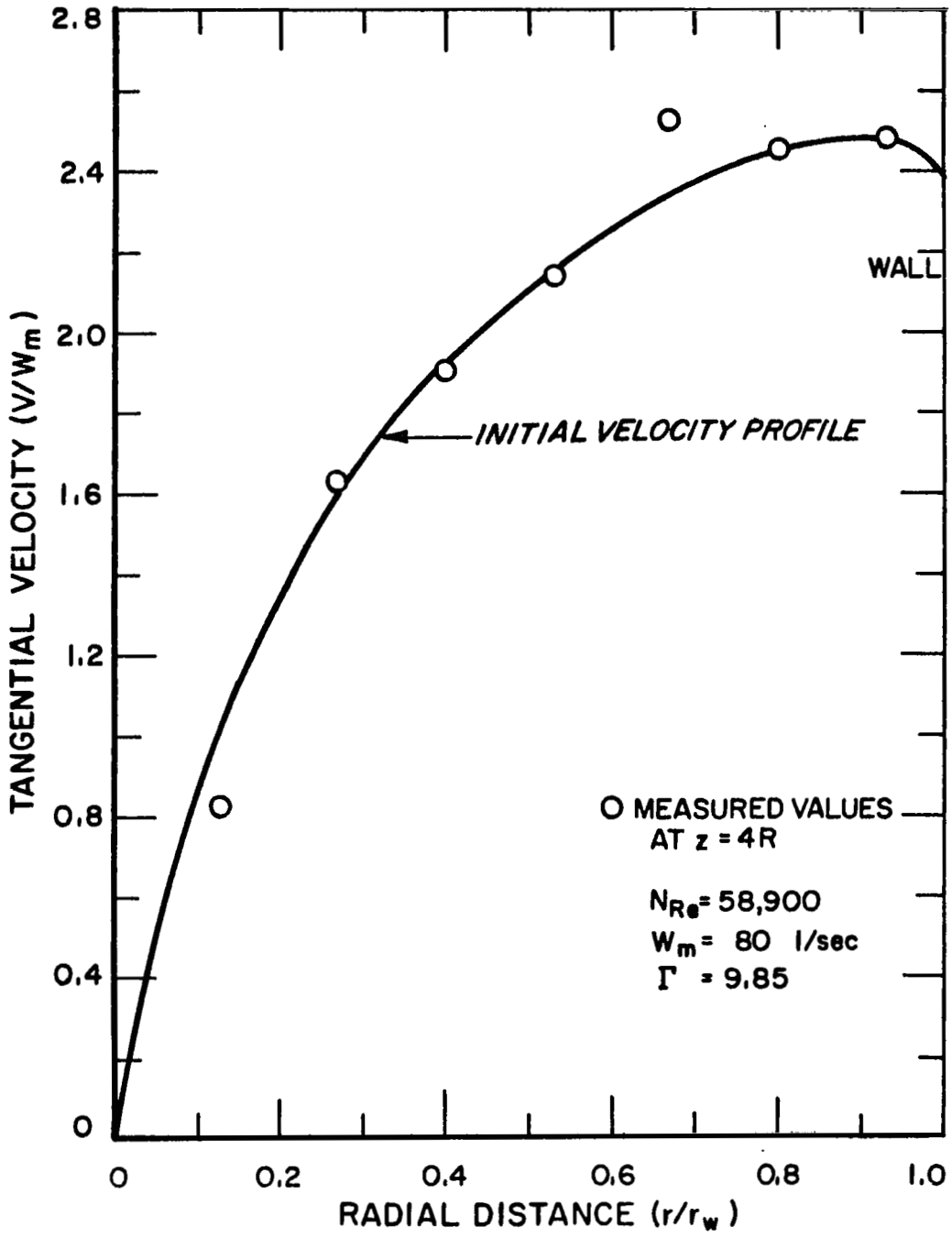

FIGURE 14. MEASURED TANGENTIAL VELOCITY PROFILE.

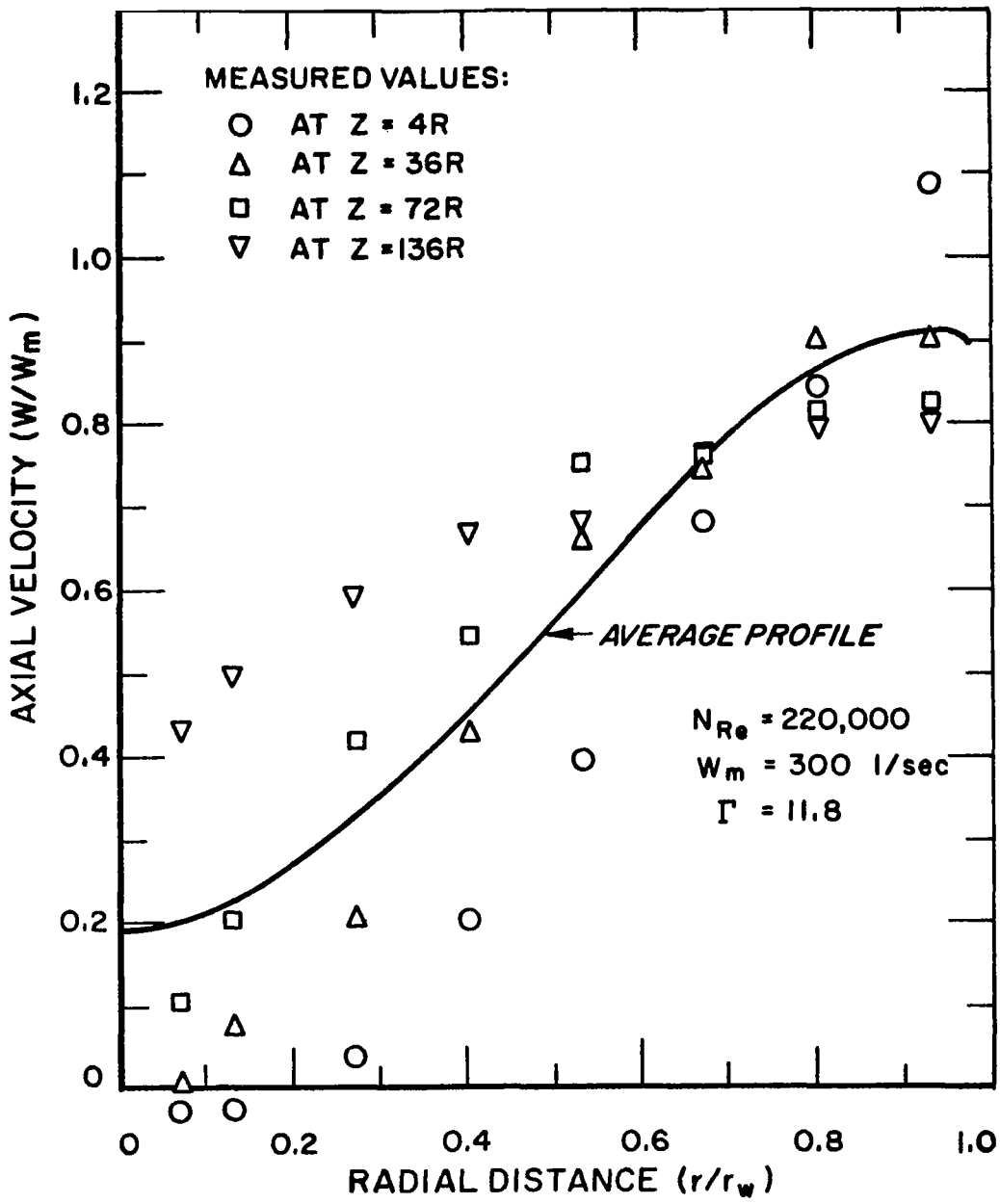

FIGURE 15. AVERAGE RADIAL DISTRIBUTION OF AXIAL VELOCITY.

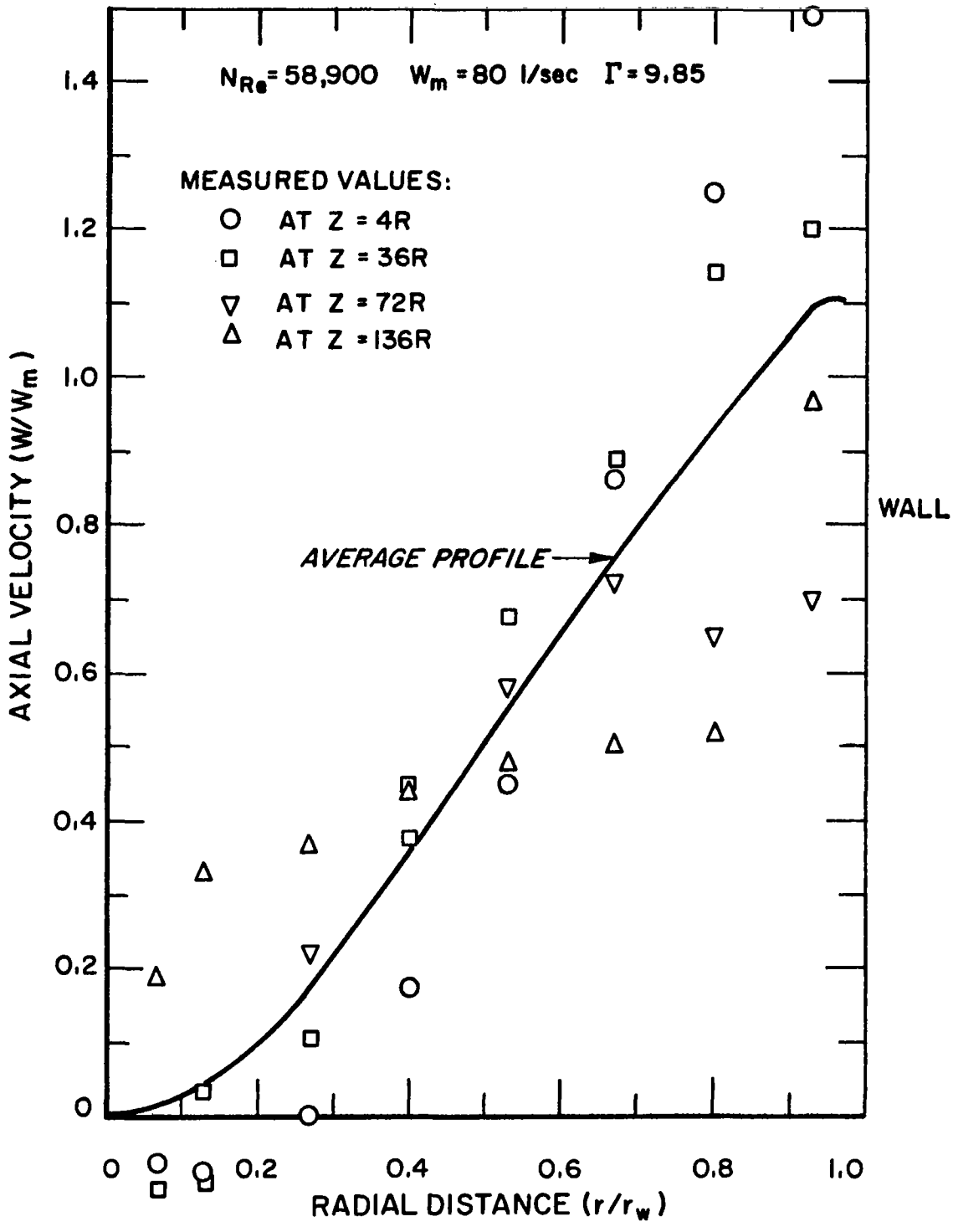

FIGURE 16. AVERAGE RADIAL DISTRIBUTION OF AXIAL VELOCITY.

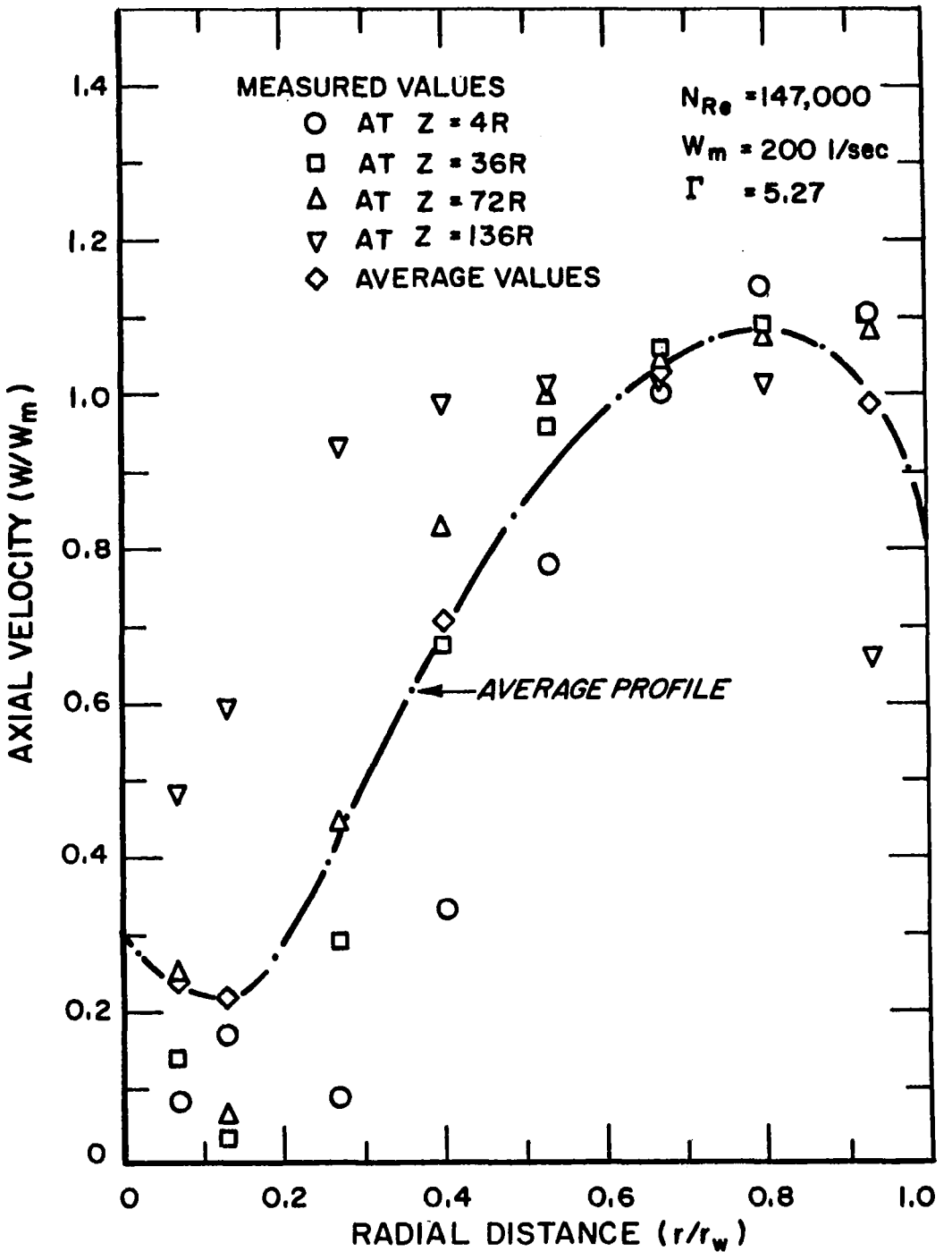

FIGURE 17. AVERAGE RADIAL DISTRIBUTION OF AXIAL VELOCITY.

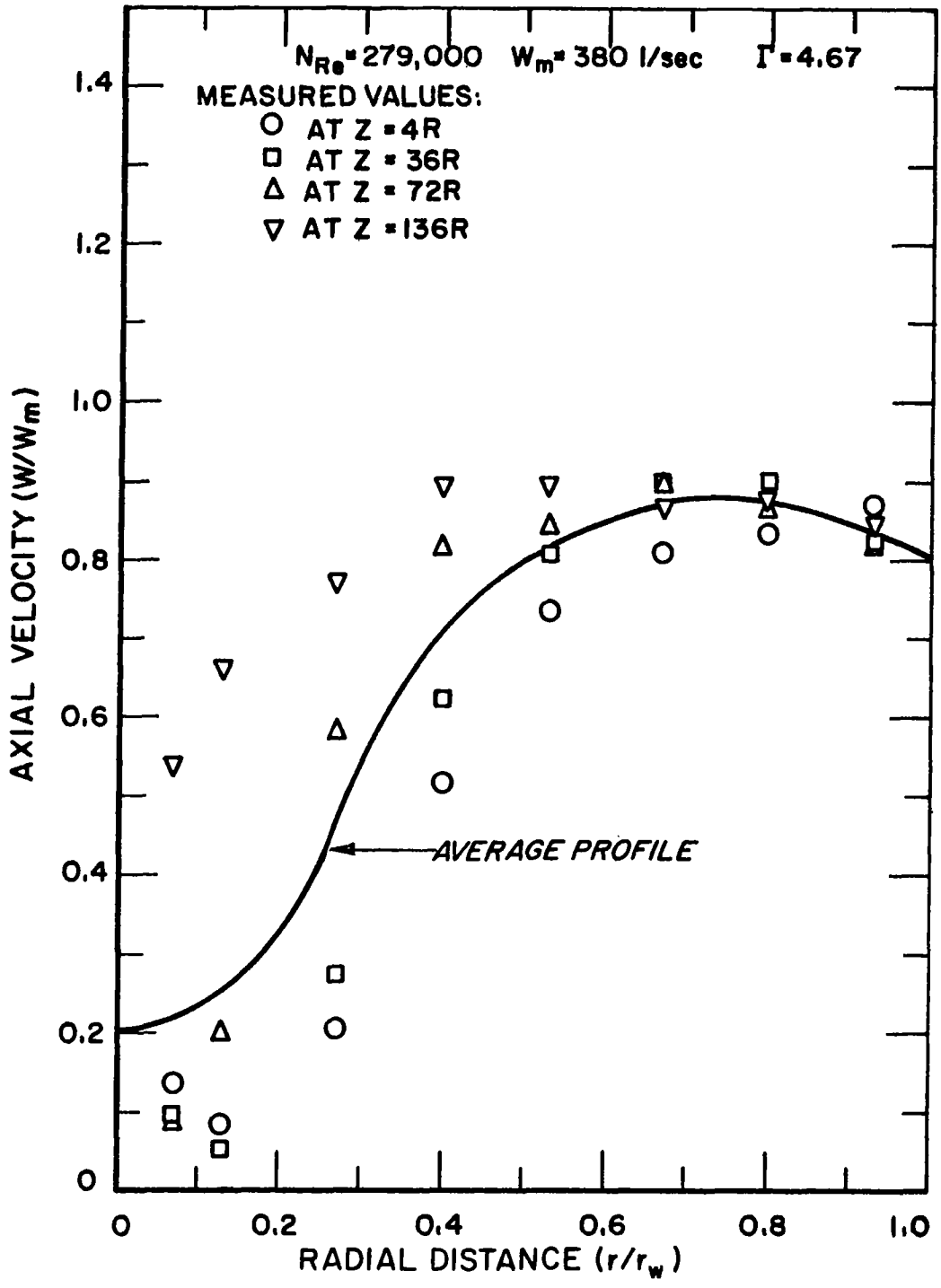

FIGURE 18. AVERAGE RADIAL DISTRIBUTION OF AXIAL VELOCITY.

of the mean axial velocity is also shown in Figures 15 to 18. It should be noted that an initial backflow occurs near the center of the pipe, for the first two cases.

3. Discussion of Results

After the initial condition and the average axial velocity profile were established, the numerical solution of the angular momentum equation was obtained.

The results are shown in Figures 19 to 26. The data shown were obtained at Reynold's Numbers of 220,000, 58,900, 147,000 and 279,000. Figures 19 and 20 show a comparison between the predicted and measured values of the radial distribution of angular momentum at different downstream positions. An examination of the measured data indicates that as the flow proceeds downstream, the region that exhibits an irrotational behavior widens and progressses towards the center of the pipe. As a result, the point of maximum tangential velocity shifts radially inward as can be seen in Figures 21 to 24 that show a comparison between the computed and experimental values of the tangential velocity at different radial and axial positions of the flow field.

An inspection of Figures 19 to 24 show a reasonably good agreement between theory and experiment. Figures 19 and 20, which represent a case where the Reynold's Number as well as the swirl ratio is high, show an excellent agreement between theory and experiment in the outer region all the way to the last station downstream ($z = 136$ R). In the region near the center there is a discrepancy which is due to a number of reasons. Firstly, in this region there is an initial backflow as seen in the axial velocity measurements at $z = 4R$ (Figure 15), while the average radial

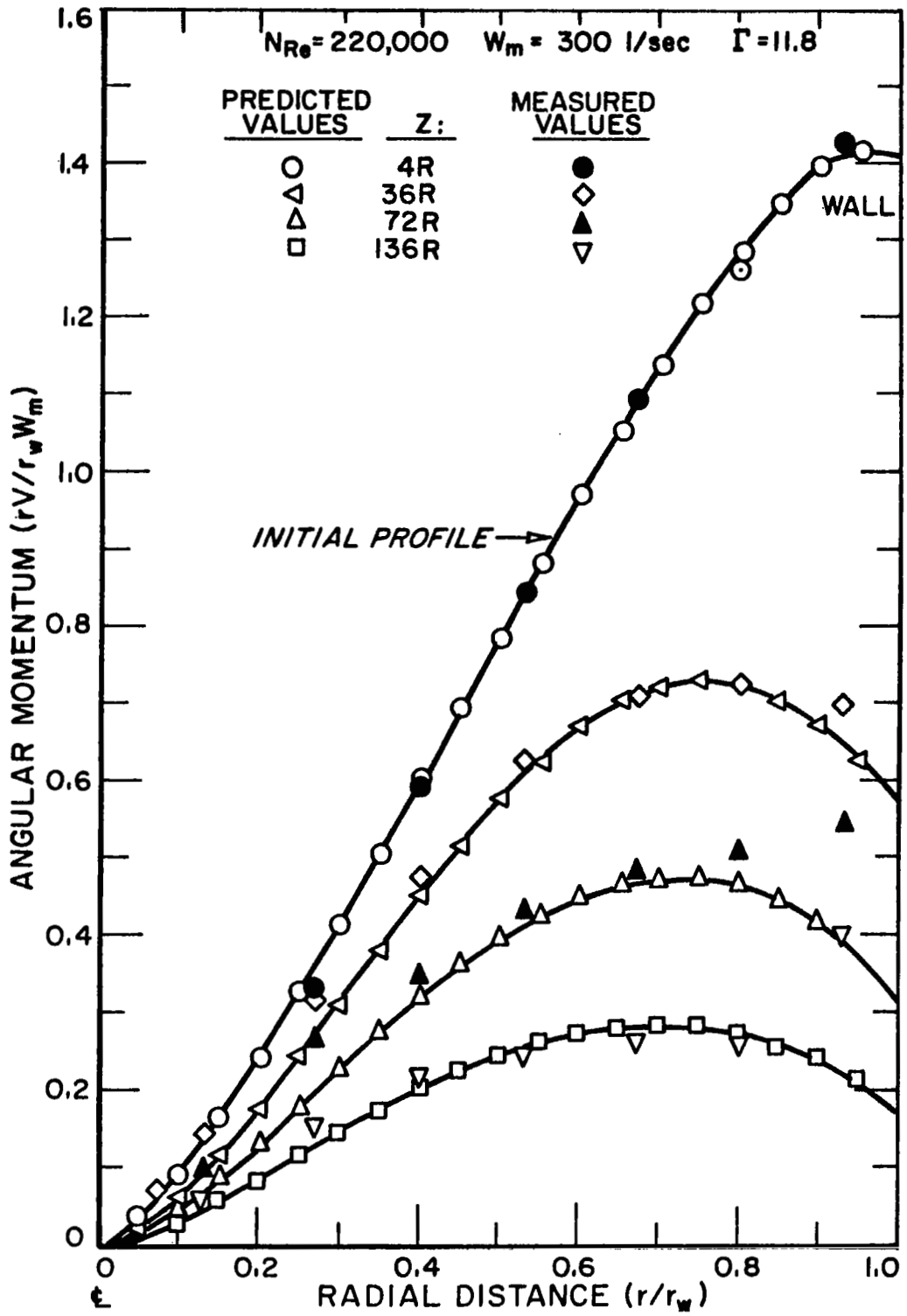

FIGURE 19. COMPARISON OF MEASURED AND PREDICTED RADIAL DISTRIBUTIONS OF ANGULAR MOMENTUM.

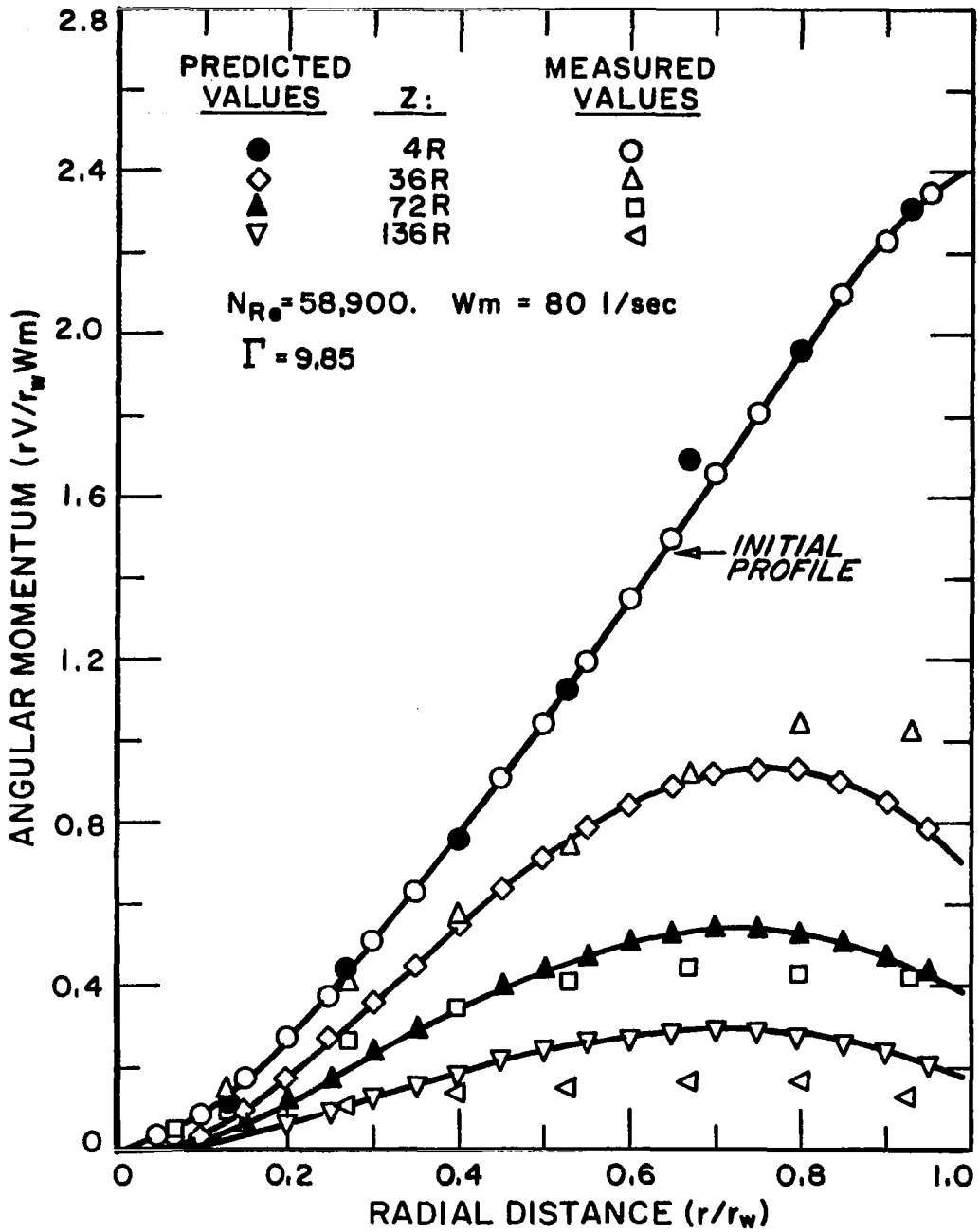

FIGURE 20. COMPARISON OF MEASURED AND PREDICTED RADIAL DISTRIBUTIONS OF ANGULAR MOMENTUM.

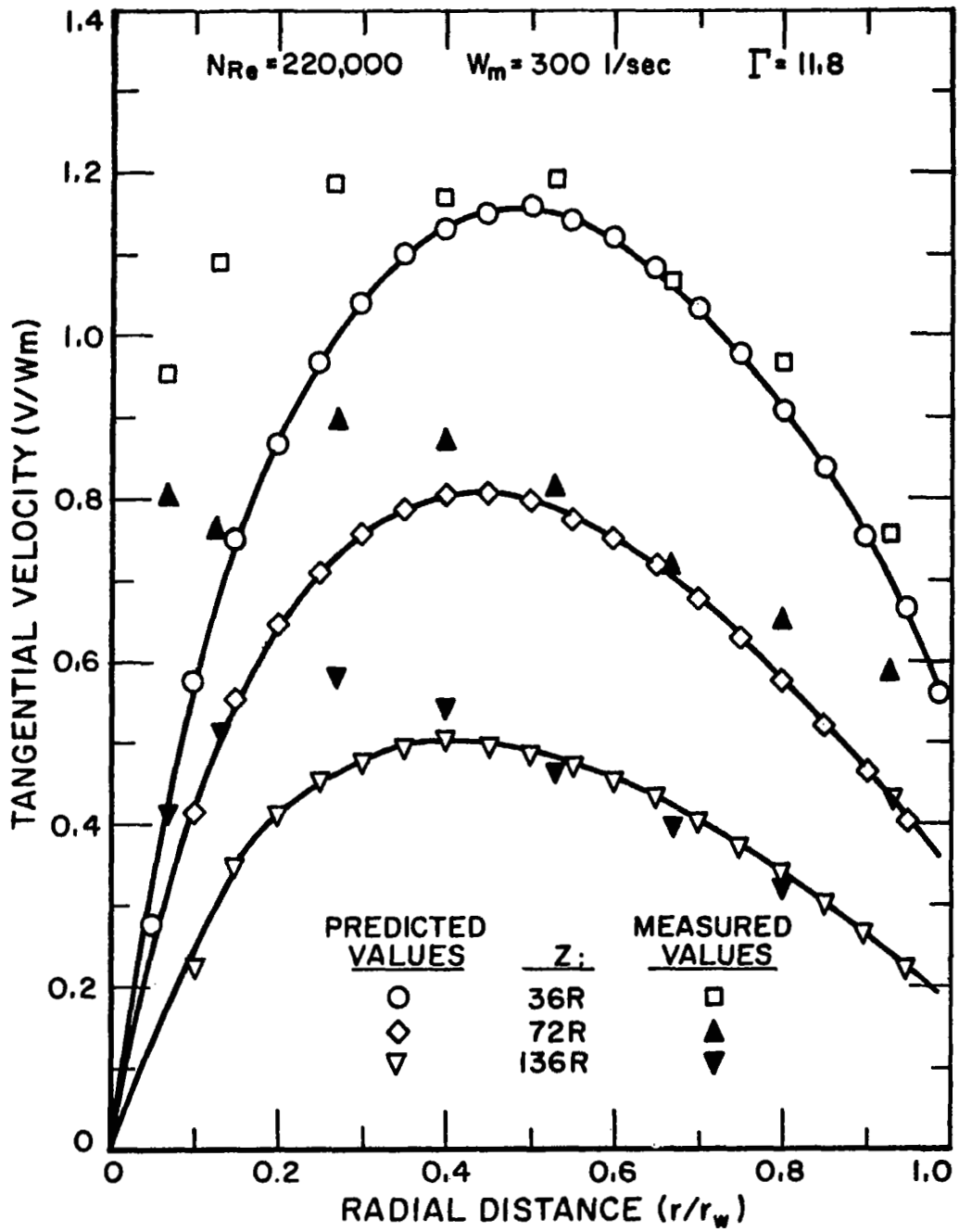

FIGURE 21. COMPARISON OF MEASURED AND PREDICTED RADIAL DISTRIBUTIONS OF TANGENTIAL VELOCITY.

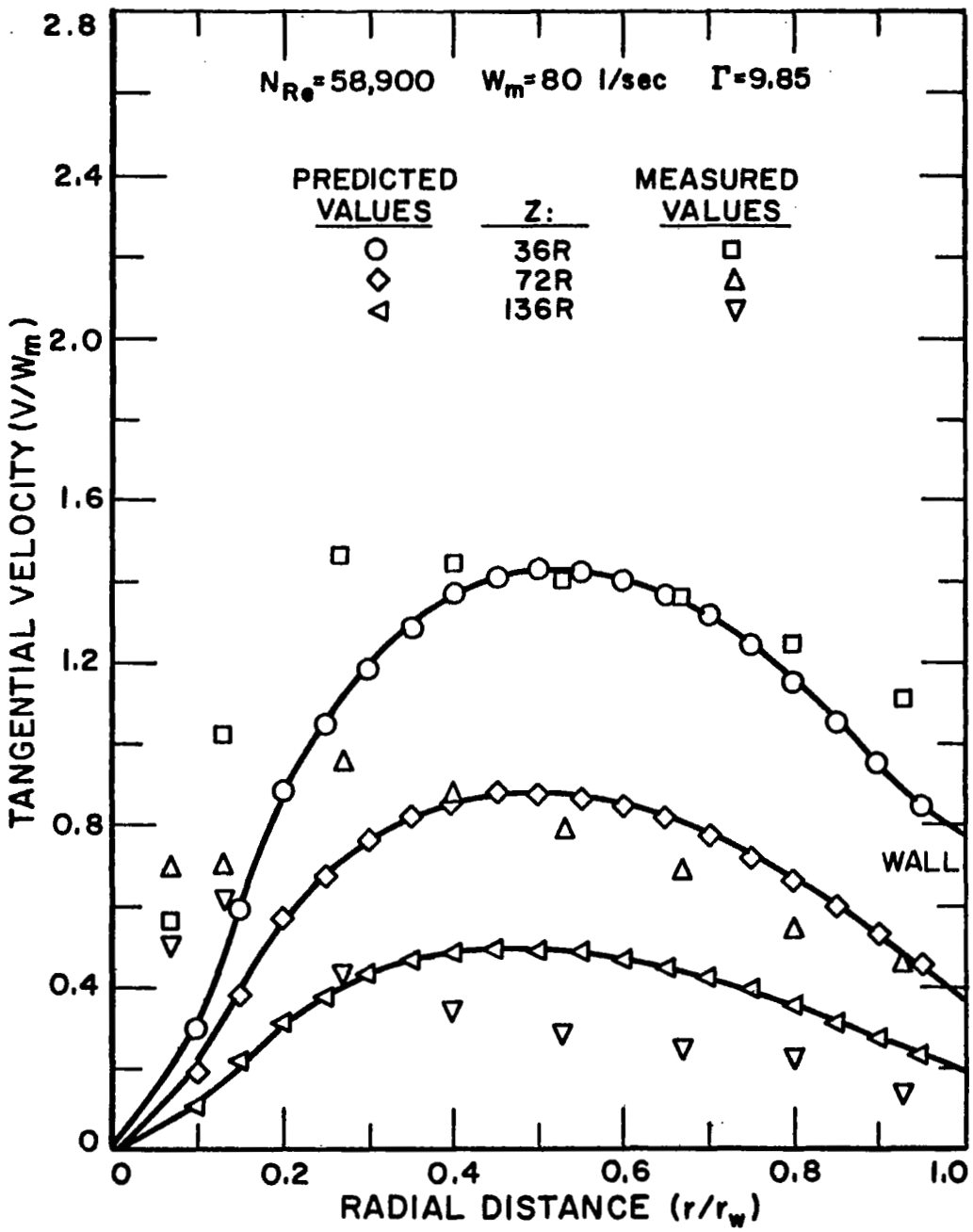

FIGURE 22. COMPARISON OF MEASURED AND PREDICTED RADIAL DISTRIBUTIONS OF TANGENTIAL VELOCITY.

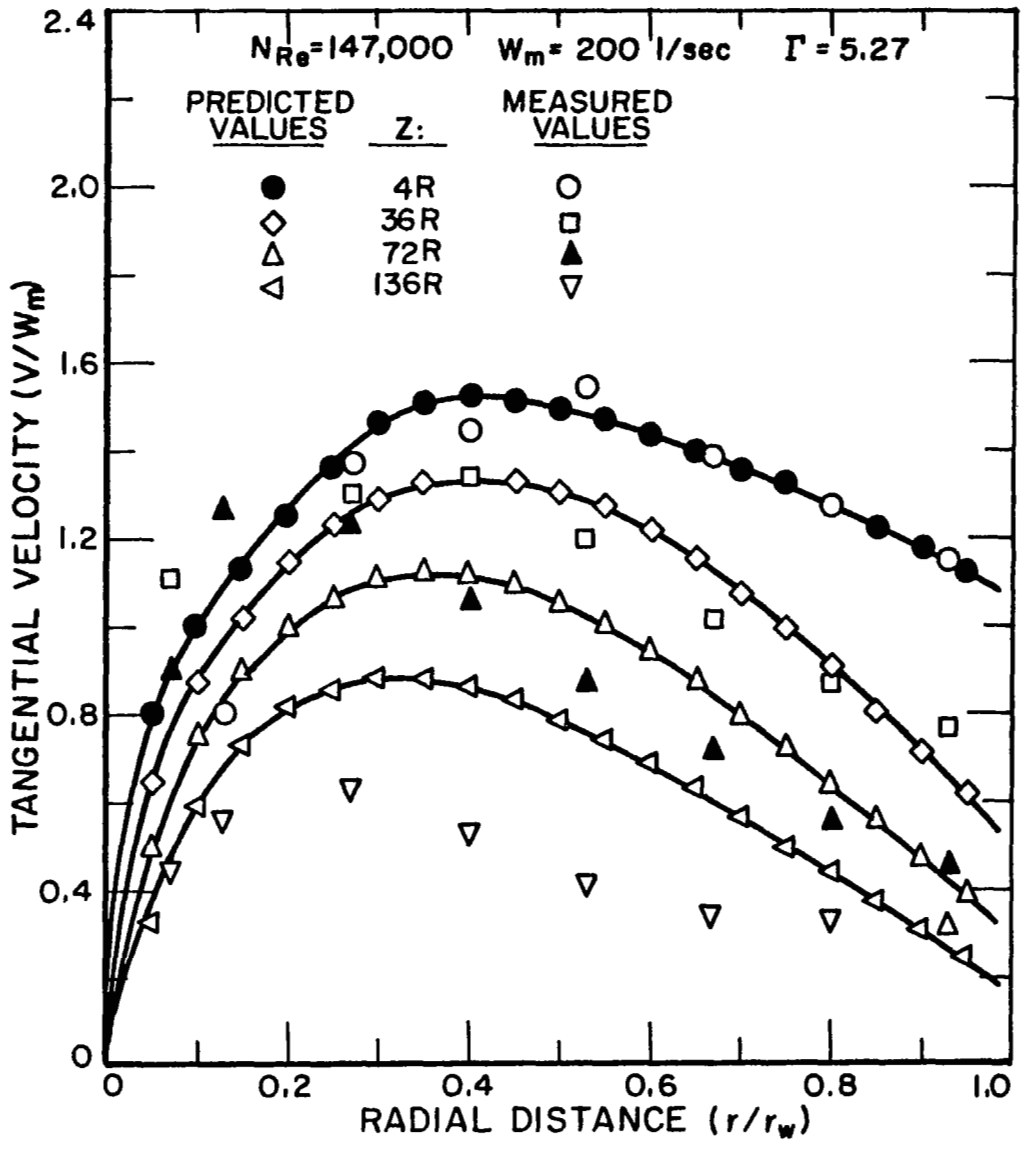

FIGURE 23. COMPARISON OF MEASURED AND PREDICTED RADIAL DISTRIBUTIONS OF TANGENTIAL VELOCITY.

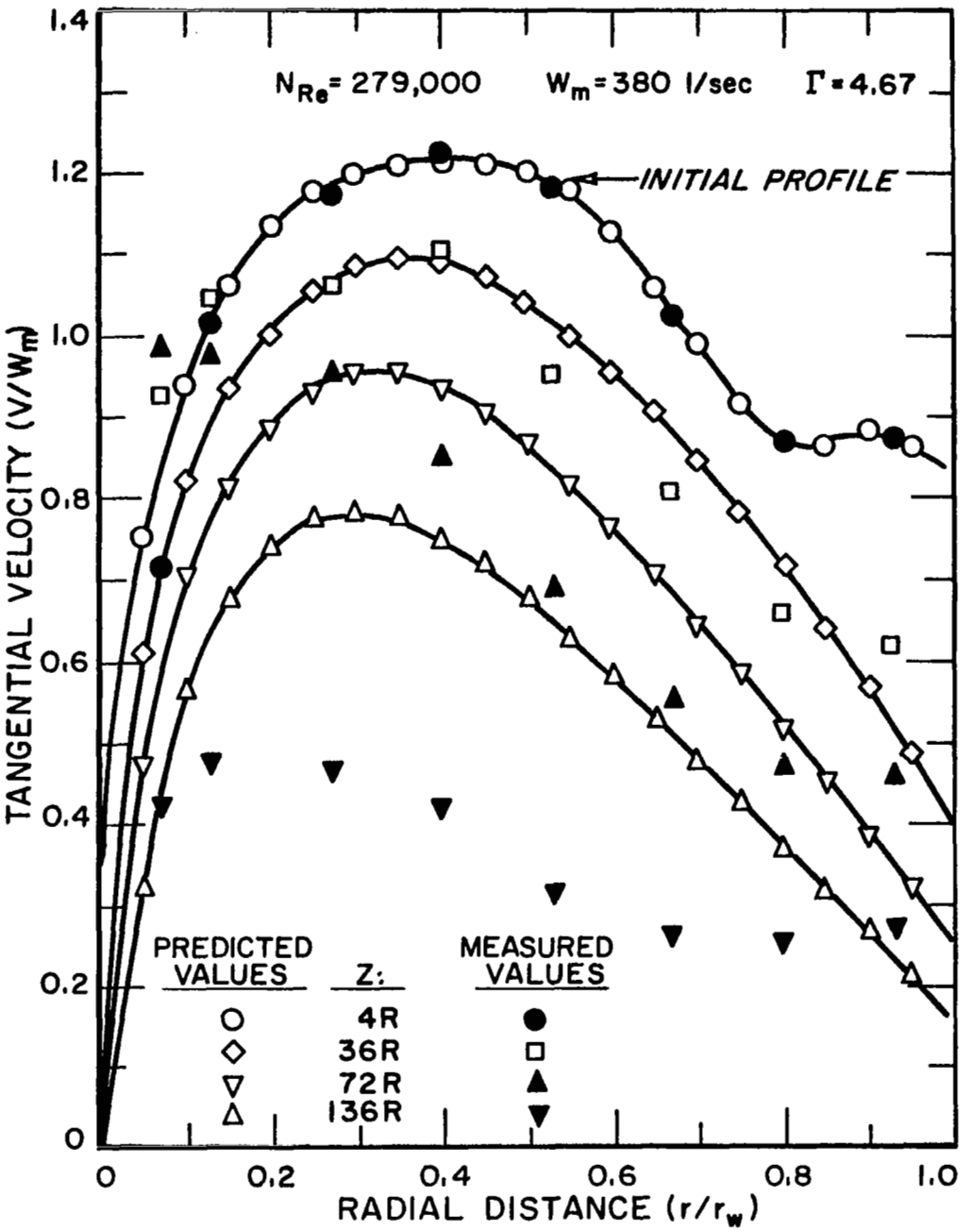

FIGURE 24. COMPARISON OF MEASURED AND PREDICTED RADIAL DISTRIBUTIONS OF TANGENTIAL VELOCITY.

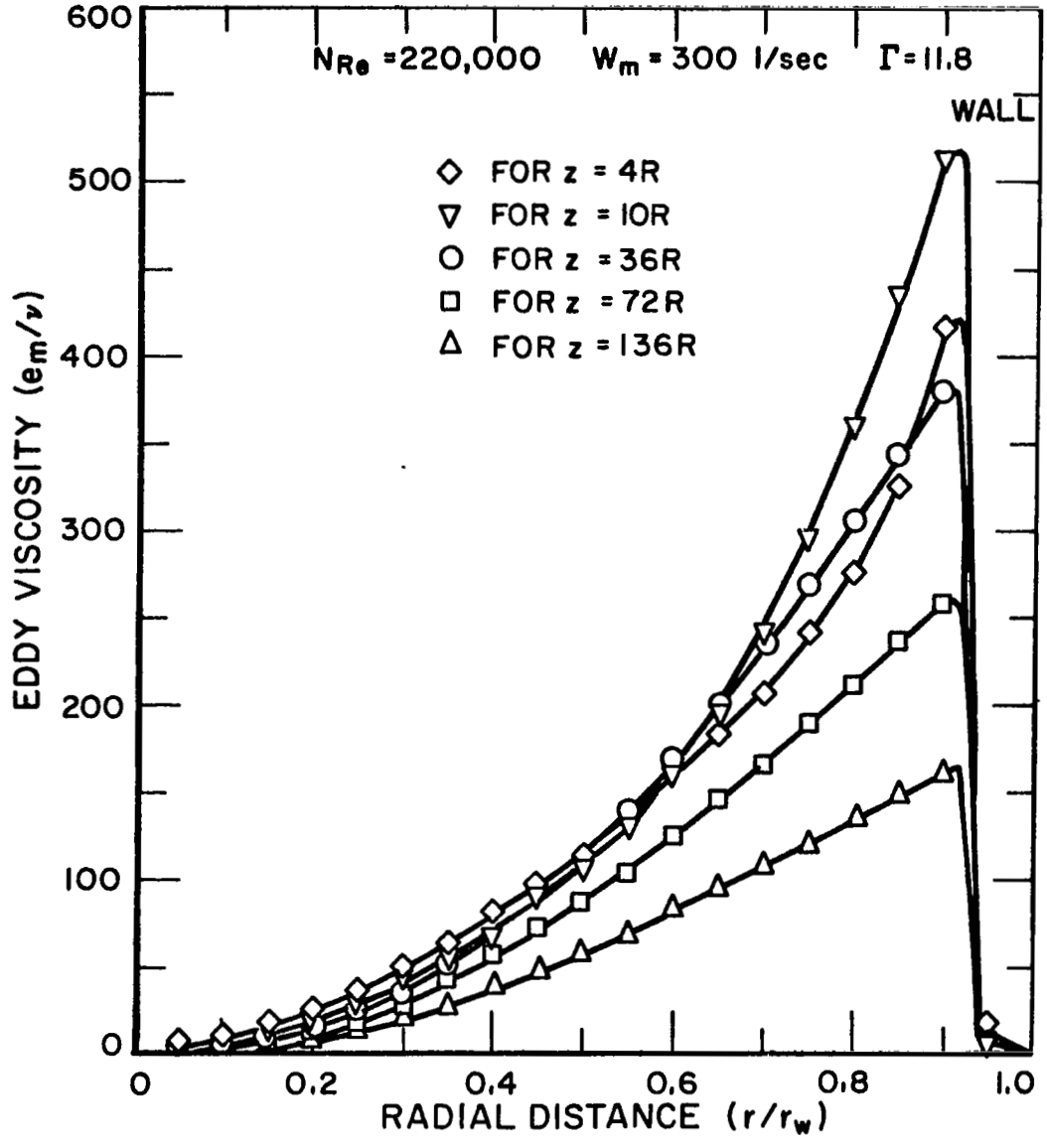

FIGURE 25. PREDICTED RADIAL DISTRIBUTION OF EDDY VISCOSITY.

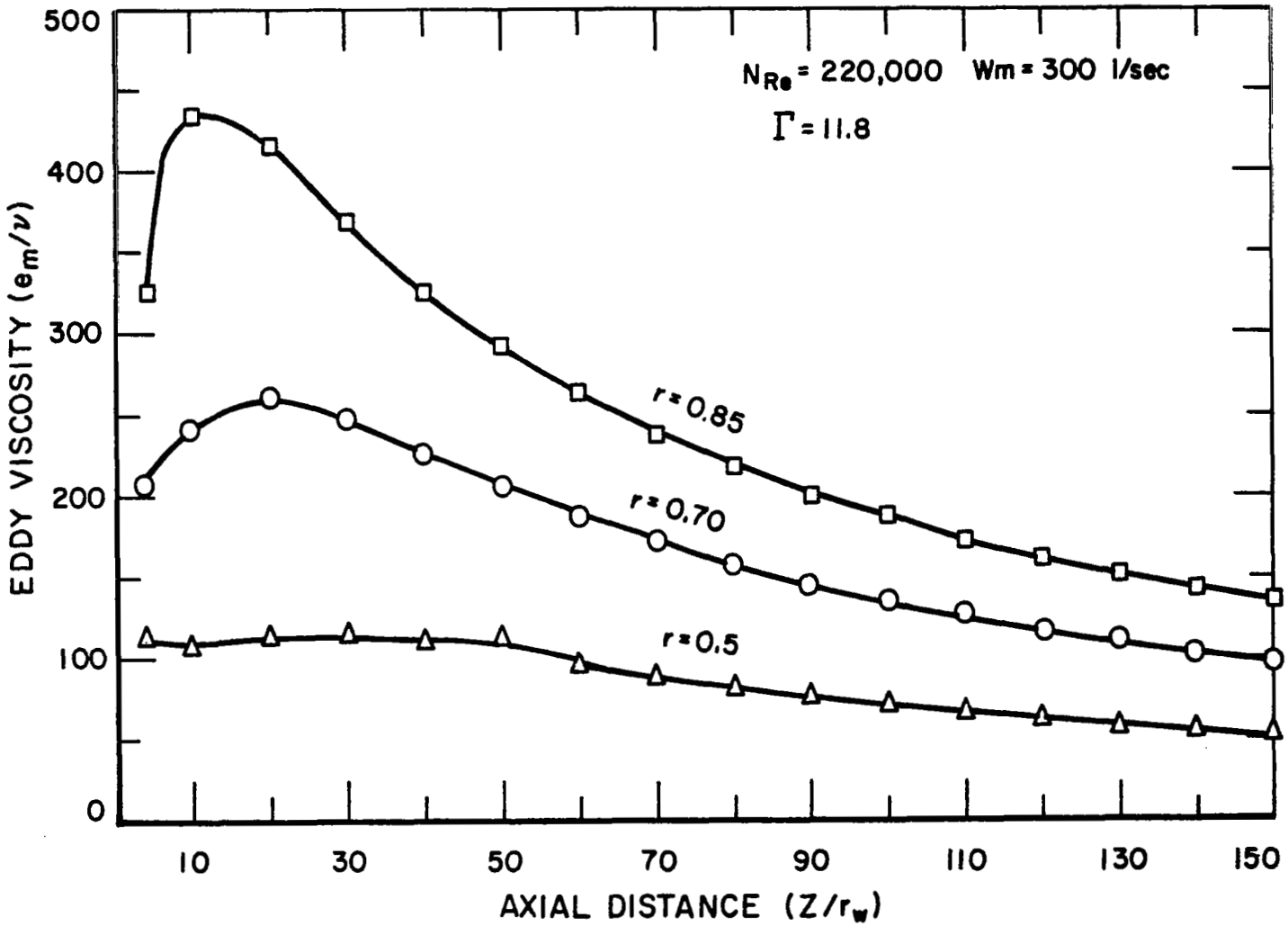

FIGURE 26. PREDICTED AXIAL DISTRIBUTION OF EDDY VISCOSITY.

distribution of axial velocity used in the analysis was always positive for this case.

An inspection of the swirl equation,

$$\frac{\partial V}{\partial z} = \frac{\left(\frac{1}{N_{Re}} + e_m\right)}{W} \frac{\partial \zeta}{\partial r} - \frac{U}{W} \cdot \zeta$$

indicates that if W is negative, $\frac{\partial \zeta}{\partial r}$ being always negative , the first term on the right hand side will represent production rather than dissipation. The noted discrepancy for this region is therefore easily explained if we recall that in the analysis U was neglected and W was always positive. Secondly, an examination of Figure 15 reveals that in the central region, the axial velocity changes markedly as the flow progresses downstream. Hence, even if W is always positive, $\frac{\partial W}{\partial z}$ is large and it may not be justified to neglect U here. It is conceivable that the convective term $\frac{U}{W} \cdot \zeta$ may be larger than the diffusive term. Lastly, the discrepancy may also be in part due to the fact that the experimental probing of rotating flows near the axis is extremely difficult and the data cannot be considered accurate.

Both Figures 20 and 22 that depict flow at low Reynold's Numbers with high swirl ratio, as well as in Figures 23 and 24 that represent high Reynold's Numbers with low swirl ratio, show good agreement between theory and experiment up to an axial distance of about 72R. Further downstream the actual decay is faster than predicted. An examination of the measured radial distribution of the angular momentum for $z \geq 72R$, reveals that a large part of the radial flow field has an irrotational behavior. It has been pointed out previously that for this type of flow some of the similarity conditions

are either infinite or indeterminate. As a result, the eddy viscosity model that was used is not strictly applicable here.

Figures 25 and 26 show the radial distribution of the predicted eddy viscosity at different downstream position, and its axial variation at r = 0.85, 0.70 and 0.50 for a Reynold's Number of 220,000. An inspection of Figure 25 reveals that the eddy viscosity increases with radius up to the vicinity of the wall, and then decreases rapidly. In the axial direction it initially increases and then decreases further downstream. These variations decrease with radius so that the eddy viscosity tends to attain a constant value for all downstream positions in the inner region.

The theory was also applied to a swirling flow field generated by twisted tape inducers inserted in the inlet section of the pipe. This is discussed in the next section.

B. COMPARISON OF THEORETICAL RESULTS WITH MUSOLF'S MEASUREMENTS

The theory was also applied to analyze the decay of the tangential velocity as well as the angular momentum profiles for a tape-induced, fully developed turbulent swirling flow field in a pipe. The predicted values are compared with measurements made by Musolf[33] in 1963 in a 2-inch I.D. tube. This problem was also considered by Kraith and Sonju[21] in 1965. They used an empirically determined constant value of eddy viscosity for the swirl equation and obtained an analytical solution in terms of Bessel-Fourier series for the resulting linear equation. The resulting velocity profiles agree qualitatively with experimental data at distances less than 20 diameters downstream.

1. Initial Conditions and the Mean Axial Velocity Distribution

Figure 27 (after Smithberg and Landis[23]) depicts the average swirl velocity profile at the point of generation where a twisted tape insert having a pitch of 10 pipe diameters was used. Kreith and Sonju[21] approximated the given profile by the expression

$$V(r,0) = f(r) = \frac{1}{H}\left[\, 6.3r - 0.013\,(1.1 - r)^{-2.68} \,\right]$$

where H = pitch of the inducer tape.

Smithberg and Landis also reported a mean axial velocity distribution at the same point in the flow field. This profile, shown in Figure 28, was used in the present analysis in solving the swirl equation.

2. The Eddy Viscosity Model and Results

An inspection of the initial swirl velocity distribution (Figure 27) indicates a predominantly solid body rotation in a large part of the flow field. Since the eddy viscosity model which was derived from similarity theory does not apply here, a different expression will be used. Figure 26 shown that the eddy viscosity is approximately a constant in the inner region where the mean flow tends to be rotational. Following this trend it will be assumed that the eddy viscosity is independent of r and z in the region of predominantly rotational mean flow. This region was arbitrarily assumed to extend up to the radius of maximum tangential velocity.

Ragsdale[25] suggested that for vortex flow, e_m should be directly proportional to the tangential Reynold's Number. Following his suggestion with a slight modification such that the axial Reynold's Number will be used

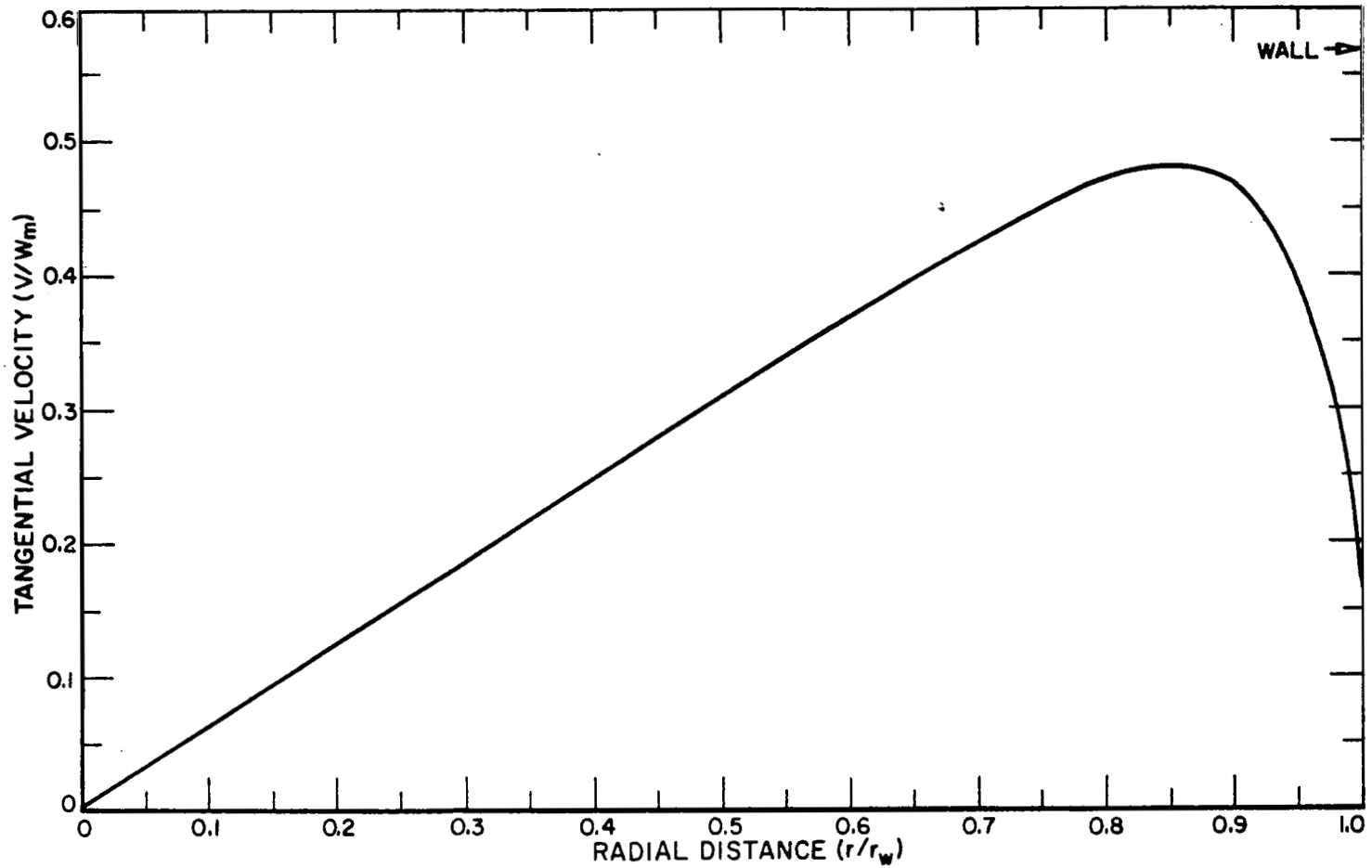

FIGURE 27. INITIAL SWIRL VELOCITY DISTRIBUTION FOR A TAPE INDUCED SWIRL (PITCH = 10) AFTER SMITHBERG AND LANDIS.

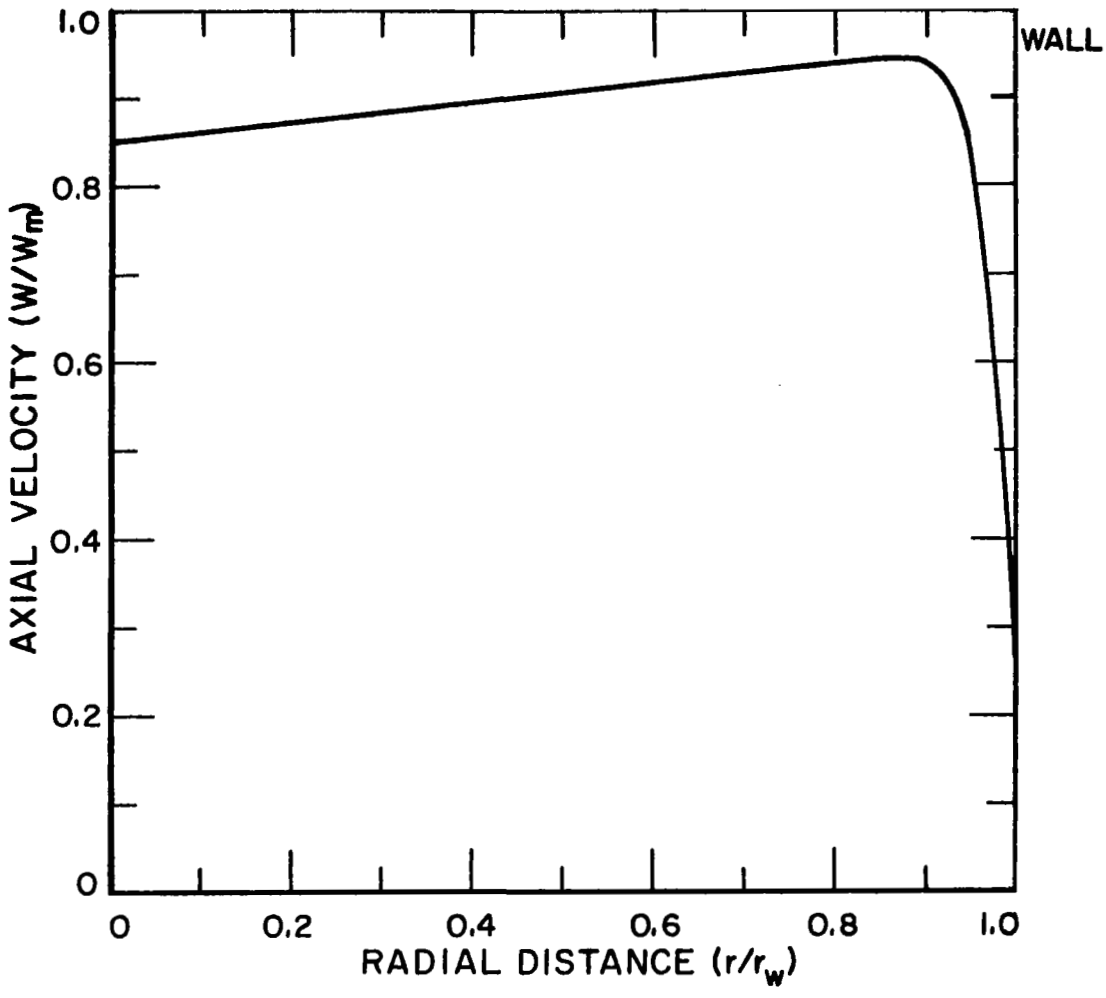

FIGURE 28. RADIAL DISTRIBUTION OF AXIAL VELOCITY AT Z = 0 AFTER SMITHBERG AND LANDIS.[23]

in the present case, the eddy viscosity expression in the region mentioned above takes the following form:

$$e_m = C \cdot N_{Re} \quad 0 \leq r \leq r_{max} \tag{99}$$

where C = Constant.

r_{max} = radius with maximum tangential velocity.

An approximate value of the constant was obtained by considering only the region with rotational mean flow. Assuming that the mean axial velocity is a constant (see Figure 28) the swirl equation was solved by the method of separation of variables and the solution was expressed in a Fourier-Bessel series. It was observed that for large values of z, V(r,z) is practically determined by the first term of the series. Hence, substituting Musolf's measurements which were taken at the farthest downstream position (100R), an average value of C was found to be approximately 0.00246.

At the outer region, that is at radii larger than the radius of maximum tangential velocity, the expression for the eddy viscosity was the same as that used previously (Equation 90).

Figure 29 shows a comparison between the calculated values of the tangential velocity and the measurements obtained by Musolf[33] at a Reynold's Number of 48,000. Figure 30 shows the predicted and measured angular momentum profiles for the same flow conditions. An inspection of these figures reveals qualitatively good agreement between theory and experiment.

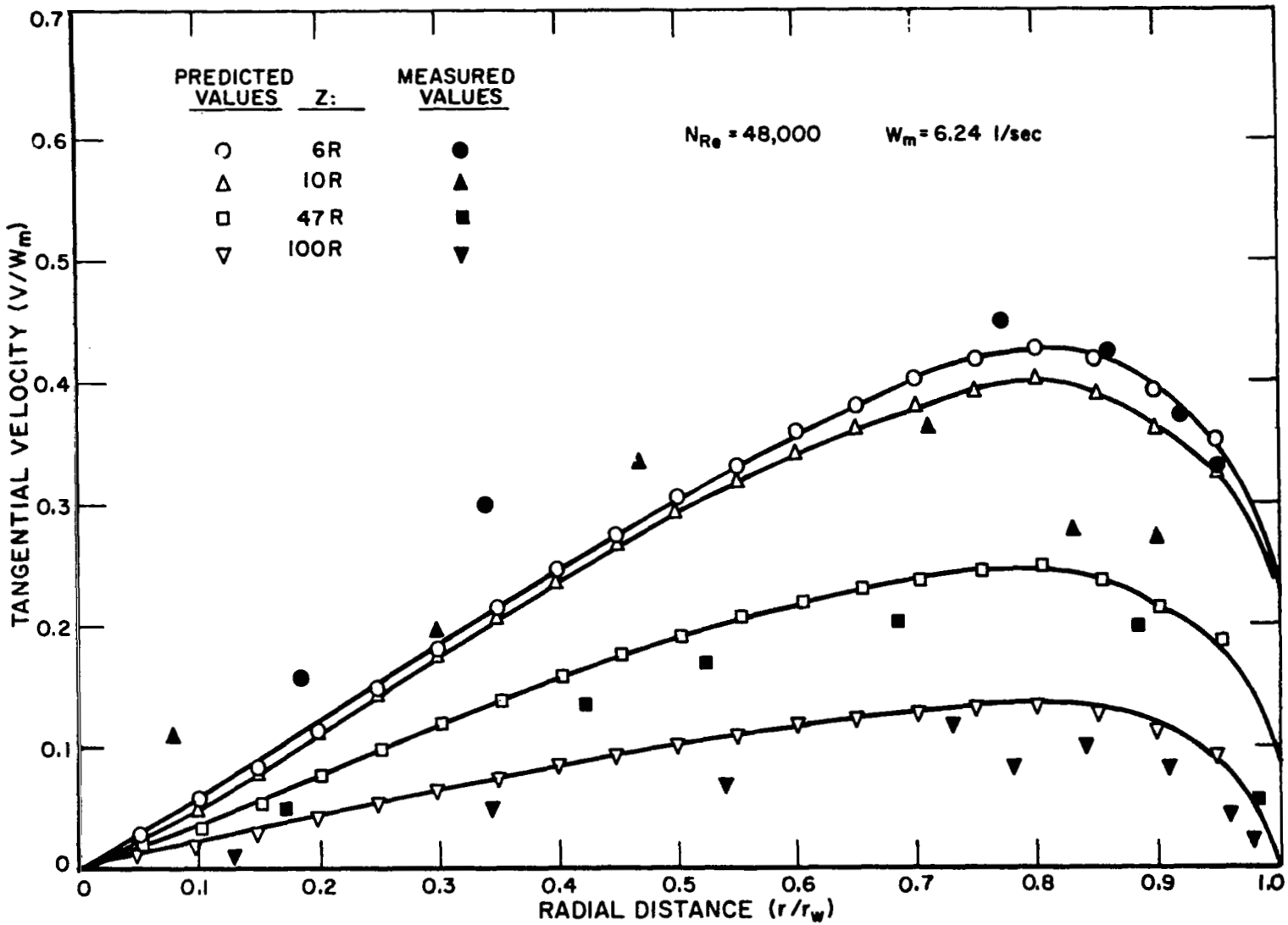

FIGURE 29. COMPARISON BETWEEN PREDICTED AND MEASURED SWIRL VELOCITY PROFILES.

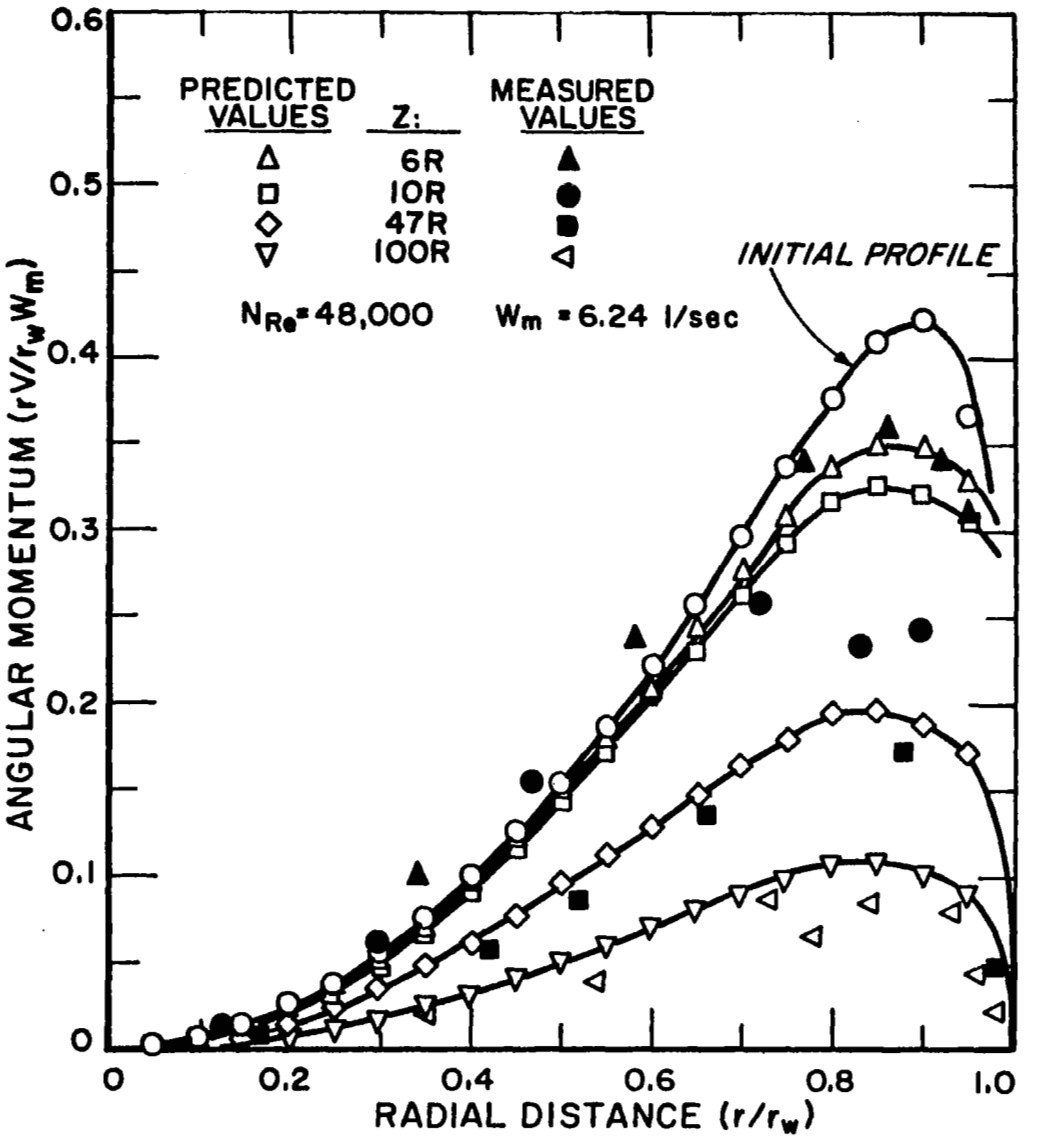

FIGURE 30. COMPARISON OF MEASURED AND PREDICTED RADIAL DISTRIBUTIONS OF ANGULAR MOMENTUM.

X. CONCLUSIONS AND RECOMMENDATIONS

1. Turbulent swirling flows with constant physical properties were investigated analytically using mixing length theories. The tangential equation of motion (swirl equation) derived by applying G. I. Taylor's modified transport theory and the concept of isotropic transport coefficients, is of the same form as the tangential component of Navier-Stokes equations for fluids with constant viscosity.

2. Theodore von Karman's similarity theory for the turbulent mechanism was extended to rotating as well as swirling flow in a cylindrical geometry. A three-dimensional fluctuating velocity field was considered in both cases, and similarity conditions were obtained. It appears that for rotating flows, the shearing stress ($T_{r\theta}$) is proportional to both shear velocity and mean rotation of the fluid. According to the usual concept of a mixing length, this indicates that the fluctuating velocity field is related to the radial transport of angular velocity and to the exchange of angular momentum between concentric layers of fluid. It can also be shown from the similarity conditions that the shear velocity and mean rotation are related to the radial transport of vorticity.

3. Assuming that the similarity conditions are simultaneously satisfied in the flow field, more than one form of similar velocity profiles were found to be possible for rotating flows. This is in agreement with the experimental observations of G. I. Taylor who found two very different turbulent velocity profiles depending on which of the concentric cylinders was rotated.

The similarity conditions indicate that different forms of similar velocity profiles may exist at different regions of the flow field at the same time. This is in accord with the well known structure of rotating flows; there is a gradual change of flow characteristics in the radial direction, starting with predominantly solid body rotation near the center to $V = \text{Constant} \cdot (r^{-m})$, in the outer region (m varying from 0.50 to 1.0).

4. For a fully developed turbulent swirling flow in pipes, von Karman's similarity theory gives similarity conditions identical to those for rotating flows, and also additional conditions which reveal that the fluctuating velocity field (hence, the turbulent stresses too), are also related to the transport of angular momentum in the axial direction. This results in a turbulent shear stress distribution in a plane perpendicular to the z-axis and in the θ direction ($T_{z\theta}$) in addition to the shear stress, $T_{r\theta}$, which arises due to the radial transport of both angular velocity and angular momentum.

5. The presence of turbulent stresses $T_{r\theta}$ and $T_{z\theta}$ in swirling flow give rise to eddy viscosities at different planes of a fluid element. A resultant expression for kinematic eddy viscosity (assumed always positive) was formulated using the assumption that the similarity conditions are simultaneously satisfied in the flow field. The expression is:

$$e_m = K^2 r^2 \left(\frac{\partial V}{\partial r} - \frac{V}{r} \right) \qquad 0 \leq r \leq 0.90$$

The constant K was found to be equal to 0.0333. This value was deduced from the one evaluated by R. B. Kinney (1967) for rotating flow using the experimental data of G. I. Taylor.

6. For the region near the wall, $0.90 < r \leq 1.0$, the mixing length was assumed proportional to the wall distance. The assumed expression is analogous to that made by L. Prandtl in his studies on parallel flows in channels and the region of validity is based on the result of experimental studies of parallel flow in pipes. The proportionality constant was assumed to be equal to that used in the interior. Thus, near the wall, we have:

$$e_m = K^2(1 - r)^2 \left|\frac{\partial V}{\partial r} - \frac{V}{r}\right| \qquad 0.90 < r \leq 1.0$$

7. Some of the similarity conditions become indeterminate or infinite in value for a purely rotational (solid body rotation) as well as for irrotational flows. This invalidates the assumption that the similarity conditions are simultaneously satisfied in the flow field. As a result, the eddy viscosity expression is not strictly applicable for these cases.

8. The derived swirl and eddy viscosity expressions were used to study the decay of angular momentum of a turbulent swirling flow field inside a stationary pipe. Two sets of measurements were used for comparison between theory and experiment. The first which was taken at IITRI (1967) considered swirl generated by radial blades with measurements taken as far as 136R downstream. The second set was obtained by Musolf (1963) for swirls generated by tape inserts inside the pipe.

In the first set, the agreement between theory and experiment was very good all the way up to z = 136R for the case when both axial Reynolds Number and swirl ratio were high (220,000 and 11.8 respectively). For cases where

the axial Reynold's Numbers are high but the swirl ratios are low or vice versa, good agreements were obtained only up to z = 72R. Further downstream, the actual decay is faster than predicted.

An inspection of the measured data revealed that as the flow progresses downstream in the latter case, a small region near the wall first exhibits an irrotational behavior. This region widens further downstream until a large part of the flow field has constant angular momentum for which the kinematic eddy viscosity model used, does not strictly apply as was pointed out in item 7.

In the second set of data, the agreement between theory and experiment was also good.

9. Due to the tendency of the outer region to exhibit irrotational motion as the flow progresses downstream, the radial position of the point with maximum tangential velocity shifts towards the center. This characteristic of the flow field is manifested also in the theoretical results using the derived mathematical model of eddy viscosity.

An attempt was made to find an eddy viscosity model that is independent of the radial and axial distances, but the calculated results using such a model did not agree with the measured data. The point of maximum tangential velocity shifts away from the center, contrary to experimental observations.

APPENDIX I

DERIVATION OF THE EXPRESSION FOR THE FLUCTUATING VORTICITY VECTOR IN A TURBULENT FIELD

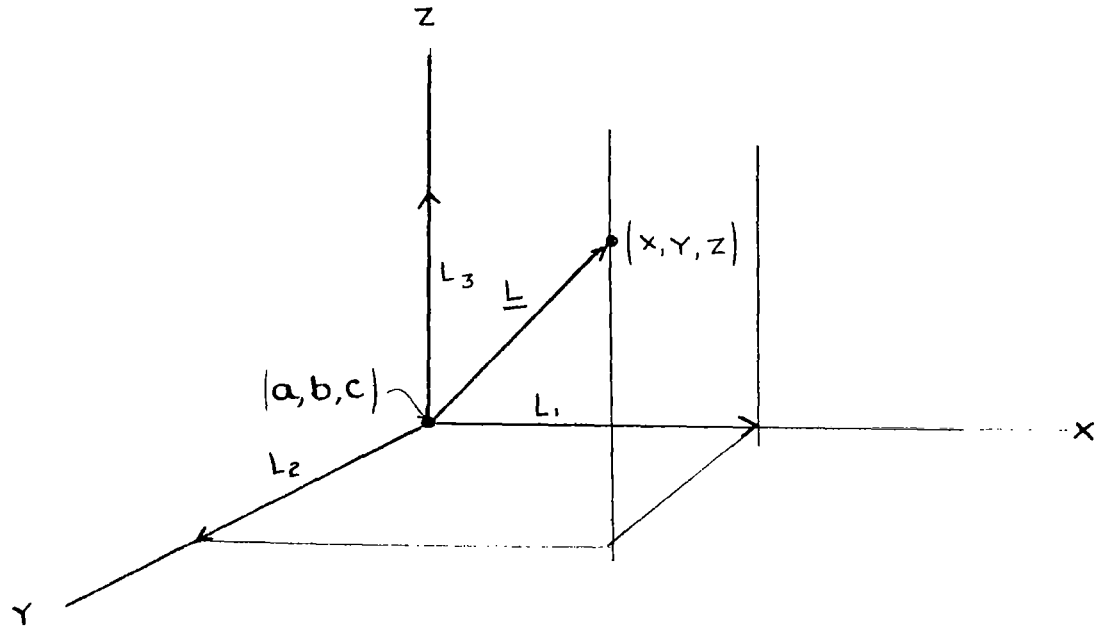

Figure A-1

Assumptions:

1. The components of the mixing length vector (see Figure A-1) are very small.
2. The space derivatives of the L's are also very small.
3. As a result of assumptions 1 and 2, terms quadratic in the L's and their space derivatives can be neglected.

Let:

(ξ_o, η_o, ζ_o) = vorticity of the fluid element at point (a,b,c) at time t_o. This is also the mean vorticity at (a,b,c).

(ξ, η, ζ) = the mean vorticity components at some point (x,y,z) after travelling the mixing length L.

(ξ', η', ζ') = fluctuating vorticity components at (x,y,z).

By Taylor series and neglecting higher order terms:

$$\begin{aligned}
\xi_o &= \xi - L_1 \frac{\partial \xi}{\partial x} - L_2 \frac{\partial \xi}{\partial y} - L_3 \frac{\partial \xi}{\partial z} \\
\eta_o &= \eta - L_1 \frac{\partial \eta}{\partial x} - L_2 \frac{\partial \eta}{\partial y} - L_3 \frac{\partial \eta}{\partial z} \qquad \text{(I-1)} \\
\zeta_o &= \zeta - L_1 \frac{\partial \zeta}{\partial x} - L_2 \frac{\partial \zeta}{\partial y} - L_3 \frac{\partial \zeta}{\partial z}
\end{aligned}$$

At point (x,y,z), the vorticity of the fluid element is $(\xi+\xi', \eta+\eta', \zeta+\zeta')$. Using Cauchy's equation of expressing the vorticity at any point in terms of its vorticity components at some previous time:[3]

$$\begin{aligned}
\xi + \xi' &= \xi_o \frac{\partial x}{\partial a} + \eta_o \frac{\partial x}{\partial b} + \zeta_o \frac{\partial x}{\partial c} \\
\eta + \eta' &= \xi_o \frac{\partial y}{\partial a} + \eta_o \frac{\partial y}{\partial b} + \zeta_o \frac{\partial y}{\partial c} \qquad \text{(I-2)} \\
\zeta + \zeta' &= \xi_o \frac{\partial z}{\partial a} + \eta_o \frac{\partial z}{\partial b} + \zeta_o \frac{\partial z}{\partial c}
\end{aligned}$$

The equation of continuity in lagrangian form is:

$$\frac{\partial(x, y, z)}{\partial(a, b, c)} = 1 \qquad \text{or} \qquad \frac{\partial(a, b, c)}{\partial(x, y, z)} = 1 \tag{I-3}$$

From Figure A-1, the following relations are obvious:

$$L_1 = x - a, \qquad L_2 = y - b, \qquad L_3 = z - c \tag{I-4}$$

Thus:

$$\frac{\partial a}{\partial x} = 1 - \frac{\partial L_1}{\partial x}, \quad \frac{\partial b}{\partial y} = 1 - \frac{\partial L_2}{\partial y}, \quad \frac{\partial c}{\partial z} = 1 - \frac{\partial L_3}{\partial z}$$

$$\frac{\partial a}{\partial y} = -\frac{\partial L_1}{\partial y}, \quad \frac{\partial b}{\partial x} = -\frac{\partial L_2}{\partial x}, \quad \frac{\partial c}{\partial x} = -\frac{\partial L_3}{\partial x} \tag{I-5}$$

$$\frac{\partial a}{\partial z} = -\frac{\partial L_1}{\partial x}, \quad \frac{\partial b}{\partial z} = -\frac{\partial L_2}{\partial z}, \quad \frac{\partial c}{\partial y} = -\frac{\partial L_3}{\partial y}$$

Expanding the determinant of the continuity equation (I-3), and substituting the values of $\frac{\partial a}{\partial x}$, $\frac{\partial a}{\partial y}$, ..., from Equation I-5) and using assumptions 1, 2 and 3, one obtains:

$$\frac{\partial L_1}{\partial x} + \frac{\partial L_2}{\partial y} + \frac{\partial L_3}{\partial z} = 0 \tag{I-6}$$

or in vector form:

$$\nabla \cdot \underline{L} = 0 \tag{I-6'}$$

This is the continuity equation in terms of the mixing length vector, $\underline{L}$.

With the aid of the continuity equation, the derivatives of x, y and z with respect to a, b or c, can be expressed in terms of the derivatives of

a, b and c with respect to x, y or z.[40] Thus:

$$\frac{\partial(a,\ b,\ c)}{\partial(x,\ y,\ c)} = \frac{\partial a}{\partial x}\left[\frac{\partial(b,\ c)}{\partial(y,\ z)}\right] - \frac{\partial b}{\partial x}\left[\frac{\partial(a,\ c)}{\partial(y,\ z)}\right] + \frac{\partial c}{\partial x}\left[\frac{\partial(a,\ b)}{\partial(y,\ z)}\right] = 1$$

Hence:

$$\frac{\partial x}{\partial a} = \frac{\partial(b,\ c)}{\partial(y,\ z)}$$

$$\frac{\partial x}{\partial b} = \frac{\partial(a,\ c)}{\partial(y,\ z)} \qquad \text{(I-7)}$$

$$\frac{\partial x}{\partial c} = \frac{\partial(a,\ b)}{\partial(y,\ z)}$$

Substituting Equation I-5 into Equation I-7 we have:

$$\frac{\partial x}{\partial a} = \frac{\partial b}{\partial y} \cdot \frac{\partial c}{\partial z} - \frac{\partial b}{\partial z} \cdot \frac{\partial c}{\partial y}$$

$$= \left(1 - \frac{\partial L_2}{\partial y}\right)\left(1 - \frac{\partial L_3}{\partial z}\right) - \left(-\frac{\partial L_2}{\partial z}\right)\left(-\frac{\partial L_3}{\partial y}\right)$$

$$= 1 - \frac{\partial L_2}{\partial y} - \frac{\partial L_3}{\partial z}$$

But from Equation I-6, the last two terms can be represented by $\frac{\partial L_1}{\partial x}$. Hence,

$$\frac{\partial x}{\partial a} = 1 + \frac{\partial L_1}{\partial x}$$

Similarly,

$$\frac{\partial x}{\partial b} = \frac{\partial L_1}{\partial y} \qquad \text{(I-8)}$$

$$\frac{\partial x}{\partial c} = \frac{\partial L_1}{\partial z}$$

The derivatives of y and z with respect to a, b or c can be derived using the same procedure as above. Substitute Equation I-8 into I-2, and using Equation I-1 and then solving for the fluctuating vorticity results in the following relations:

$$\xi' = \xi \frac{\partial L_1}{\partial x} + \eta \frac{\partial L_1}{\partial y} + \zeta \frac{\partial L_1}{\partial z} - L_1 \frac{\partial \xi}{\partial x} - L_2 \frac{\partial \xi}{\partial y} - L_3 \frac{\partial \xi}{\partial z} \quad \text{(a)}$$

Similarly for η' and ζ': (I-10)

$$\eta' = \xi \frac{\partial L_2}{\partial x} + \eta \frac{\partial L_2}{\partial y} + \zeta \frac{\partial L_2}{\partial z} - L_1 \frac{\partial \eta}{\partial x} - L_2 \frac{\partial \eta}{\partial y} - L_3 \frac{\partial \eta}{\partial z} \quad \text{(b)}$$

$$\zeta' = \xi \frac{\partial L_3}{\partial x} + \eta \frac{\partial L_3}{\partial y} + \zeta \frac{\partial L_3}{\partial z} - L_1 \frac{\partial \zeta}{\partial x} - L_2 \frac{\partial \zeta}{\partial y} - L_3 \frac{\partial \zeta}{\partial z} \quad \text{(c)}$$

From vector analysis:

$$\nabla \cdot \underline{\Omega} = 0 \quad \text{(I-11)}$$

or

$$\frac{\partial \xi}{\partial x} + \frac{\partial \eta}{\partial y} + \frac{\partial \zeta}{\partial z} = 0 \quad \text{(I-11')}$$

Solving for $\frac{\partial \xi}{\partial x}$ in I-11' and $\frac{\partial L_1}{\partial x}$ in Equation I-6 and substituting these into Equation I-10a, the following expression for the vorticity in the x-direction results after simplification:

$$\xi' = \frac{\partial}{\partial y}(L_1\eta - L_2\xi) - \frac{\partial}{\partial z}(L_3\xi - L_1\zeta) \quad \text{(a)}$$

Similarly for the vorticity in the y and z directions:

$$\eta' = \frac{\partial}{\partial z}(L_2\zeta - L_3\eta) - \frac{\partial}{\partial x}(L_1\eta - L_2\xi) \quad \text{(b)}$$

(I-12)

$$\zeta' = \frac{\partial}{\partial x}(L_3\xi - L_1\zeta) - \frac{\partial}{\partial y}(L_2\zeta - L_3\eta) \qquad (c)$$

Vectorially, Equation I-12 can be written as:

$$\underline{\Omega}' = \nabla \times (\underline{L} \times \overline{\Omega}) \qquad (I\text{-}13)$$

APPENDIX II

APPLICATION OF THE MODIFIED VORTICITY TRANSPORT THEORY TO THE ANALYSIS OF TURBULENT FLOW

With the use of Cauchy's Equation (I-2), the component of vorticity at any point can be expressed in terms of its vorticity components at some previous time.

$$\xi + \xi' = \xi_o \frac{\partial x}{\partial a} + \eta_o \frac{\partial x}{\partial b} + \zeta_o \frac{\partial x}{\partial c}$$

$$\eta + \eta' = \xi_o \frac{\partial y}{\partial a} + \eta_o \frac{\partial y}{\partial b} + \zeta_o \frac{\partial y}{\partial c} \qquad \text{(I-2)}$$

$$\zeta + \zeta' = \xi_o \frac{\partial z}{\partial a} + \eta_o \frac{\partial z}{\partial b} + \zeta_o \frac{\partial z}{\partial c}$$

The modified vorticity transport theory asserts that a lump of fluid leaving a certain position with vorticity components of the mean motion, and upon traversing the mixing length, the vorticity components are retained until it mixes with the surrounding fluid in the new position.

Mathematically, the above condition implies that:

$$\xi + \xi' = \xi_o$$

$$\eta + \eta' = \eta_o \qquad \text{(II-1)}$$

$$\zeta + \zeta' = \zeta_o$$

Comparing Equations I-2 and II-1, it follows that the following relations hold:

$$\frac{\partial x}{\partial a} = \frac{\partial y}{\partial b} = \frac{\partial z}{\partial c} = 1$$

$$\frac{\partial x}{\partial b} = \frac{\partial x}{\partial x} = \frac{\partial y}{\partial a} = \frac{\partial y}{\partial c} = \frac{\partial z}{\partial a} = \frac{\partial z}{\partial b} = 0 \qquad \text{(II-2)}$$

From Equation I-8,

$$\frac{\partial x}{\partial a} = 1 + \frac{\partial L_1}{\partial x}, \qquad \frac{\partial y}{\partial b} = 1 + \frac{\partial L_2}{\partial y}$$

$$\frac{\partial x}{\partial b} = \frac{\partial L_1}{\partial y}, \qquad \frac{\partial y}{\partial a} = \frac{\partial L_2}{\partial x}$$

$$\frac{\partial x}{\partial c} = \frac{\partial L_1}{\partial z}, \qquad \frac{\partial y}{\partial c} = \frac{\partial L_2}{\partial z}$$

$$\frac{\partial z}{\partial c} = 1 + \frac{\partial L_3}{\partial z}, \quad \frac{\partial z}{\partial a} = \frac{\partial L_3}{\partial x}, \quad \frac{\partial z}{\partial b} = \frac{\partial L_3}{\partial y}$$

Substituting the values from Equation II-2 into Equation I-8 results in the following values of the space derivatives of the components of the mixing length vector:

$$\frac{\partial L_1}{\partial x} = 0$$

$$\frac{\partial L_1}{\partial y} = 0$$

$$\frac{\partial L_1}{\partial z} = 0$$

This means that the component L_1 is a constant. Similarly,

$$\frac{\partial L_2}{\partial x} = \frac{\partial L_2}{\partial y} = \frac{\partial L_2}{\partial z} = 0$$

$$\frac{\partial L_3}{\partial x} = \frac{\partial L_3}{\partial y} = \frac{\partial L_3}{\partial z} = 0$$

From the above results it appears that the concept of the modified vorticity transport theory requires that the components of the mixing length vector are constants. This also means that,

$$\underline{L} = \text{Constant} \qquad \text{(II-3)}$$

where $\underline{L}$ is the mixing length vector.

APPENDIX III

STABILITY ANALYSIS OF THE EXPLICIT DIFFERENCE EQUATION

The solution of the finite-difference equation represented by Equation 96 can be written as a Fourier series, the form of which is:

$$\beta_j^n = \sum_j \psi^n \cdot e^{i(j\Delta r)} \qquad \text{(III-1)}$$

where:

ψ = amplification factor

$i = \sqrt{-1}$

n and j are positive integers

Substituting Equation (III-1) into Equation 96, we obtain, after some algebraic manipulations:

$$\sum_j \left[\psi^{n+1} - \psi^n \left(1 - \tau + \gamma e^{i(j\Delta r)} + \phi e^{-i(j\Delta r)} \right) \right] \cdot e^{i(j\Delta r)} = 0$$

or

$$\psi = 1 - \tau + \gamma e^{i(j\Delta r)} + \phi e^{-i(j\Delta r)} \qquad \text{(III-2)}$$

Since

$$e^{\pm i(j\Delta r)} = \cos(j\Delta r) \pm i \sin(j\Delta r)$$

Equation III-2 further reduces to

$$\psi = 1 - \tau + (\gamma + \phi) \cos(j\Delta r) + (\gamma - \phi)\, i \sin(j\Delta r) \qquad \text{(III-3)}$$

Where:

$$\tau = \left(\frac{2D}{(\Delta r)^2} + \frac{B}{r\Delta r} \right) \Delta z$$

$$\gamma = \left(\frac{D}{(\Delta r)^2} + \frac{B}{r\Delta r} \right) \Delta z$$

$$\phi = \frac{D}{(\Delta r)^2} \Delta z$$

The condition of stability according to von Neumann[41] is

$$|\Psi| \leq 1 \qquad \text{(III-4)}$$

Taking the worst case of Equation III-3, i.e., where

$$\cos(j\Delta r) = -1$$

$$\sin(j\Delta r) = 0$$

we have

$$\Psi = 1 - (\tau + \gamma + \phi) \qquad \text{(III-5)}$$

To satisfy the stability condition as given by Equation III-4, the following inequality must be true in Equation III-5:

$$-2 \leq -(\tau + \gamma + \phi) \leq 0 \qquad \text{(III-6)}$$

Since the right inequality of Equation III-6 is always satisfied, the stability criterion will be obtained if we consider the left inequality. Thus:

$$(\tau + \gamma + \phi) \leq 2$$

Substituting the values of τ, γ and ϕ, the stability criterion becomes:

$$\left[\frac{2D}{(\Delta r)^2} + \frac{B}{r\Delta r} \right] \Delta z \leqq 1 \qquad \text{(III-7)}$$

This is the same expression as that given in Equation 97.

REFERENCES

1. Hinze, J. O., "Turbulence", McGraw-Hill Book Company, New York, 1959.

2. Lin, C. C. (Editor), "Turbulent Flows and Heat Transfer", Princeton University Press, 1959.

3. Lamb, H., "Hydrodynamics", Dover Publications, New York, 1932, p. 205.

4. Schlichting, H., "Boundary Layer Theory", McGraw-Hill Book Company, New York, 1962.

5. Goldstein, S., "Similarity Theory of Turbulence and Flow between Planes and through Pipes", Proc. Roy. Soc. Vol. 159, Series A, p. 496, 1937.

6. Taylor, G. I., "Flow in Pipes and between Parallel Planes", Proc. Roy. Soc., Vol. 159, Series A, p. 496, 1937.

7. Taylor, G. I., "Distribution of Velocity and Temperature between Concentric Rotating Cylinders", Proc. Roy. Soc., Vol. 151, Series A, 1935. "The Transport of Vorticity and Heat through Fluids in Turbulent Motion", Proc. Roy. Soc., Vol. 135, Series A, 1932.

8. Reynolds, O., "An Experimental Investigation of the Circumstances which Determine whether the Motion of Water Shall Be Direct or Sinuous, and of the Laws of Resistance in Parallel Channels", Phil. Trans. CLXXIV, p. 935, 1883.

9. Mallock, "Determination of the Viscosity of Water", Proc. Roy. Soc. XLV, p. 126, 1888. "Experiments on Fluid Viscosity", Phil. Trans. A, CLXXXVII, p. 41.

10. Taylor, G. I., "Stability of a Viscous Liquid Contained between Two Rotating Cylinders", Phil. Trans. A, CCXXIII, 1922.

11. Watendorf, F. L., "A Study of the Effect of Curvature on Fully Developed Turbulent Flow", Proc. Roy. Soc., Vol. 148, Series A, p. 565, 1935.

12. Kassner, R. and Knoernschild, E., "Friction Laws and Energy Transfer in Circular Flow", Technical Report No. F-TR-2198-ND, GS-USAF Wright Patterson Air Force, 1948.

13. Ragsdale, R. G., "Applicability of Mixing Length Theory to a Turbulent Vortex System", NASA TN D-1051, 1961.

References (Cont'd)

14. Prandtl, L., "Essentials of Fluid Dynamics", Hafner Publishing Company, New York, 1952, p. 125.

15. von Karman, Th., "Mechanische Ahnlickeit und Turbulenz", Nach. Ges. Wiss, Gottingen, Math. Phys. Klasse; Vol. 58, 1930 and Proc. 3rd International Congress of Applied Mechanics, Stockholm, Part I. 85, 1930; also NACA TM 611, 1931.

16. Einstein, H. A. and Li, H., "Steady Vortex Flow in a Real Fluid", 1951, Proceedings, Heat Transfer and Fluid Mechanics Institute, Stanford University, Palo Alto, California, June 1951.

17. Deissler, R. G. and Perlmutter, M., "Analysis of the Flow and Energy Separation in a Turbulent Vortex Flow", Int. Jour. Heat and Mass Transfer, Vol. 1, No. 2, Pergamon Press, 1960.

18. Hartnett, J. P. and Eckert, E. R., "Experimental Study of the Velocity and Temperature Distribution in a High Velocity Vortex Type Flow", Trans. ASME, Vol. 79, No. 4, p. 751, May 1957.

19. Reynolds, A. J., "On the Dynamics of Turbulent Vortical Flow", ZAMP, Vol. 12, p. 149, 1961(a). "Energy Flows in a Vortex Tube", ZAMP, Vol. 12, p. 343, 1961(b).

20. Sibulkin, M., "Unsteady Viscous Circular Flow", Part 3: Application to the Ranque-Hilsch Vortex Tube", Jour. Fluid Mechanics, Vol. 12, p. 269, 1962.

21. Kreith, F. and Sonju, O., "The Decay of Turbulent Swirl in a Pipe", Jour. Fluid Mechanics, Vol. 22, Part 2, p. 257, 1965.

22. Kreith, F. and Margolis, D., "Heat Transfer and Friction in a Turbulent Vortex Flow", App. Sci. Res. A, Vol. 8, p. 457, 1959.

23. Smithberg, E. and Landis, F., "Friction and Forced Convection Heat Transfer Characteristics in Tubes with Twisted Tape Swirl Generators", Trans. ASME, J. Heat Transfer, Vol. 86, p. 1, 1964.

24. Gambil, W., Bundy, R. D. and Wansbrough, R. W., "Heat Transfer, Burnout and Pressure Drop for Water in Swirl Flow through Tubes with Internal Twisted Tape", Chem. Eng. Symp., Series 5, p. 127, 1961.

25. Ragsdale, R. G., "NASA Research on the Hydrodynamics in High Velocity Vortex Flow", NASA TND-288, September 1960.

26. Keyes, J. J., "An Experimental Study of Gas Dynamics in High Velocity Vortex Flow", Proc. Heat Transfer and Fluid Mech. Institute, Palo Alto, California, Stanford University Press, 1960.

27. Kerrebrook, J. L. and Meghreblian, R. V., "Vortex Containment for the Gaseous Fission Rocket", J. Aerospace Science, Vol. 28, p. 710, 1961.

28. Lavan, Z. and Fejer, A. A., "Investigation of Swirling Flows in Ducts", ARL 66-0083, Aerospace Research Laboratories, USAF, Wright-Patterson Air Force Base, Ohio, May 1966.

29. Collatz, L. and Goertler, G., "Rohrstromung mit Schwachem Drall", ZAMP, V(1954).

30. Talbot, L., "Laminar Swirling Flow", Journal Applied Mechanics, Vol. 76, 1954.

31. Kinney, R. B., "Universal Velocity Similarity in Fully Turbulent Rotating Flow", Paper No. 67-APM-23 - Contributed by the Applied Mechanics Div. for Presentation at the Applied Mechanics Conference, Pasadena, California, June 26-28, 1967 of the ASME.

32. Taylor, G. I., "Fluid Friction between Rotating Cylinders, Part I: Torque Measurements. Part II: Distribution of Velocity between Concentric Cylinders when the Outer One is Rotating and the Inner One is at Rest", Proc. Roy. Soc., London, Vol. 157, Series A, pp. 546-578, 1936.

33. Musolf, A. O., "An Experimental Investigation of the Decay of a Turbulent Swirl Flow in a Pipe", Thesis, University of Colorado, 1963.

34. Experimental investigation of rotating swirling flows presently carried out at IITRI under an Air Force Contract. Private Communications with L. Wolf and Z. Lavan.

35. Boussinesq, J., "Theory de l'ecoulement tourbillant", Mem. Pre. par. div. Sav. XXIII, Paris, 1977.

36. Stanisic, M. M. and Groves. R. N., "On the Eddy Viscosity of Incompressible Turbulent Flow", ZAMP, Vol. 16, 1965, p. 709.

37. Sutton, O. G., "Atmospheric Turbulence", London, 1949, p. 30, 35.

38. Hoffman, E. R. and Joubert, P. N., "Turbulent Line Vortices", Jour. of Fluid Mechanics, Vol. 13, Part 2, 1963.

39. Barakat, et. al., "Transient Natural Convection Flows in Closed Containers", Technical Report No. 2, Microfilm No. N65-33973, University of Michigan.

40. Goldstein, S., "A Note on the Vorticity Transport Theory of Turbulent Motion", Proc. Camb. Phil. Soc., Vol. 31, p. 351.

References (Cont'd)

41 Richtmyer, R., "Difference Methods for Initial Value Problems", Interscience, New York.

42. Goldstein, S., "Modern Developments in Fluid Dynamics", Vol. I and II, Oxford Clarendon Press, 1938.

43. McCracken, D. and Dorn, W., "Numerical Methods and Fortran Programming", John Wiley and Sons, New York, 1964.